Modeling of multimodal transportation systems of large networks

Kwami Sossoe

THÈSE DE DOCTORAT

DE L'UNIVERSITÉ PARIS-EST

Spécialité

MATHÉMATIQUES

(Ecole doctorale : 532)

Présentée par

Kwami Seyram SOSSOE

pour obtenir le grade de

DOCTEUR DE L'UNIVERSITÉ PARIS-EST

Sujet de thèse:

Modélisation des systèmes de transport multimodaux de grands réseaux

Thèse présentée et soutenue à l'IFSTTAR (Champs-sur-Marne) le 10 Juillet 2017.

Composition du Jury:

M. Saïd MAMMAR	Professeur des universités, Université d'Evry	Rapporteur
M. Florian DE VUYST	CMLA, ENS Paris-Saclay	Rapporteur
M. Lionel SCREMIN	Directeur du projet MIC, IRT SystemX	Examinateur
M. Patrice AKNIN	Directeur scientifique, IRT SystemX	Examinateur
Mme Alix MUNIER	Professeure des universités, LIP6	Examinateur
M. Fabien LEURENT	Professeur ENPC, directeur de recherche - LVMT	Examinateur
M. Habib HAJ-SALEM	HDR, Directeur de recherche - IFSTTAR/GRETTIA	Directeur de thèse
M. Jean-Patrick LEBACQUE	IGPEF, Directeur de IFSTTAR/GRETTIA	Directeur de thèse

DISSERTATION

Submitted in partial satisfaction of the requirements for the degree of

DOCTOR OF PHILOSOPHY

in

MATHEMATICS

in the

UNIVERSITÉ PARIS-EST

(Doctoral school : 532)

Presented by

Kwami Seyram SOSSOE

Thesis subject:

Modeling of multimodal transportation systems of large networks

PhD presented and defended at IFSTTAR (Champs-sur-Marne) on July 10, 2017.

Composition of the Jury:

M. Saïd MAMMAR	Professor of universities, Université d'Evry	Reviewer
M. Florian DE VUYST	CMLA, ENS Paris-Saclay	Reviewer
M. Lionel SCREMIN	MIC project director, IRT SystemX	Examiner
M. Patrice AKNIN	Scientific director, IRT SystemX	Examiner
Mme Alix MUNIER	Professor of universities, LIP6	Examiner
M. Fabien LEURENT	Professor ENPC, Research director - LVMT	Examiner
M. Habib HAJ-SALEM	HDR, Research director - IFSTTAR/GRETTIA	Supervisor
M. Jean-Patrick LEBACQUE	IGEPF, Director of IFSTTAR/GRETTIA	Supervisor

Résumé: **Modélisation des systèmes de transport Multimodaux de Grands réseaux**

L'objectif de ce travail consiste en la modélisation des flux de véhicules d'un grand et dense réseau de transport multimodal. Le travail s'organise en deux parties: un aspect théorique et un aspect développement. L'étude théorique met l'accent sur la façon dont un réseau multimodal peut être modélisé et comment sa performance en termes d'offre peut être optimisée. Pour ce faire, trois études principales sont réalisées: la prévision et la régulation des flux de trafic sur les grands réseaux de surface, la multimodalité véhiculaire dans les grands réseaux de surface prenant en compte les nouvelles formes de mobilité, et enfin l'impact de l'information sur le coût des itinéraires. La partie développement consiste en la conception d'un simulateur de flux de trafic pour réguler le trafic multimodal véhiculaire. Le simulateur développé devrait aider les opérateurs de transport et les collectivités territoriales dans leurs stratégies de gestion des flux de trafic.

<u>Mots-clés:</u> modélisation bidimensionnel du trafic, offre et demande du trafic, affectation dynamique réactive, optimisation.

Abstract: **Modeling of Multimodal transportation systems of Large networks**

The objective of this work consists on the modeling of traffic flow of a large multimodal transportation network. The work is organized in two parts: a theoretical study part and a development part. The theoretical study emphasizes on how a multimodal network can be model and how its performance in terms of supply can be optimized. To do so, three main studies are discussed: the traffic flow prediction and regulation on large surface networks, the vehicular multimodality in big surface networks taking into account new forms of mobility, and finally the impact of the information on the cost of the itineraries. The development part consists on the conception of a traffic flow simulator to regulate the vehicular multimodal traffic. The developed simulator should assist transport operators and territorial communities in their traffic flow management strategies.

<u>Key-words:</u> bi-dimensional traffic modeling, traffic supply and demand, reactive dynamic assignment, optimization.

This page is intentionally left blank.

à ma très chère femme Amele, à notre fils Maximilien,

et à mes chers amis.

This page is intentionally left blank.

Je remercie tout particulièrement mon ami Gédéon pour son soutien morale indéfectible. Mes derniers remerciements et non les moindres, s'adressent à ma femme Amele, qui, pour mon plus grand bonheur partage ma vie et mes exp'eriences professionnelles depuis leurs origines. Je rends grÃćce au Seigneur Dieu pour la naissance de notre enfant Maximilien durant ces travaux de recherche. Sa venue a booster mon 'elan à l'achèvement de mes projets.

Contents

This page is intentionally left blank.

LIST OF TABLES

This page is intentionally left blank.

"Experience: that most brutal of teachers. But you learn, my God do you learn. "

– C.S. Lewis

This page is intentionally left blank.

Chapter 1

General introduction

This chapter motivates our research, defines its context, and eases the readability of the remainder of this report as it is indicated in the table of contents below. In Sec. 1.1 we present the context of this report. Next in Sec. 1.2 we summarize the objectives of our work in more detail, which all focus on the development of vehicular multimodal traffic flow model for traffic flow management of big multimodal transportation systems. Finally, we provide an overview of (i) all conventions & notations that we frequently use in the remainder of this report in Sec. 1.3, and (ii) the structure of this remainder in Sec. 1.5.

Contents

The report lies on the crossroad of system of hyperbolic partial differential equations, traffic flow theory, convex optimization, and transport simulation. In our work we use mathematical approaches to develop right vehicular traffic flow models specific to the type and the topology of the transport networks. The models can be used as decision supports for the management of the traffic of urban networks.

1.1 Context & Problem formulation

Naturally, transport models are complex. Most advanced models that allow a relative understanding of large systems are majority in static. Dynamic models have just emerged. Their

resolution is very complex and it requires a prohibitive computational time. In a dynamic setting, macroscopic models do allow to get several properties of traffic flow on a road's stretch (meaning the highway). It is therefore quite reasonable to think to get a new generation of models which provide efficiency in a larger scale. That means to develop right transport models for very large networks. This report provides solid mathematical models able to reproduce traffic flows of transport networks at certain level-of-details. The models are capable of reliability with large surface network where traffic data are difficult to acquire due to insufficient traffic count sensors over such networks.

The challenge of the thesis is to design a dynamic and multimodal realistic macroscopic model that takes into account particular vehicles, electric and autonomous vehicles, and buses for the mass transportation. The final model is handy for the numerical calculations. It understands and performs several tasks such like:

- calculation of traffic indicators as travel costs, instantaneous travel times;

- calculation of dynamic multimodal shortest paths taking into account the variability of the traffic, and the sudden changes derived from a huge number of interactions of vehicles within a dense network;

- computation of traffic flow, traffic density and traffic speed in any location of a considered surface network.

1.2   Research objectives

The research we present in this thesis is a part of the MIC (Modeling - Interoperability - Cooperation) project of the 'Smart Territories' program at IRT SYSTEM X (an Institute for Technological Research). The MIC project aims at (refering to `http://www.irt-systemx.fr/en/project/mic/`):

- develop technologies that improve multimodal travel, principally in urban areas, firstly by optimizing the means of transport (capacity, performance, and energy consumption) and, secondly, by providing supervision within transport systems, allowing optimal operational running within the day-to-day reality of needs and unpredictable factors;

- demonstrate the usability of the technological components developed through the use

of demonstrators representative of real-life situations, and evaluate the associated economic models;

- extend the capabilities of system development environments, to effectively implement a "systems of systems" dimension compliant with security of operation requirements;

- specify the open systems of systems architecture with regards to an attractive number of project models for the various players in transport systems;

- facilitate the analysis of alternatives, from both a "business" and "technical" angle, by constructing a modeling framework interlinked with these two aspects, allowing the description of different "structured" scenarios, and enabling their verification and comparison.

Within the MIC project, this Report comes up with solutions to efficiently reduce traffic congestion on large surface networks by means of Reactive Dynamic Traffic Management. In the sake of improving congestion management, our approaches consider the freeway networks and the underlying urban and rural networks in an integrated way. We develop a multi-scale model in response to traffic congestion issues on very large networks. In our study, we account intelligent demand responsive systems. We then integrate in the proposed multi-scale model an archetype transport model of an intelligent transportation system. This transport mode is coordinated - rather than isolated from - with the other transport modes of the multimodal system. Therefore, the thesis develops an archetype multimodal macroscopic transport model for large networks comprising a surface network, the transit lines and an automated system such as a railway intelligent transportation system. We propose a developing multi-scale model comprising three specific traffic flow models:

- microscopic transport model for an intelligent transportation system, in particular for a personal rapid transit system.

- model of multimodal traffic flow relying on main road links and public transport lines. This model consists of two coupled models of similar structures. They are the following: the GSOM (Generic Second Order Modeling [50]) family model (or a multiclass traffic flow model) and the dynamic model of transport based on users' activities (developed by Ma in [61]). The former model expresses a system of conservation equations on a graph. Its Lagrangian form is implemented. Afterwards, it is coupled with

the latter model which distinguishes the passenger flow and vehicle traffic (see [60] and the references therein).

- two-dimensional (or bi-dimensional) dynamic traffic flow model applied to very large surface networks. Given the fact that, road stretches in dense transport networks are very numerous, and it is impractical to collect data on each one of them, we provide a high level aggregation of the large and dense road networks. This consists on two approximations. The first is the approximation of the corresponding network domain of the large surface network by an anisotropic medium with preferred directions of propagation of the traffic flow. The second is the approximation of the traffic flow by a two-dimensional fluid flow. We take as a starting point the works on bi-dimensional models introduced in Saumtally [77].

The validation process of the developed multi-scale traffic flow model is supported by quasi-real data of a multimodal transportation system.

1.3   Conventions & Notations

We use some terms of transport mobility, traffic flow theory, partial differential equations and scientific computing that one may not be familiar with. Thus, here are some brief definitions listed in the table below.

PRT	personal rapid transit
MTF	macroscopic traffic flow
BTF	bi-dimensional traffic flow
DRS	demand responsive system
MHI	multiscale hybrid and integrated
FD	fundamental diagram
MFD	macroscopic fundamental diagram
NFD	network fundamental diagram

Table 1.1: List of abreviations

U	• defines an open and bounded subspace of $\mathbb{R}^d$, $d = 1, 2$
$\mathfrak{C}^0([\mathbb{R}^+ \times U])$	• set of continuous functions of two variables named t and x, with $t \in \mathbb{R}^+$ and $x \in U$
$\mathfrak{C}^1_c([\mathbb{R}^+ \times U])$	• set of continuously differentiable functions with compact support in $\mathbb{R}^+ \times U$
$\mathfrak{L}^\infty(Y)$	• set of infinitely integrable functions on the space Y

Table 1.2: Some mathematical sets

t	:	the time in the space $\mathbb{R}^+$
x	:	the position/location in the open and bounded space U
$\rho(t, x)$	:	traffic density at the time t and the position x
$\tilde{\rho}(t, x)$	:	traffic lineic density at the time t and the position x in a specific direction of flow propagation
$v(t, x)$	:	traffic speed at the time t and the position x
x^-	:	the position immediately upstream to the position x
x^+	:	the position immediately downstream to the position x
$\Delta_e(\rho(t, x^-), x^-)$	:	equilibrium traffic demand upstream to the position x at the time t
$\Sigma_e(\rho(t, x^+), x^+)$	:	equilibrium traffic supply downstream to the position x at the time t
$\Delta(\rho, x)$	:	traffic demand field at the position x
$\Sigma(\rho, x)$	:	traffic supply field at the position x
$Q_e(\rho, x)$	:	equilibrium traffic flow at the position x
$q(t, x)$	:	traffic flow at the time t and the position x
$\tilde{q}(t, x)$	:	traffic lineic flow at the time t and the position x in a specific direction of flow propagation
$QI(t, x)$	:	traffic Inflow at the time t to the location x
$QO(t, x)$	:	traffic Outflow at the time t from the location x

Table 1.3: Some notations and variables

1.4 Scientific Publications

Table 1.4 below lists all our publications that have been published until the compilation of this report. The table indicate the underlying mathematical models (PRT: personal rapid transit, DRS: demand responsive system, MTF: macroscopic traffic flow, BTF: bi-dimensional traffic flow, RDTA: reactive dynamic traffic assignment, MHI: multiscale and hybrid integrated), and their contributions to the specification or computation of the final integrated model.

Publication	Model	Major Contributions
[Sossoe 2016], ICSS'16, Poland	RDTA	• Ventilation of the traffic flow through the set of directional inflows and outflows of $2d$ traffic zones • Logit assignment of vehicles • Reactive assignment scheme which describes traffic variability in time
[Sossoe 2015b], TGF'15, Netherlands	BTF	• High aggregation of road links and intersections in two-dimensional traffic zones • Specific directions of propagation of traffic flows through traffic zones • Bi-dimensional flow estimation engine
[Sossoe 2015a], EWGT'15, Netherlands	PRT & DRS	• Time-dependent arrival of passengers at portals which define passengers' travel demands • SkyTran system supply optimization to respond to passengers' travel demands
[Sossoe 2014], ICNAAM'14, Greece	MTF	• Sections, intersections, and its capacities which define road network infrastructure and supply • Multiclass multilane FDs which define specific class traffic speeds equilibrium

Table 1.4: List of our publications.

1.5 Outline of this Report

This section provides the outline of this Report and briefly gives information about each chapter.

Chapter 2 presents an overview of the state-of-the-art of multimodal network mobility and specific traffic flow models derived from the traffic flow theory. In this chapter, we discuss the advantages and disadvantages of different traffic modeling approaches: both approaches used in macroscopic and two-dimensional traffic flow modeling. Furthermore, we discuss about macroscopic transport simulators as decision supports in the traffic flow management and controlling of large scale multimodal transport networks.

Chapter 3 is based on Saumtally *et al.* [78] and Sossoe and *et al.* [81]. It focuses on the methodology of the simplification of a surface network by a high level of aggregation of its links and intersections. It specifies the type of network for which this network simplification approach fits properly. The resulted traffic flow model predicts traffic dynamics of large anisotropic network from scarce transport data.

Chapter 4 is based on personal rapid transit transport models of the literature, the work of Sossoe and Lebacque [83], on Farhi *et al.* [18] and Sossoe and Lebacque [82]. On the one side, we study in Section 4.2 a specific system, the skyTran autonomous intelligent transportation system for mass transportation. This system is a Personal Rapid Transit (PRT for short) system. It is the better way to reach one location in no time. On the other side, since other traditional modes of transportation are available as services to mobility, we develop for the traffic prediction on a multimodal road transport network, in Section 4.4, a multiclass multilane macroscopic transport model. It comprises a system of conservation laws that govern traffic dynamics on road stretches and intersections. They take into account traffic interactions of vehicles, from different transport modes, moving on shared roads and dedicated roads.

Chapter 5 concerns multiscale coupling of different traffic flow models. We present traffic interactions between highways and secondary roads, and validate the approach by numerical test. This chapter highlights further interactions between different transport modes/forms of mobility used in a multimodal transportation system. This results in a multiscale traffic flow simulation model for large multimodal transportation system.

Chapter 6 is based on Sossoe and Lebacque [84]. It is related to traffic assignment especially the reactive dynamic traffic assignment of large surface networks.

Chapter 7 concludes this Report and gives some research directions for the future.

This page is intentionally left blank.

Chapter 2

Background and Related work

2.1   Introduction

This chapter provides an introductory to mobility in transport networks, to the traffic flow theory, dynamic traffic assignment and macroscopic transport simulators. It shall highlight traffic flow models and what is called the *reactive* dynamic traffic assignment. It shall also aid to respond to below issues which are still very much alive today. How should we model a multimodal transportation system ? How can we properly estimate traffic states of large and dense surface networks ? What are solutions to traffic breakdowns and traffic congestion in the big transport networks ?

Contents

Context

Technologies have been evolved considerably in industrialized cities. We note the emergence of different intelligent transportation systems and transport services. For instance there are the personal rapid transit system, the system of communication between vehicles and also between vehicle and its environment. There are also new uses of certain modes of transport. We note carpooling services, ride and share services, users' services provided by demand responsive systems, etc. In a multimodal transportation system which is equipped with such technologies along with these uses, how can we contribute in a very truthful intermodality between the different monomodal transportation systems ? The goal will be to get a fairly realistic model of traffic flow for large multimodal transport networks.

Organization of the chapter

We shall review the mobility in multimodal transport network, some traffic flow models and macroscopic transport simulators. We discuss about these in Sec. 2.2 and Sec. 2.3. We highlight the law of the minimum between the traffic supply and the traffic demand. It induces that the performed traffic demand in a network cannot be greater than the traffic supply itself. Traffic demand and supply are very correlated by this physical law. The so-called *macroscopic* and *bi-dimensional* traffic flow theories get our intention along the review. We introduce how so far the bi-dimensional traffic flow theory can help in routing strategies within large-scale surface networks. It is a parallel framework to that related to the macroscopic fundamental diagram which provides the relation between the number of vehicles and the network performance. One can apply traffic control on these both ways of the large networks modeling: the bi-dimensional modeling and the modeling by the macroscopic fundamental diagram or the network fundamental diagram. The objective is to overcome computational complexity of network-wide control using traditional control levels of links or vehicles. Besides, still in Sec. 2.2 (i) we discuss about the topology structure and the different layers of multimodal transport network. Further, (ii) we provide an overview of different methods to extract spatial structure of cities. That is to say the spatial distribution of the population in a city. It

helps to better understand and describe the mobility in the cities.

2.2 Mobility in multimodal transport network

Mobility is fundamental in big cities. People move, travel for infinite reasons. These movements or displacements are carried through available means of mobility and transport resources. Since there are different modes of transportation in industrialized cities, to move from one location to another location, one regularity take more than one mode of transportation in daily trips. These mobilities imply interactions of solicited modes of transportation. They give rise to traffic incidents, for instance traffic jams, traffic breakdowns, traffic accident and time delays. The variability of traffic is complex. It is more complex when different transport modes operating by separated systems are involved. Such a global transport system is called a *multimodal transportation system*. The word "multimodal" refers to the different transport modes, transport services, and traffic services available for the global system. Let us give in the next section a clear definition of a multimodal transport network with respect to two major aspects: the physical and the functional points of view.

Multimodal transport network

Definitions

There are many definitions to the multimodal transportation system, since a transportation system is too complex to have a clear and straightforward definition, as it depends on the perspective. A multimodal transportation system can be defined from the point of view of transport modes. A transportation system is described in term of its components associated with specific means of transportation and its services [64]. Main components of transportation system are the corresponding network, routes, intersections, junctions, stops, terminals, stations, hub stations. There are also control centers in the case of a public transportation system, a demand responsive transport system, a personal rapid transit system, an operating center for taxi services, etc. A transport network is a set of routes and intersections. A route is simply a single physical link between two locations. An intersection is a merge or diverge junction of several road sections. Other components are the hubs, stations, exchange nodes and terminals. They are the contact or exchange points where people may change from one mode of transportation to another within a multimodal transport network. The following summarizes what is a multimodal transport network/system.

a-/ A multimodal transport network is a collection of networks (or sub-systems), each network representing one mode of transportation. Each mode of the whole system comprises routes. Some of the latter bind up the separate networks (or the monomodal networks) by the connection points or transfer nodes [89].

b-/ Multimodal transportation system is the set of several modes of transportation, their operating systems with their offered transport services.

c-/ From the user point of view, multimodal transport network is as simple as a physical network in which people could travel from one location to another location throught at least two means of mobility [64].

d-/ Multimodal transportation system is transportation system that provides to users particularly transport services of different travel models. On the one side, such global system comprises public and private vehicle modes which are divided among the network levels such like urban/suburban, regional and national levels. The service levels are the mass transportation, responsive and/or sharing services, and the personal uses. The first are such like the metro, tram, train, and bus. The second are car-sharing, demand responsive transport, carpooling, car-rent. The latter are trips via its own cars and also carpooling. On the other side, physical networks comprise transport infrastructures for the all transport modes. Figure 2.1 depicts the vehicle modes, types of function and service levels of a multimodal transportation system.

In this report, we take into account both the physical and functional standpoints of the definition of a multimodal transportation system, regarding transport modes, their corresponding physical networks (meaning the traffic services) and the transport services.

Structure of multimodal transport network

We have seen that there are two categories of transport networks:

- transport services or network services, for instance the bus or train services;

- traffic services or physical networks such as roadways or railways.

The transport service is always related to a physical network. Main characteristics of any transport network from the user's point of view are travel costs and travel time. The latter

two are computed with respect to network characteristics and the variability of the traffic. Transfer links and transfer nodes are mandatory in a multimodal transport network. Combining private transport and public transport in a truly multimodal transport system offers opportunities to capitalize on the strengths of the different monomodal transport systems. The requirements for such a multimodal transportation system, however, are high. Users have to be aware of the possibility for changing vehicle modes and the related benefits. Thus, a high quality travel information is crucial. It shall come up from an advanced user information system. Transfers between transport modes, and the transport services should be seamless. It is appeared that a multimodal transport network can be approached by the supernetwork theory. Relations between networks could be identified by the physical transfer nodes, links, and hubs, or by a virtual transfer-network. Transfer nodes of a transfer network are nodes that connect different network modes to a larger network wherein the whole system shall operate differently compared to the separate systems. Let us give some details on the following.

(a) The traffic transfers. Using at least two modes, a traffic transfert is mandatory. That is done through a transfer node. Let us recall that a transfer is related to an inter-modal transfer.

(b) The network modes and transport services. They are closely related and at the same time have different meanings. A typical example of the usage of the term *mode* is in the mode choice model, in which the user's choice is between for instance cycling, taking a personal car or a public transport. In this context the term *mode* is usually associated with the vehicle used. However, in the case of a public transportation, the term *mode* is related to the service characteristics. It is not specifically related to types of vehicle such as the bus, tram, metro neither the train. Since multimodal travel is strongly related to transport services, the term *mode* is hence usually related to service modes. Further, in the case of common transport services, different types of transport services are distinguished, because of their different characteristics as their accessibility, speed, frequency, rates and vehicles used. Multimodal trip thus concerns transfers between different transport modes and the transport services used. Figure 2.1 depicts the classification of transport modes with function levels, network levels, and service levels.
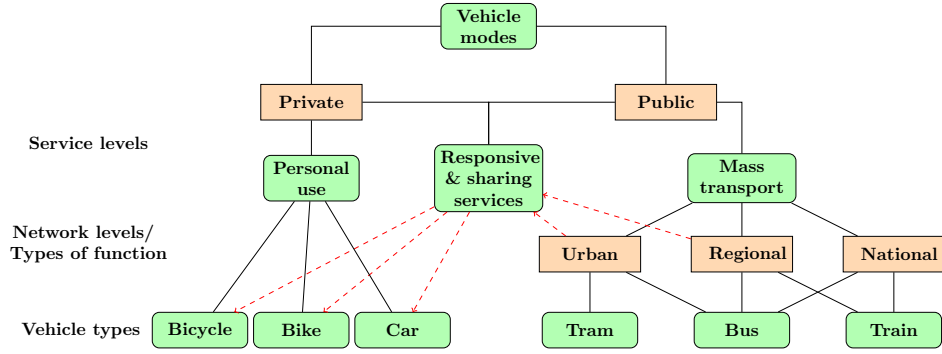
Figure 2.1: Classification of transport modes, related functions and service levels.

(c) The walking. Walking is nearly always part of a trip. Users walk from home to station, office to station and from many other locations to a station, in the hubs and also via the correspondences.

Modeling

In this subsection, we respond to the question: "How we should model properly multimodal transport network for an advanced traveler information of a multimodal transportation system". We know that transport networks modeling relies on the graph theory. Most common definition of the network is to regard it as a set of nodes together with a set of links; each link connects a pair of nodes. For public transport networks, this type of representation includes public transport lines. It results in a set of connected links, nodes and bus time tables (or bus schedules). This type of description is appropriate to transportation network modeling. It allows to describe all kinds of transportation networks found in practice. Let us denote by $G = (V, E)$ a directed multi-graph of a multimodal transport network. We assume that G has mixed weighted time-dependent and time-independent arcs. G is either a set of graphs: $G = \left(\bigcup_{\ell \in \Lambda} G_\ell \right) \cup G_b$. ℓ is the index of the network and Λ is the set of all the networks of the multimodal transport network. For $\ell \in \Lambda, G_\ell = (V_\ell, E_\ell)$ with V_ℓ the set of vertices (or nodes) of the graph G_ℓ and E_ℓ the set of its arcs. The whole transport system shall be model as a supernetwork with regard of its whole physical network and transport services. Figure 2.2 depicts the layers of a multimodal transport network, as well as the connections between the layers.
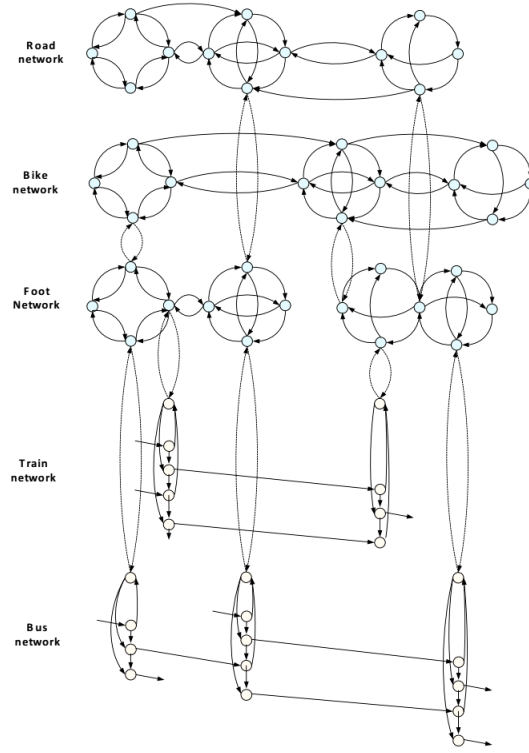
Figure 2.2: Representation of a multimodal transport network.

Mobility networks

Regarding any transportation system, it is relevant to have clear knowledge of existing forms of mobility related to the physical network. In the acquisition of transport data, one extract what it is called origins-destinations matrices. They represent the performed users' demands over the considered network. In reality, these matrices are time-dependent. Methods have been developed to extract from origin-destination matrices a spatial distribution of the population of cities. The spatial distribution determines major activities of cities concerned. In most cases, Origin-Destination (OD) matrices are classified into two types of flows: integrated flows (between residential and employment hotspots) and random flows, whose importance increases with the size of the network. Let us mention the "ICDR" method, developed by [58]. ICDR is the acronym for Integrated, Convergent, Divergent, Random. The method allows the extraction of a coarse-grained signature of mobility networks under the form of a 2×2 matrix that separates network flows into four categories (2.1).

Definition 2.1 (Coarse-grained models)**.** *Coarse-grained models are computational models that mimic the behavior of a complex system by breaking it down into simpler sub-*

components. The extent to which the system is broken down reflects the degree of granularity of the model in question.

In transportation field, a coarse-grained signature of mobility refers to one larger granularity of trajectories of displacements induced by users' mobility in the city. Such signature is obtained by analyzing for example users traffic data such as data on tickets validation from validators transport tickets. So a coarse-grained signature of mobility network gives a clear spatial distribution of users' displacements over the city whose network is considered.

The method ICDR takes into account all types of flows of networks, and is more general for the extraction of high level information of any weighted and directed graph. In that context, denoting by $\Lambda = \left(F_{ij}\right)_{i,j=1}^{n}$ an OD matrix, F_{ij} is the number of users living in the location i and commuting to the location j where they have their main and regular activities. For a given city network, the method reduces the OD matrix to a 2×2 matrix

$$\Lambda = \begin{pmatrix} I & D \\ C & R \end{pmatrix}. \tag{2.1}$$

The main variables I, C, D and R are defined as following.

$$I = \sum_{i=1...m, j=1...p} F_{ij} / \sum_{i,j=1...n} F_{ij}$$

is the proportion of Integrated flows going from residential to work hotspots.

$$C = \sum_{i=m+1...n, j=1...p} F_{ij} / \sum_{i,j=1...n} F_{ij}$$

is the proportion of Convergent flows going from random activity places to work hotspots.

$$D = \sum_{i=1...m, j=p+1...n} F_{ij} / \sum_{i,j=1...n} F_{ij}$$

is the proportion of Divergent flows going from residential hotspots to random activity places.

$$R = \sum_{i=m+1...n, j=p+1...n} F_{ij} / \sum_{i,j=1...n} F_{ij}$$

is the proportion of random flows that occur "at random" in the city. These random flows come from some places and are going to other places which both are not hotspots.
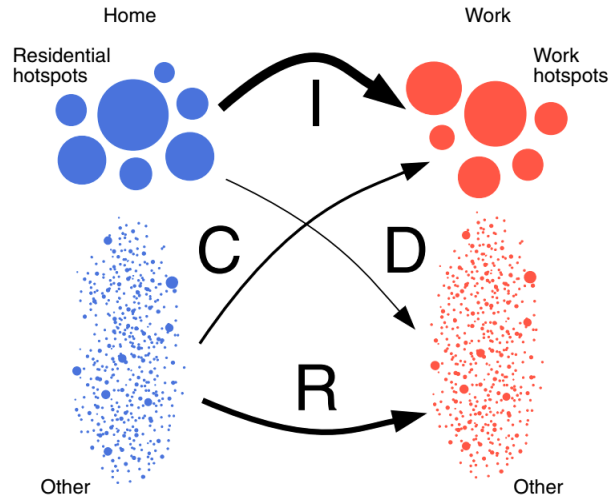
Figure 2.3: Illustration of the ICDR method - OD Matrix of city network falls down in a hotspots' classification.

Let us recall that the method decomposes the commuting flows in the city in four categories: the Integrated flows (I) from hotspot to hotspot, the Convergent flows (C) to hotspots, the Divergent flows (D) originating from hotspots and, finally the Random flows (R) which are neither starting nor ending at hotspots. For a city, from origin-destination matrices one computes the four types of flows. That gives the picture of the mobility structure in the city. The ICDR method comprises several steps. The first step relies on the identification of origin and destination hotspots. It can be performed with any reasonable method. The second step consists in aggregating the flows in four different types, depending whether they start from a hotspot or end to a hotspot or none of the above. This method shows that independently of the density threshold chosen to determine hotspots, the proportion of integrated flows (I) decreases with the city size, while the proportion of random flows (R) increases. When the size of the city increases, the largest impact relies on convergent flows (C) of the users that live in smaller residential areas (typically in the suburbs) and the commuting to important employment centers. The classification of cities based on the ICDR values highlights the relationship between the size of the urban population and its commuting structure.

Network planning

Many software and strategical processes have been developed encompassing topological design, network-synthesis, and network-realization. There are several microscopic models and macroscopic models or continuous models that have been developed so far in the literature

as tools devised for transport network planning. Algorithms of optimization are designed for networks supervision in the framework of traffic flow management and traffic controlling.

2.3   Continuum traffic models & Dynamic traffic assignment

Industrialized cities and countries mostly cope with traffic congestion and traffic incident. These are one of the major problem on the economic, social and societal front. We need to clearly understand what causes traffic congestion and traffic incidents. We need to know too how traffic operations work in order to be able to properly monitor and control traffic in any congested transport network. Infinite mobile jams often occur in dense networks. During the last fifty years and so far, research in traffic theory encompasses a rich set of mathematical and physical models. The models are often designed for specific networks according to required level-of-details. The models aim at:

- predict and estimate traffic states over different types of networks,

- calculate traffic indicators such as travel times,

- provide alternative paths or routes in case of traffic breakdowns and also when certain roads become inaccessible,

- ensure a greater safety and reduce multiple risks of traffic incidents, etc.

Many new trends of modeling and controlling emerged in the field of transportation networks modeling. They are used as decision tools for the traffic management, traffic controlling, traffic supervision, etc. In cases of networks traffic controlling, we note that specific physical/mathematical models are required according to requirements of governmental decisions makers, transport operators or transport planners. According to the level-of-details, needs and expected results, right models are appropriate. They are numerically and computationally handleable in specific tools for traffic flow management.

These assets help the decision makers for an optimized management of transport networks. Several scales of modeling exist. Each scale represents a particular aspect of what is modeling. Depending on desired level-of-details in the representation of traffic states, one uses one approach (one scale of representation) rather than the other. The main scales of traffic modeling range from microscopic, to mesoscopic, macroscopic and bi-dimensional. In

our research, we mainly dig on models of surface transport networks. In our review, we do not include microscopic models since we are more interesting on mathematical and physical models that represent the traffic flow of networks. We do not include possible interactions between vehicles and passengers within networks. The thesis concerns mostly macroscopic and bi-dimensional traffic flow models and dynamic traffic assignment deriving from related network loading models. We say mostly since we know that microscopic models are the limit of kinematic and macroscopic models.

To the best of author's knowledge, there is no available and reliable general multimodal model (or seamlessly integrated models and algorithms) for the traffic controlling that takes into account every available transport mode of a large-scale transportation system. We count several families of traffic flow models that describe vehicular dynamics given a certain traffic infrastructure and, if applicable, given additional routes choice information. The infrastructure comprises the considered road system in terms of topology (its geometry, characteristics, right-of-way laws, and traffic signaling available on it), road sections speed limits and capacities, and intersection properties, etc. Continuum traffic flow models are divided into mesoscopic/gas-kinetic traffic flow models and fluid-dynamical models also named macroscopic traffic flow models.

Continuum traffic flow modeling

In this Section, we discuss on principal macroscopic and two-dimensional traffic flow models introduced so far in the literature. We highlight their advantages and drawbacks according to expected results and the types of considered surface networks.

Among macroscopic models, we distinguish first-order models, second-order models, multi-class models, multi-lane models and stochastic models, all in a mathematical formalism and computer unit.

The major advantages of macroscopic models are their:

- flexible mathematical structures, and

- low number of parameters (compared to microscopic transport models).

The macroscopic models presented here are classified as hydrodynamic models regarding the fact that they are derived from an hydrodynamic approach. Field quantities (or macroscopic variables) are the density, the traffic flow and the traffic speed.

- The density $\rho(t, x)$ is the number of vehicles passing through the location x at the time t, for all $t \in$ T and for all $x \in$ X. T denotes the space of the time and X denotes the space of the location.

- The traffic flow $q(t, x)$ is the number of vehicles passing the location x at the time t, for all $(t, x) \in$ T $\times$ X.

- The traffic speed $v(t, x)$ is the velocity field of vehicles flow on the road at the location x and at the time t, for all $(t, x) \in$ T $\times$ X.

These physical quantities fields are assumed to be continuous (or at least piecewise continuous) functions with respect to the position space X and the time space T. The three functions q, ρ, v are related by the following continuity relationship (2.2).

$$q(t, x) = \rho(t, x) \times v(t, x) \quad \forall (t, x) \in \text{T} \times \text{X}. \tag{2.2}$$

This relationship defines, in macroscopic traffic models, the speed $v(t, x)$ in any position x and time t given the flow $q(t, x)$ and the density $\rho(t, x)$ at the position x and at the time t.

First-order traffic models

The motorway network is viewed as an oriented graph. Traffic models have been developed to simulate the dynamic aspects of the traffic flow. To do that, ones modeled the different elements constituting the network. Traffic dynamics, on both arcs and nodes, are hence studied and modeled. The main difficulties with modeling traffic on sections and intersections lie with choosing the correct definition of the boundary conditions.

Let us consider the macroscopic first order LWR (Lighthill-Whitham-Richards) model [57, 76]. It is a continuous traffic flow model that describes vehicles flow on a road stretch without intersection. The flow $q(t, x)$, the density $\rho(t, x)$ and the speed $v(t, x)$ are its key variables. These variables are solution of a system of relations-equation:

(i) The speed-concentration relation. The speed v is a function of ρ which shapes the so-called density-speed fundamental diagram.

(ii) The continuity equation $q = \rho v$ derived from an analogy between traffic flow and a one-dimensional compressible fluid.

(iii) The conservation law on the density and the flow, which results in an hyperbolic partial differential equation $\rho_t + q_x = s$, where t and x denote the time and the position variables, and s denotes the source term. s is a function of the time t and the position x.

Let us consider the section (a, b) with a the upstream node of the section and b its downstream node (see figure 2.4).

Figure 2.4: Boundary condition of a section.

Notations are the following.
- q_a is the in-flow at the node (a),
- q_b is the out-flow at the node (b),
- Δ_u is upstream demand,
- Ω_a is the link supply,
- Δ_b is the link demand,
- Ω_d is the downstream traffic supply.

The subscripts u and d mean downstream and upstream respectively.

The traffic road is described by a nonlinear hyperbolic continuum Equation (2.3) which expresses the conservation of vehicles flow and density:

$$\partial_t \rho(t,x) + \partial_x q(t,x) = 0 \quad \forall (t,x) \in \mathrm{T} \times \mathrm{X}. \tag{2.3}$$

This equation is completed by the law of the minimum between the link demand and the traffic supply, stated in [51], and the relation (2.2) above. The law of minimum implies that performing users' demands are constrained by traffic supplies. The demand and supply are respectively an increasing function and a decreasing function of the density. They are constrained by the network flow capacity which is the maximal supply of the network when the network is empty.

In [51], boundary conditions of a section are defined. They show for instance that

$$q_a = \min\left(\Delta_u, \Omega_a\right) \text{ and } q_b = \min\left(\Delta_b, \Omega_d\right) \tag{2.4}$$

Link-demand and traffic-supply for the LWR model The function minimum of the demand and the supply functions yields a fundamental diagram, depicted by the Figure 2.5. The function link demand at equilibrium is shown to be: $\Delta_e(\rho, x) = \max_{r \leq \rho} Q_e(r, x)$. Correspondingly, ones find the traffic supply at equilibrium being defined as follows: $\Sigma_e(\rho, x) = \max_{r \geq \rho} Q_e(r, x)$.

At the time t and at the position x, the local demand and the local supply are set to:

$$
\begin{aligned}
\Delta(t, x) &= \Delta_e\left(\rho(t, x^-), x^-\right) \\
\Sigma(t, x) &= \Sigma_e\left(\rho(t, x^+), x^+\right)
\end{aligned}
\tag{2.5}
$$

The formulation (2.6)

$$q(t, x) = \min\left(\Sigma(t, x), \Delta(t, x)\right) \tag{2.6}$$

represents the Fundamental Diagram (FD for short). (2.6) is still valid if the function $x \longmapsto Q_e(\rho, x)$ is piecewise continuous. This relation defines dynamics of traffic on motorways sections.

Properties of LWR models that one can mention are characteristics, shock-waves and rarefaction waves. They take into account the acceleration and the deceleration of vehicles on road sections. They lead to LWR bounded-acceleration model and other related traffic flow models.
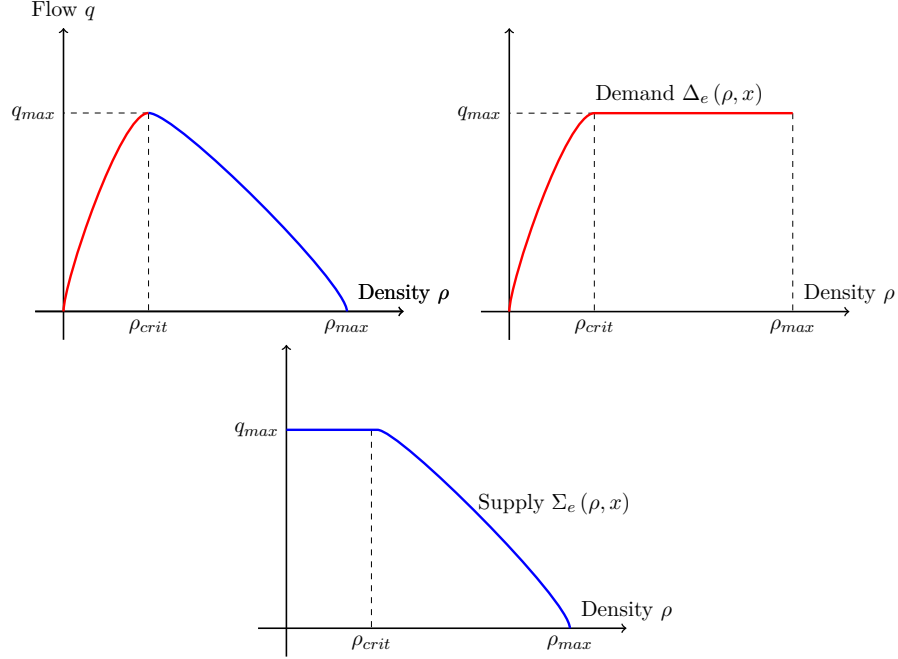
Figure 2.5: The fundamental diagram $q = \min(\Sigma, \Delta)$, the link demand and the link supply functions (respectively from the left to right to the bottom).

Σ_e denotes the traffic supply at equilibrium (drawn with a red line) and Δ_e denotes the link demand at equilibrium (drawn with a blue line).

The LWR models have a crucial disadvantage: they do not take into account the driver attributes such as the inter-vehicular distance between a leader vehicle and its follower vehicle. The inter-vehicular distance increases with the velocity. The LWR models are nonetheless more suitable for freeway traffic as explained by [88]. Among them, we note a systematic methodology of data fitted first-order traffic models construction using an historic data collection of the fundamental diagram. It is introduced by [17]. The methodology allows to treat the flow per section and lane. The research efforts around the LWR models has led to the so-called second-order traffic flow models.

Multi-attribute models

Several different first-order traffic flow models have been developed. The differences between them derive from the very definition of their fundamental diagram. Most of them are designed at the mesoscopic and macroscopic scales. Multi-class models of [5, 37, 39] and multi-lane models of authors [69, 44, 18, 82] are derived from this standard model. An other type of model of a higher order is classified as attribute model. It is the GSOM model [50, 53]. We review it in Section 2.3 in the sequel.

Multi-attribute models describe traffic interactions such as

- overtaking lanes interactions,

- interactions between different classes of vehicles,

- interactions between different transportation vehicles modes that shared same physical road lanes or roads.

The notion of multi-class refers to the classe of users as passengers or vehicles (such as the personal car, the bus for mass transportation, the car for specific use, and/or the different types of transport services, etc). It often raises the issue of using the right transport model, or technology and strategies to optimize traffic interactions between transport modes, and regularize access on motorways. On the one hand, depending on the type of the network and its characteristics, and on the other hand with respect to purposes of the traffic controlling a right model does not easy to build.

We see that the multi-class models developped by [5] take into account the behaviors of different type of vehicles (cars, trucks, buses, etc.) and drivers. They are designed for single lane traffic and are described by a nonlinear hyperbolic system of three conservation laws. They introduce a function that describes the difference between the velocity and some equilibrium velocity where they take into account the length of cars. The model is written via a system. The authors of multi-class models [5] introduce a grid (or cell) in time and space and prove the convergence of the Godunov scheme to a weak entropy solution to the initial value problem, as the step-size of space and of time tend to 0 with a fixed ratio satisfying the CFL (Couran–Friedrichs–Lewy) condition. They compute the solution in every cell to obtain an approximation of the flow with piecewise-constant initial data.

Gas-kinetic models

The gas-kinetic traffic flow models are based on descriptions of the dynamics of the phase-space (or time-location) density, that is, the dynamics of the speed distribution functions of vehicles in the traffic flow. Given the knowledge of the phase profile of density, one can determine the macroscopic traffic variables such as density, mean speed, or flow rate, by means of the method of moments.

These models have been developed starting from the works presented in Prigogine and Herman (1971) [75] by analogy with the kinetic theory of gases of Boltzmann.

This section mainly discusses the model of Prigogine and Herman (1971) [75]. The model assumes that the dynamic changes of the so called phase-space density (PSD for short) function (denoted by $\rho(x, v, t)$ where x is the location, v the traffic speed and t the time) are caused by a number of processes which are described in the following equation:

$$\frac{\partial \rho}{\partial t} + \underbrace{v \frac{\partial \rho}{\partial x}}_{\text{convection}} = \underbrace{\left(\frac{\partial \rho}{\partial t}\right)_{int}}_{\text{interaction}} + \underbrace{\left(\frac{\partial \rho}{\partial t}\right)_{rel}}_{\text{relaxation}} \tag{2.7}$$

The phase-space density function is interpreted as follows: "at the instant time t, the expected number of vehicles present at a small cell $[x, x + dx]$ driving with the speed v in the region $[v, v + dv]$ is equal to $\rho(x, v, t)dxdv$". Based on the conservation law, the equation for the dynamics of $\rho(x, v, t)$ can be found.

The left hand side of Equation (2.7) describes the changes of the phase-space density due to the motion of vehicles along the road, while the right hand side describes the changes of the phase-space density due to events such as deceleration or relaxation. The model consists of convection, interaction and relaxation, which are described in detail below:

- the *convection* term describes the continuous change of the PSD due to the inflow into and outflow from a small cell $[x, x + dx]$ within the time period $[t, t + dt]$.

- the *relaxation* term reflects the continuous change of the phase-space density due to the tendency of drivers to relax to the desired speed distribution.

- the *interaction* term describes the discontinuous change of the phase-space density due to the interaction between fast and slow vehicles. When a faster vehicle catches up with a slower one, it has to slow down to avoid a collision.

Interaction process In the model of Prigogine and Herman (1971), it is assumed that when a faster vehicle driving with speed v catches up with a slower one driving with speed w ($w < v$), the former either slows down to the speed of the latter or overtakes in order to avoid a collision. To determine the interaction term in equation (2.7), the following assumptions are used:

- If the faster vehicle overtakes, it does not change its speed.

- The slower vehicle is not influenced by the vehicle behind.

- The vehicles are considered 'points' (the length of vehicles is neglected).

- The fast vehicle slows down instantaneously.

- The vehicles are uncorrelated (vehicular chaos).

- Interactions affecting more than two vehicles are neglected.

Based on these assumptions, the interaction term in equation (2.7) is determined as follows:

$$\left(\frac{\partial \rho}{\partial t}\right)_{int} = (1-p)\int_v^\infty (w-v)f(x,t,v,w)dw - (1-p)\int_0^v (v-w)f(x,t,v,w)dw. \quad (2.8)$$

In equation (2.8), p denotes the probability for overtaking; $f(x,t,v,w)$ is the pair-distribution function of density. The assumption of vehicular chaos means that the correlation between vehicles is neglected. That is, the pair-distribution function can be decomposed as follows:

$$f(x,t,v,w) = \rho(x,v,t)\rho(x,w,t) \quad (2.9)$$

By substituting equation (2.9) into equation (2.8) the interaction term is reduced to:

$$\begin{aligned}\left(\frac{\partial \rho}{\partial t}\right)_{int} &= (1-p)\rho(x,v,t)\int_v^\infty |w-v|\rho(x,w,t)dw - \\ &\quad (1-p)\rho(x,v,t)\int_0^v |w-v|\rho(x,w,t)dw.\end{aligned} \quad (2.10)$$

Equation (2.10) reflects the fact that faster vehicles with speed w interact with slower vehicles with speed v at a rate $|wv|\rho(x,v,t)\rho(x,w,t)$, describing how often vehicles with speed w and v encounter at location x and time instant t. If the faster vehicle can not overtake, it decelerates to the speed of the slower vehicle. This deceleration process increases the phase-space density $\rho(x,v,t)$ accordingly (the plus term of the right hand side). When a vehicle with speed v catches up with a slower vehicle with speed w, if the faster vehicle is unable to overtake, it decelerates to the speed w. This process decreases the phase-space density $\rho(x,v,t)$ (the minus term of the right hand side).

Relaxation process Prigogine and Herman (1971) proposed the relaxation term in equation (2.7) as follows:

$$\left(\frac{\partial \rho}{\partial t}\right)_{rel} = -\frac{\partial}{\partial t}\left(\rho\frac{V_{max}(v|x,t)-v}{\tau}\right) \quad (2.11)$$

In equation (2.11), $V_{max}(v|x,t)$ denotes the desired speed distribution; τ is the density-dependent relaxation time. With this model, Prigogine and Herman (1971) found that the

transition from the free to the congested traffic state occurs when the density is higher than a certain critical value. This congested state is characterized by the appearance of a second maximum of the speed distribution at $v = 0$. That means, there are some vehicles still moving, while the others are at standstill. Since the works of [72], an extra degree of freedom has been added, by introducing the joint distribution of speed and desired speed of users. Many relevant researchs based on gas-kinetic approach can be cited such like [72, 73, 68, 29, 30, 92, 47, 33, 34, 35, 85, 69, 39]. That is as far as we had go because we do not use the gas-kinetic modeling approach for our current developments.

GSOM traffic flow models

The traffic flow models such as the Payne-Whitham model, the ARZ model [4], the GSOM family models [50, 53] (and generalizations thereof) are models of second order. They are all characterized as (GSOM) generic second order modeling family models. They come up with precisions on traffic waves such like shock waves, rarefactions and phantom traffic jams named jamitons. In the sequel, we recall the GSOM traffic flow models with driver specific-attributes. We give some examples of second order traffic flow models.

Structure of GSOM models   GSOM traffic flow family models combines the LWR model with dynamics of driver-specific attributes and is expressed as a system of conservation laws. It is stated as

$$
\left|
\begin{aligned}
&\partial_t \rho + \partial_x (\rho v) = 0 \\
&\partial_t (\rho I) + \partial_x (\rho v I) = \rho \varphi(I) \\
&v = \mathscr{I}(\rho, I)
\end{aligned}
\right.
\tag{2.12}
$$

with ρ the density as usual, v the speed, t the time, x the position, and I the driver-specific attribute. The first equation of (2.12) expresses the conservation of vehicles. The second equation represents dynamics of the driver attribute I. The third equation states the speed-density fundamental diagram which depends on the driver-specific attribute I. The attribute I can be a vector, and, depending on the model it can be related to an aspect of the traffic, the network or its infrastructure or further the mode of transport involved. The possible attributes fall down to the following.

1. The type of vehicle or the modal attribute. The modal attribute is typically the mode of transportation that users take during their trips. It can be therefore a taxi, or a demand responsive transport, or a bus, a private car used for carpooling or for ride-

and-share services. This attribute also could be the motorization as an electrical vehicle deployed for example in a car-sharing system. We note for instance the Autolib system, implemented in the city of Paris, France.

2. The driver attribute related to origin-destination. It is just simply called the driver destination. It is relevant when conducting a (dynamic) traffic flow assignment or evaluating traffic volumes per destination. This attribute is pertinent in multi-class traffic flow model performed for the simulation of multimodal transportation systems. The driver attribute refers also to route choice and the driver behavior itself along the routes taken during a trip.

3. The lane attribute. Mostly Logit lane assignment models or multi-lane traffic flow models are governed by a system of conservation laws with source terms. The source terms capture the change of traffic volumes between lanes of the road section. It is calculated or predicted based on the probability of vehicles for changing lane according to the transport utility, the mission of the vehicles, the destination. The list is not exhaustive. It is the issue of lane choice. The lane choice is furthermore responsive to the congestion on a target lane compared to traffic states on neighboring lanes. Besides, certain lanes can be dedicated to specific category of vehicles. These lanes are called segregated lanes or dedicated lanes. For instance it is the case of buses for mass transportation along dedicated traffic lines. We notice the taxi mode for individual (or sometimes collective) services. Most of the time, this works within a demand responsive operational system.

4. The traffic attribute. Because of the variability of the traffic on the one side, and the perspective of the transport simulation model on the other side, it is necessary to model and simulate the traffic accounting on stochastic perturbations. This type of pertubations refers to the traffic attribute. Further, there exists other traffic attribute related to the type of the vehicle engine. Vehicles are either equipped with a hot engine or with a cold engine. Particularly, this type of traffic attribute permits to estimate, based on traffic flow models, the volume of the emission of pollutants. A third example of the traffic attribute relies on the traffc model with a relaxation towards the norm.

Therefore, we see that GSOM family models are perfect match for modeling multimodal

transportation system by combining different driver-specific attributes.

Some examples of GSOM models

1. The LWR model itself of course is a GSOM model (with no driver-specific attribute).

2. The Aw-Rascle model introduced in [4] and successively refined in several papers, (see for instance [3, 5, 21, 22, 23, 45, 31, 67, 79] and the references therein) is a GSOM model too. We recall in the following the system of equations that states the dynamics of vehicles, modeled by the AR model.

   We have:

$$
\begin{cases}
\partial_t \rho + \partial_x[\rho v(\rho, y)] = 0 \\
\partial_t \rho + \partial_x[\rho v(\rho, y)] = 0
\end{cases}
\quad \text{with} \quad v(\rho, y) = \frac{y}{\rho} - p(\rho) \qquad (2.13)
$$

   where p is the traffic pressure which depends on the density ρ.

   The general form of the model is the ARZ model. It is a GSOM model with attribute $I = v - V_e(\rho)$, where $V_e(\rho)$ expresses an "average" fundamental diagram around which the fundamental diagram $v = V_e(\rho) + I$ tends to. The "average" fundamental diagram, $V_e(\rho)$, evokes a fundamental diagram of equilibrium, depicts by Figure 2.6.
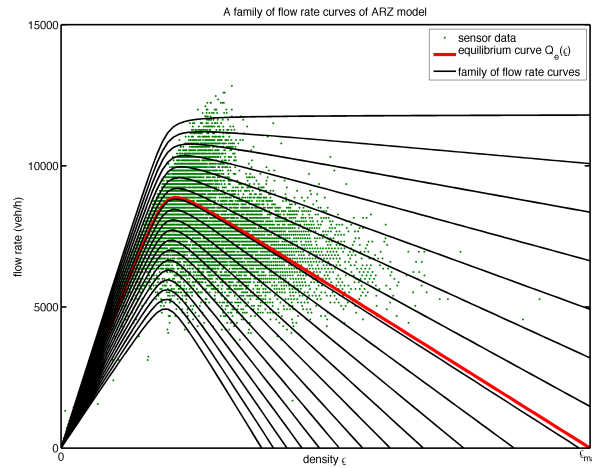
Figure 2.6: Flow rate curves of ARZ model.

3. Multi-commodity GSOM models. Here it is assumed that different drivers may have different speeds at a same traffic density. It leads to different density-speed fundamentals diagrams. Drivers speeds, however may be different even at the same density, they are limited by a maximal speed that no driver exceeds.

4. The Colombo 1—phase model.

5. The stochastic GSOM model.

6. The multi-lane impact model of [46].

7. Various models with eulerian source terms (such as (SMMR 09)), including higher order traffic flow models such as (ZWD 09).

Supply and demand formulations of GSOM family models   In case of a higher order traffic flow model, the fundamental diagram depends on the driver specific attribute I under the following properties:

1. $x \longmapsto Q_e(\rho, I, x)$ is a piecewise continuous function.

2. The function $\rho, I \longmapsto Q_e(\rho, I)$ is piecewise continuously differentiable.

Kinematic waves   There are two (2) kinematic waves of the density: the velocity of characteristics $\partial_\rho Q_e$ and the fundamental diagram FD $\rho \longmapsto Q_e(\rho, I, x)$. The attribute I is continuous when traversing a shock wave.

Waves of attribute of contact discontinuity   The velocity of waves of the attribute I, $V_e(\rho, I, x)$ by definition is set to be: $V_e(\rho, I, x) \stackrel{def}{=} \dfrac{Q_e}{\rho}$. It is shown that the velocity of waves is always greater than or equal to the velocity of kinematic waves. The former is continuous when traversing a contact discontinuity.

Riemann problem   To compute numerically the conservation law, the network domain is discretized in cells, and the time space in time-steps. The calculation of flow crossing every cells lead to the Riemann problem. Such situation is represented in the figure 2.7.
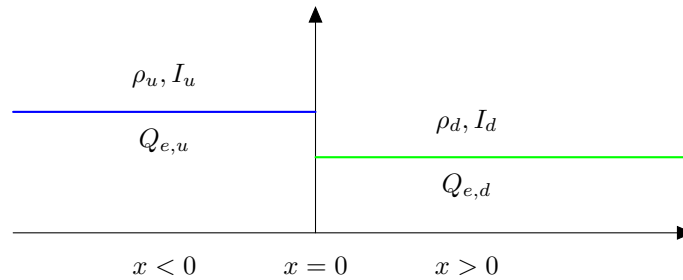
Figure 2.7: Riemann problem with the attribute I.

The driver-specific attribute fundamental diagram $Q_e(\rho, I, x)$ is set to be:

$$Q_e(\rho, I, x) = \begin{cases} Q_{e,u}(\rho, I) & \text{if } x < 0 \\ Q_{e,d}(\rho, I) & \text{if } x > 0 \end{cases} \tag{2.14}$$

At the downstream, the velocity is: $v_d = V_{e,d}(\rho_d, I_d)$. FDs at upstream and downstream are depicted by the below figure 2.8.
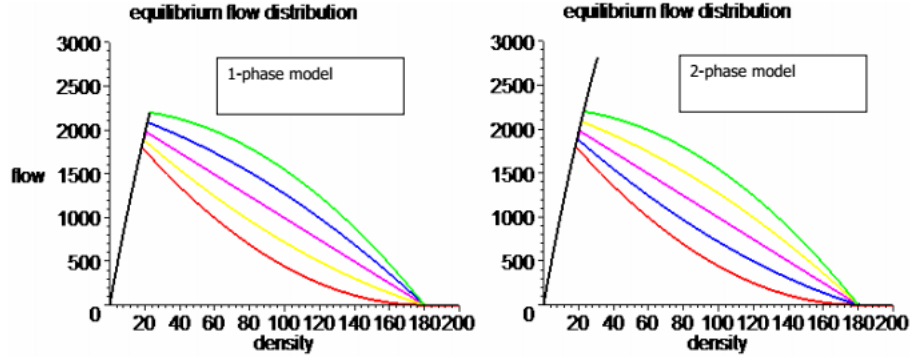
Figure 2.8: Colombo 1-phase and 2-phase fundamentals diagrams.

Since FD depends on I, and that $(\rho, I) \longmapsto Q_e(\rho, I)$ is assumed to be piecewise continuous differentiable, it is proved that the discontinuity of the variable I moves at the traffic speed, which is in this case the speed at downstream v_d. The calculation of the density, denoted by ρ_m at the discontinuity point is the solution of the following equation (2.15).

$$V_{e,d}(\rho_m, I_d) = v_d \tag{2.15}$$

The variable density ρ_m is pointed out in the the figure 2.9.
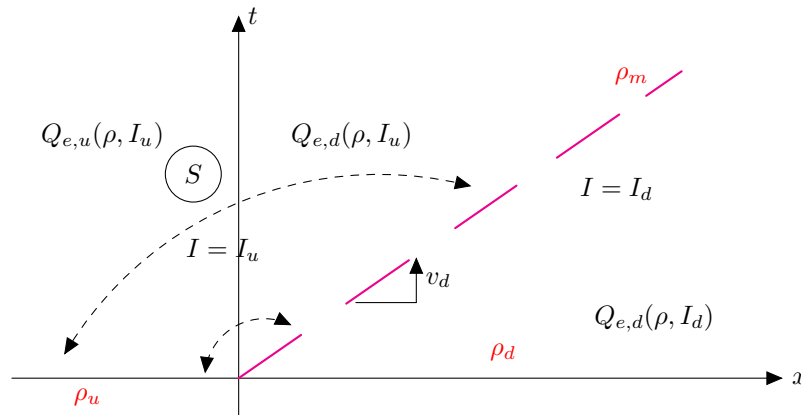
Figure 2.9: Riemann problem for the density at the discontinuity contact in (x, t)-plan.

The function $\rho \longmapsto V_{e,d}(\rho_m, I_d)$ is continuous and bijective function. Therefore, its inverse function $V_{e,d}^{-1}(.,.)$ exists. One has:

$$\rho_m \quad = V_{e,d}^{-1}(v_d, I_u) = V_{e,d}^{-1}\left(V_{e,d}(\rho_m, I_d), I_u\right) \tag{2.16}$$

Hence the flow at the origin q_0 of the link can be calculate simply, after compute the demand and the supply:

$$\left[\begin{array}{l} \Delta_u = \Delta_{e,u}(\rho_u, I_u) \\[2mm] \Sigma_d = \Sigma_{e,u}(\rho_m, I_u) = \Sigma_{e,u}\left[V_{e,d}^{-1}\left(V_{e,d}(\rho_m, I_d), I_u\right), I_u\right] \end{array} \right. \tag{2.17}$$

Whence, $q_0 = \min(\delta_u, \Sigma_d)$. To close the section on GSOM models, let us now give properly relations about driver-specific demand and supply, regarding the Riemann problem we study above. At the equilibrium, similarly in the LWR model, the link-demand and the traffic-supply are respectively defined as

$$\left[\begin{array}{l} \Delta_e(\rho, I, x) = \max_{r \leq \rho} Q_e(r, I, x) \\[2mm] \Sigma_e(\rho, I, x) = \max_{r \geq \rho} Q_e(r, I, x) \end{array} \right. \tag{2.18}$$

The local demand and local supply are then derived. One has:

$$\left[\begin{array}{l} \Delta(t, x) = \Delta_e\left(\rho(t, x^-), I(t, x^-), x^-\right) \\[2mm] \Sigma(t, x) = \Sigma_e^\star\left[\rho(t, x^+), I(t, x^+), I(t, x^-)\right] \end{array} \right. \tag{2.19}$$

with

$$\Sigma_e^\star\left[\rho(t, x^+), I(t, x^+), I(t, x^-)\right] \overset{def}{=}$$
$$\Sigma_e\left[Ve^{-1}\left(V_e\left(\rho(t, x^+), I(t, x^+), x^+\right), I(t, x^-), x^+\right), I(t, x^+), x^+\right]$$

By applying the law of the minimum, one obtains the flow at the position x and at the time t.

$$q(t, x) = \min\left[\Delta(t, x), \Sigma(t, x)\right] \tag{2.20}$$

Inhomogeneous Riemann problems and boundary conditions are properly solved with the GSOM family models. Therefore they capture in details shock-waves or rarefaction fans occurred during breakdowns and traffic congestion.

On one hand, they enable a good estimation of traffic densities, traffic flows, cumulative flows of roads networks with respect of driver-specific attribute. On the other hand, higher

order macroscopic traffic flow models require many traffic count locations and more significant traffic data. Therefore applied to very large networks, high order models may lead to cumbersome computations and computer complexities in data assimilation and calculation of links flows.

Junction traffic models

Concerning modeling of network nodes, one distinguishes single and multiple nodes. Multiples nodes are junction or intersection of nodes. A junction defines merge nodes or else diverge nodes while intersection has a more general configuration with many incoming and outgoing links, as in Figure 2.10. One may refer to [28] and [9] for modeling approaches of a complex urban road intersections.
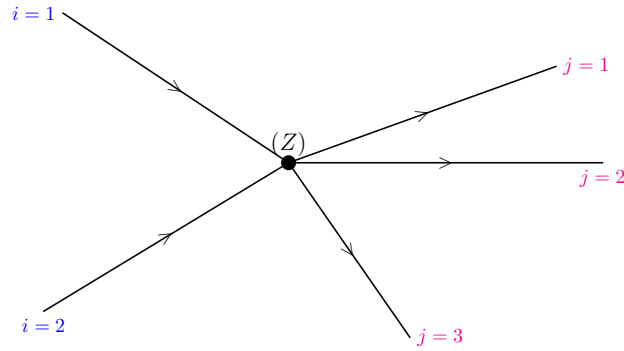
Figure 2.10: A general intersection with I-ingoing links indexed by $i = 1, 2, \cdots, I$ and J-outgoing links indexed by $j = 1, 2, \cdots, J$.

The min-formula of the demand and supply (which yields to the fundamental diagram and then to the definition of flow rate which really passes through) reflects the self-evident constraint that local traffic flow is bounded by:

- the flow that can be dismissed from the immediate upstream location, and

- the flow that can be absorbed by the immediately downstream location.

Three main principles are applied to an intersection:

- every upstream link provides a demand equal to its greatest possible inflow into the intersection,

- every downstream link provides a supply equal to the greatest possible outflow it accepts from the intersection, and

- the conservation of vehicles.

It is also applied to the intersection principle of local flow maximization subject to all phenomenological constraints. Indeed, one notices the statement of drivers' ride impulse which is equivalently expressed by "Drive as fast as you can and stop only if you have to". [9] defines a class of a node model that maximizes a concave function of the flow. It comprises the models of [32] and [7]. The study of dynamics of flow through node or intersection yields to an optimization problem: the maximization of the inflow at the intersection under constraints and principles. One notices the following:

- $\forall i, j, \ 0 \leq \gamma_{ij} \leq 1$ where γ_{ij} is the turning fractions from upstream (incoming) link (i) to downstream (outgoing) link (j). and $\forall j, \ \sum_{i=1}^{I} \gamma_{ij} = 1$.

- the inflow is superiorly bounded by the link-demand.

- the outflow is superiorly bounded by the traffic-supply.

- the flow rate satisfies the invariance principle. The invariance principle is the also refered to the consistency principle. It states that traffic waves originating from a node travel in the right directon (with negative speed at upstream and positive speed at downstream).

- the flow is conserved: $\forall j, \ q_j = \sum_{i=1}^{I} \gamma_{ij} q_i$.

- the flow rate satisfies a supply constraint interaction rule.

- the flow rate satisfies node supply constraints.

The conservation of vehicles within the node and the compliance with turning fractions requires that inflows and outflows do not exceed respectively link-demands and traffic-supplies. The invariance principle also states that the throughput does not change:

- when the link-demand on an incoming link (i) at upstream of the node (Z), tends to the flow capacity at downstream of any outgoing link (j);

- when the traffic-supply at downstream of the node (Z) of a link (j), tends to the flow capacity of the same link (j);

- with respect to the node supply constraints, which are data specific to the intersection (or the node), arising from signaling and/or conflicts inside the node itself. It is seen that such constraint is not easy to compute and it complicate substantially the intersection modeling.

Afterwards, Flottërod et *al.* [19] have found a specification of node supply constraints. They developed reliable algorithms for intersection traffic simulation.

LWR intersection model   Let us mention that the LWR model is a GSOM model without driver-specific attribute. It does not modify the fundamental diagram such we see it above, at the beginning of the sub-subsection 2.3. In the next paragraph, we discuss about intersection model with driver-specific attribute which modify the fundamental diagram.

The principle of the LWR intersection model concerns the outflow q_i and the inflow r_j, for $i = 1, \cdots, I$, $j = 1, \cdots, J$, and their dynamics at intersection. In, it is shown that there exist concave increasing functions Φ_i and Ψ_j such that the dynamics of vehicles at intersection reflects an optimization of

$$\max_{(q_i)_i, (r_j)_j} \left(\sum_i \Phi_i(q_i) + \sum_j \Psi_j(r_j) \right) \tag{2.21}$$

This objective function has following constraints.

i/ At the node, there is conservation of flow: $r_j = \sum_i \gamma_{ij} q_i$ at the entry of the link (j). $\left(\gamma_{ij} \right)_{i,j}$ are directional coefficients (also named turning movements) within the intersection (Z). These coefficients can be set by a static assignment or could be time-depending in case of a dynamic assignment applied to the LWR model for transport simulation.

ii/ At the entry of the link (j), the inflow r_j is constrained as follows. $0 \leqslant r_j \leqslant \sigma_j$, with σ_j the supply of the link (j).

iii/ Symmetrically, at the exit of the link (i), the outflow q_i is such that $0 \leqslant q_i \leqslant \delta_i$, with δ_i the (i)-link-demand.

The function Φ_i corresponds to the supply of the intersection in the direction (i), for each $i \in I$. Respectively, the function Ψ_j corresponds to the demand of the intersection in the direction (j), for each $j \in J$.

GSOM intersection model   There is attribute I to include in the LWR intersection model for corresponding to the GSOM intersection theory. The fundamental diagram of GSOM model is modified compared to fundamental diagram of LWR model. Demand and supply depend on the attribute I. It is found that the demand σ_j in the direction (j) is equal to $\sum_j^\star \left(\rho_j, I_j, I_j^\star \right)$. ρ_j is the density at the entry of the intersection from direction (j), and I_j is the attribute in the direction (j). Regarding $I_j^\star$, it expresses the intersection attribute of the traffic passing through the intersection and that goes to the direction (j).

$$\forall j \in J,\ I_j^\star = \frac{\sum_{i \in I} \gamma_{ij} q_i I_i}{r_j}.$$ (2.22)

The calculation of $I_j^\star$ is difficult because its depends of unknowns q_i and r_j, while σ_j depends on q_i and r_j; the former being dependent of σ_j. It is a problem of fixed-point solvable via specific fixed-point algorithms. This is not the subject of the thesis. It will not address in this manuscript. Besides, let us mention that to address the general intersection of the GSOM one shall use a buffer which is not also discuss in the thesis.

Two-dimensional traffic models

These models are simplified models and they concern very big and dense anisotropic networks. [93] deals with networks of several highly compact central business districts and provides traffic flow model derived from continuum approximation of network flow with variable users transport demands. The works of [74, 77, 81] are of the order of two-dimensional modeling, and they are relevant by reducing computation efforts.

Towards development of dynamic two-dimensional traffic model, Saumtally used the fact that, at any point P of coordinates (a, b) of the considered network area, local conservations of vehicles are unavoidable. This is expressed by Equation (2.23).

$$\forall j,\ \forall P(a, b)\ q_j(a, b) = \sum_{i=1}^{4} \gamma_{ij}(a, b) q_i(a, b).$$ (2.23)

That is the local conservation of the traffic per direction of propagation taking into account percentages of turning movements. $\gamma_{ij}(a, b)$ is the turning rate of flow that going from the direction (i) to the direction (j). It is therefore a traffic model at intersections.

Particularly, let us state the traffic two-dimensional model introduced in [78]. They authors provide a global conservation equation (2.25) in the elementary cells of the concerned net-

work area. The governing system of the model is the following.

$$\begin{cases} \partial_t \rho_1 + \partial_x f_1 + \partial_y \left(\dfrac{f_2\gamma_{21} - f_4\gamma_{41}}{2} + \dfrac{\lambda_2}{\lambda_1}\dfrac{f_1\gamma_{12} - f_1\gamma_{14}}{2} \right) = 0 \\[3mm] \partial_t \rho_2 + \partial_x \left(\dfrac{f_1\gamma_{12} - f_3\gamma_{32}}{2} + \dfrac{\lambda_1}{\lambda_2}\dfrac{f_2\gamma_{21} - f_2\gamma_{23}}{2} \right) + \partial_y f_2 = 0 \\[3mm] \partial_t \rho_3 + \partial_x(-f_3) + \partial_y \left(\dfrac{f_2\gamma_{23} - f_4\gamma_{43}}{2} + \dfrac{\lambda_2}{\lambda_1}\dfrac{f_3\gamma_{32} - f_3\gamma_{34}}{2} \right) = 0 \\[3mm] \partial_t \rho_4 + \partial_x \left(\dfrac{f_1\gamma_{14} - f_3\gamma_{34}}{2} + \dfrac{\lambda_1}{\lambda_2}\dfrac{f_4\gamma_{41} - f_4\gamma_{43}}{2} \right) + \partial_y(-f_4) = 0 \end{cases} \tag{2.24}$$

That is a system of 4 variables which are density per direction of propagation (i), $i \in \{1, 2, 3, 4\}$ since it is assumed that at any point of the network area there is 4 possible directions for vehicles in their displacement.

The variable the total density is set to $\rho = \rho_1 + \rho_2 + \rho_3 + \rho_4$. It is easily showed that ρ verifies the simple conservation equation (2.25).

$$\partial_t \rho + \partial_x f_1 + \partial_x \left(f_1 - f_3 + \frac{1}{2}\left[1 + \frac{\lambda_1}{\lambda_2} \right][(1 - \gamma_{11})f_1 - (1 - \gamma_{33})f_3] \right)$$
$$+ \partial_y \left(f_2 - f_4 + \frac{1}{2}\left[1 + \frac{\lambda_2}{\lambda_1} \right][(1 - \gamma_{22})f_2 - (1 - \gamma_{44})f_4] \right) = 0. \tag{2.25}$$

This two-dimensional model is a static model. It is however right for the prediction of average displacements of vehicles over network, without properly looking on details of vehicles' dynamics. The results extracted are depicted by the Figure 2.11. Let us recall that the equation (2.25) reduces to equation (2.26) in the particular case $\lambda_1 = \lambda_2$.

$$\partial_t \rho + \partial_x \Big((2 - \gamma_{11})f_1 - (2 - \gamma_{33})f_3 \Big) + \partial_y \Big((2 - \gamma_{22})f_2 - (2 - \gamma_{44})f_4 \Big) = 0. \tag{2.26}$$
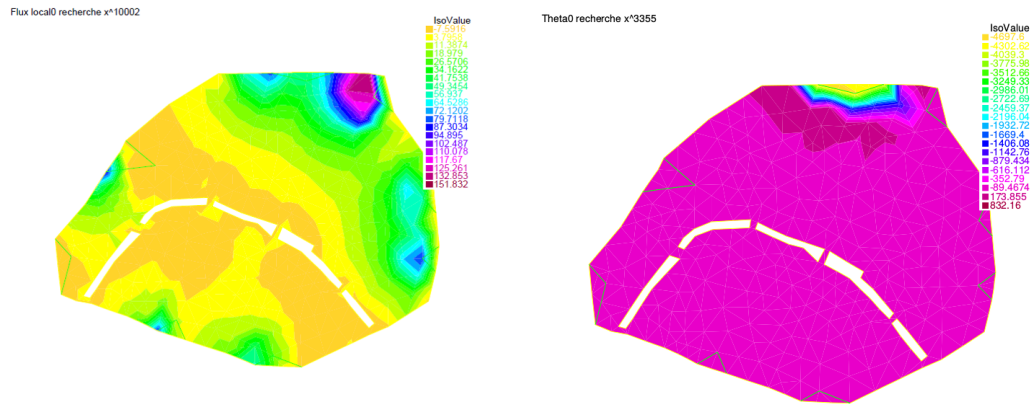
Figure 2.11: At the left, traffic load from West to East. The traffic load increases as the demand to the destinations increases. Denote that the number of iterations to reach an approximated solution increases too. In every case, there are no network congestion.
At the right, Generation function Θ_m for $m =$ North destination. [77].

It is a basic case scenario where the surface network of the city of Paris is considered. Network domain of the surface network is cosntructed. It is meshed in $2d$-cells. The simulation is done with the mesh and simulation software Freefem++. It shows traffic states in each zones of the network domain (see Fig. 2.11 and [77]).

The macroscopic fundamental diagram (MFD)   Let us mention that there are other modeling approaches of traffic flows derived in the notion of the macroscopic or network fundamental diagram (MFD or NFD) and the feedback-based gating concepts [6, 10, 40, 54, 48, 42, 41] and the references therein.

Under specific conditions, the network fundamental diagram describes a crisp relationship between the average flow and the average density in an entire network. The limiting condition is being that traffic conditions must be relatively homogeneous over the whole network. The network fundamental diagram is hence not well adapted for great networks in which traffic is extremely inhomogeneous.

Numerical methods applied to traffic flow models

Partial differential equations (shortly "PDE") arise in a number of physical problems such as fluid flow, heat transfer, solid mechanics and biological processes. In this section we only concerned with the hyperbolic partial differential equations, and more on system of partial differential equations. Hyperbolic systems of PDE or hyperbolic PDE fall into conservation laws of mass, flow, momentum, etc. The book [87] are our primary asset to study the system of hyperbolic PDE or the conservation laws we have developed along the scientific works presented with this thesis. As we already see in the section 2.4 above, traffic flow models are written based on conservation laws with respect to the flow and the density variables. Numerical methods are essentials in solving partial differential equations where in theory analytical solutions have been not find. Basic conservation law, defined on a bounded domain,

is the linear advection equation (which is a variable coefficient conservation law):

$$\frac{\partial u}{\partial t} + \frac{\partial (cu)}{\partial x} = 0 \text{ for all } a < x < b \text{ for all } t > 0,$$

$$u(a, t) = v(t) \text{ for all } t > 0,$$

$$u(x, 0) = u_0(x) \text{ for all } a < x < b.$$

(2.27)

where u is the physical conservative quantity, and c the velocity of u. The interval $[a, b]$ represents the interval domain of the study of u on where the latter is defined. The quantity u represented a density $i.e.$ the conserved quantity per length. In numerical analysis or scientific computing courses, basics of numerical methods are discretization of the spacial domain and the domain of time by a finite increasing sequence of grid points and time points, follow-up to the definition of computational grid cells and timesteps. See Figure 2.12 spatial and temporal discretization.
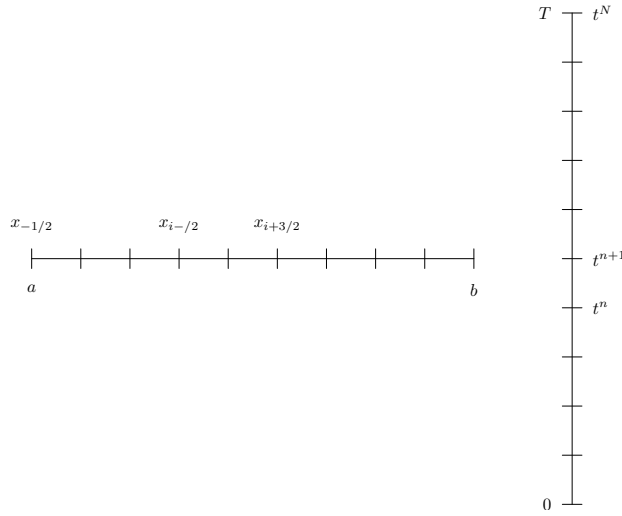
Figure 2.12: Spatial and temporal discretizations.

The simplest numerical approximation to the linear advection equation is the explicit upwind difference method:

$$u_i^{n+1} = u_i^n - \left[u_i^n - u_i^n\right]\frac{c\Delta t^{n+1/2}}{\Delta x_i}, \quad 0 < i < I$$

$$u_0^{n+1} = u_0^n - \left[cu_0^n - f_{-1/2}^{n+1/2}\right]\frac{c\Delta t^{n+1/2}}{\Delta x_i}.$$

(2.28)

(a) $CFL < 1$ (b) $CFL > 1$
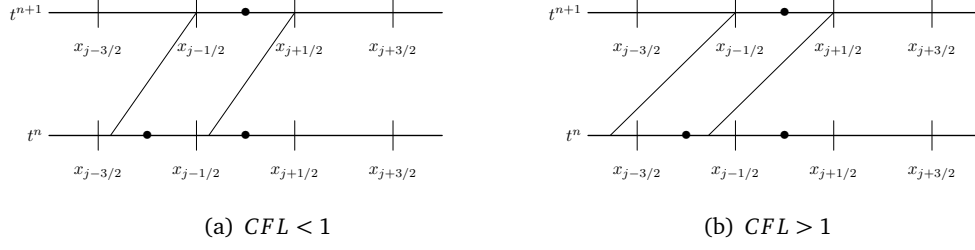
Figure 2.13: Explicit upwind stencil

It is a conservative difference scheme in which the numerical fluxes are computed by $f_{i+1/2}^{n+1/2} = cu_i^n$ for all $0 \leq i < I$ and by the below equation

$$f_{-1/2}^{n+1/2} = \frac{1}{\Delta t^{n+1/2}} \int_{x_{i-1/2}}^{x_{i+1/2}} f(v(t)) dt$$

for all $0 \leq n < N$, at the inflow boundary $i = 0$.

For other numerical methods, we are referred to finite volume methods, and these introduced by Daganzo in [13, 14]. Lagrangian remapping schemes are best schemes to keep both advantages of numerical solutions obtained from partial differential equation in Eulerian and Lagrangian forms. The scheme is fully studied in [15].

Dynamic assignment

Traffic equilibrium

Facing the mass-production of automobiles and a rising demand for public transportation, analysts, economists, mathematician and computer scientists have considered ways of coping with road congestion and queuing. Wardrop [91] pointed out in his Second Principle, that congestion can only occur if users choose their routes userly to optimize their own utility functions. The transportation system is said at user traffic equilibrium state when all traffic patterns stabilize and no driver (for car road system) or no passenger (for public system) have any incentive to change their current route (Wardrop's First Principle, [91]). By the way, there is a central decision maker that assigns routes to drivers or passengers in order to collectively optimize the utilization of the network. In this context, the system is said at a social optimum state or social traffic equilibrium when the goal of the optimization is achieved. Anyway, the evaluation of (alternative) routes is based on objective quantitative criteria with respect to cost, travel time, comfort of the transportation mode up to use etc. The cost depends on used path cost (according to network supply) and is a function of flow

and capacity bound. A commonly used function is that of "Bureau of Public Roads" [27] where the cost of an arc is function of its flow. It is a cost function which is strictly increasing and differentiable. But it has the disadvantage of allowing assignment that exceeds road capacity. And for that reason the cost function of Bureau of Public Roads is only valid in fluid phase. In congested phase, one can apply the method of cross-entropy field of multimodal dynamic assignment [28] which is also valid in fluid phase. In [29], authors have used the notion of traffic intensity for proposing a variant of the problem of optimal transportation cost taking into account congestion and Wardrop equilibrium. In static assignment, one has to consider:

- fixed (stationary) demands since dynamics effects and traffic propagation are neglected and

- the choice of routes for traveling to a target from one source in multimodal framework.

For the road network, there are many possible routes to reach a target from one source, for instance, one notes the multiplicity of paths, and the use of combinatory paths. So they lead to some difficulties as non-uniqueness of multimodality and the choice of departure time (in dynamic case). Since there are a larger number of origins and destinations with multiple paths connecting each origin-destination pair, during rush hours, the travel time on numerous routes changes substantially due to traffic congestion, and thus alternative paths may become competitive. On the other hand, change of environmental conditions, exceptional events and incidents can alter the traffic condition in an unpredictable way. One needs some strategies qualified as feedback or iterative strategies. They are highly efficient in establishing appropriate user-optimal conditions on the basis of current traffic measurements. They have the advantage of simplicity and low computational effort. One cites reactive feedback strategies based on instantaneous reactive travel times [30]. For dynamic multimodal assignment, the principle is based on superposition of path choice and choice departure time interval while dynamic cost contributes to dynamics pheromone levels per OD. Using the cross-entropy method [28], the assignment is described in terms of path choice probabilities and probabilities of choice of departure time. However the optimal choice constitutes a very rare event, in the probabilistic sense, among possible events. It is obtained with a sequence of probability laws that converge towards a law expressing equilibrium conditions

that concentrated on optimal paths, where the convergence is measured by the Kullback-Leibler distance (close to entropy for the estimation of OD matrices). This optimal law is obtained heuristically from best paths configurations.

Reactive dynamic assignment

For a very large network, there are many challenges. The Dynamic Traffic Assignment (DTA) has substantially evolved. [65, 66] are well-known as initial fieldwork on the DTA problems. Many development have been deployed for dynamic traffic assignment problem. The dynamic traffic asignment refers to a broad spectrum of problems, especially when large datum of dense and large network is concerned, explained in [63, 62, 71, 38]. Thus it is important to mention the type of dynamic assignment is related in this dissertation. We are not concerned in user equilibrium problems neither in dynamic user equilibrium problems. Since one of the major expectations from this thesis work is the modeling of flows of large transport networks, the corresponding network loading model provided by this thesis work (see Chapters 3 and 6) shall be loaded with reactive assignment. A reactive assignment refers to

(i) the ways vehicles change their routes during trips according to instantaneous traffic information, and the fact that

(ii) knowing the shortest path, there are nevertheless some users who use other roads because their behaviors are more liable to a Logit based assignment model. That is to say there is nonzero probability of users that use other routes other than shortest paths between origin-destination points.

2.4   Macroscopic transport simulators

Generality

Computer simulation is more and more popular discipline in the filed of science in general. There exist many strategies to simulate traffic systems which fall under the following three categories:

1. The microscopic simulation including cellular automata, multi-agent simulation, particles system simulation.

2. The macroscopic simulation including statistical dispersion models, freeway traffic models, generic second order modeling family models.

3. The two-dimensional simulation including macroscopic fundamental diagram based traffic models, two-dimensional traffic models and continuous approach based traffic models.

Computer scientists have come up with theses above models and with strategies of hybridization to cope with traffic issues. We are interesting on macroscopic simulators and two-dimensional simulators since they are appropriate tools for large-scale traffic management. There are plenty of macroscopic traffic simulators such like Transims, Transmodeler, Dynamit, Dynasmart-P, Magister, Matsim [36]. The list is not exhaustive. The choice of simulators we deployed in the rest of the manuscript comes up with the simulators' accessibility. They are essentially macroscopic simulators. That means that the simulators result from implementation of mathematical/physical macroscopic traffic flow models, and/or stochastic multi-agent transport models.

These are appropriate tools for traffic analysis and traffic controlling. They allow to make dynamic traffic assignment and rerouting of network flows in order to achieve dynamic user equilibrium, and other purposes relevant for transportation safety and re-liabilities.

Let us talk a little bit about few well known and widely used traffic simulation packages:

1. TRANSIMS. The Transportation Analysis and Simulation System (TRANSIMS) is an open source transportation modeling and simulation toolbox. It is an integrated set of tools developed to conduct regional transportation system analyses. With the goal of establishing TRANSIMS as an ongoing public resource available to the transportation community, TRANSIMS is made available under the NASA Open Source Agreement Version 1.3 and is supported by this online community.

2. TransModeler. TransModeler is a versatile traffic simulator with many advanced features including support for key aspects of Intelligent Transportation Systems. TransModeler simulates a wide variety of facility types, including mixed urban and freeway networks, and can be applied to specific geographic areas such as downtowns, highway corridors, or beltways. It integrates traffic simulation models such as:

   - model for freeway and urban networks
   - model rotaries with driver behavior models that capture the unique interactions between vehicles entering and vehicles inside the rotary,

63

- model high occupancy vehicle (HOV) lanes, bus lanes and toll facilities to better understand their effects on traffic system dynamics,

- model evacuation plans and scenarios for response to natural disasters, hazardous spills, and other emergencies

- model work zones to manage traffic during the construction and maintenance projects.

3. DynaMIT. DynaMIT aims to operate an ATIS (Advanced Traveler Information System) to improve travel decisions. Its applications include:

   - Generation of unbiased and consistent information to drivers.

   - Optimizing the operation of TMCs through the provision of real-time predictions.

   - Efficient operation of Variable Message Signs (VMS).

   - Real-time incident management and control.

   - Off-line evaluation of real-time incident management strategies.

   - Evaluation of alternative traffic signals and ramp meters operation strategies.

   - Co-ordination of evacuation and rescue operations in real-time emergencies (natural disasters, etc.) that could block highway links.

   - Generating historical databases.

4. DYNASMART-P.

5. MAGISTER. It is a simulator with a graphical user interface. It is developed in C++. Macroscopic models such as the bounded LWR model, the model of Daganzo (1-phase and 2-phase), the GSOM model (with driver-specific attribute equals to the flow speed minus the fundamental diagram equilibrium velocity). We means by the latter model, the ARZ model.

6. MATSim. MATSim means Multi-Agent Transport Simulation.

It is appeared to us more pertinent to works with MATSim which sounds pretty well compared to the other transport simulation packages, regarding numerous cases studies applied for. Let us make focus on the MATSim transport simulator. We deploy it to perform on flow estimates big surface networks.

MATSim

The core components of MATSim is shown in the Figure 2.14.
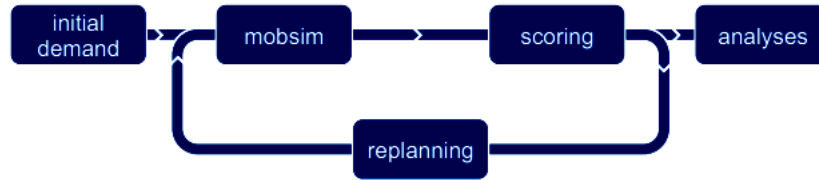
Figure 2.14: Core components of MATSim.

The *"initial demand"* refers to input data to the simulation part. It comprises transport network (the graph with information needed on the infrastructure and topology of the considered network). The module *"mobsim"* is the MATSim engine for traffic estimates on the graph. The *"replanning"* module is important in case of re-routing due to the change of departure times in locations, or change of routes of passengers in order to achieve some scores.

The software come up with many functionalities (see Figure 2.15) for planning, contol, multimodal simulation. It can account traffic signals during microsimulation. Its main function being to simulate passengers and vehicles as agents over the network at the macroscopic level.
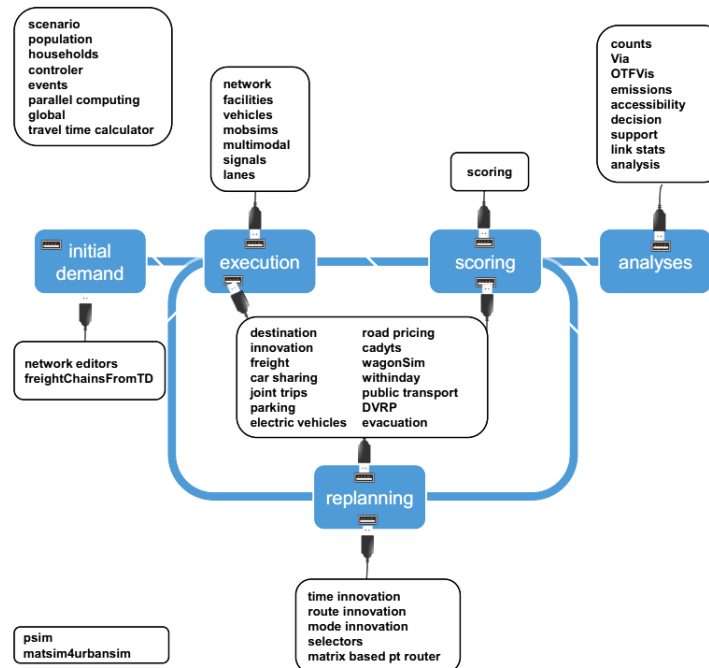
Figure 2.15: MATSim full functionality.

Configuring and running MATSim It is designed so far to simulate any transportation system such urban network, public transit system, multimodal system, etc. It comprises several transport models.
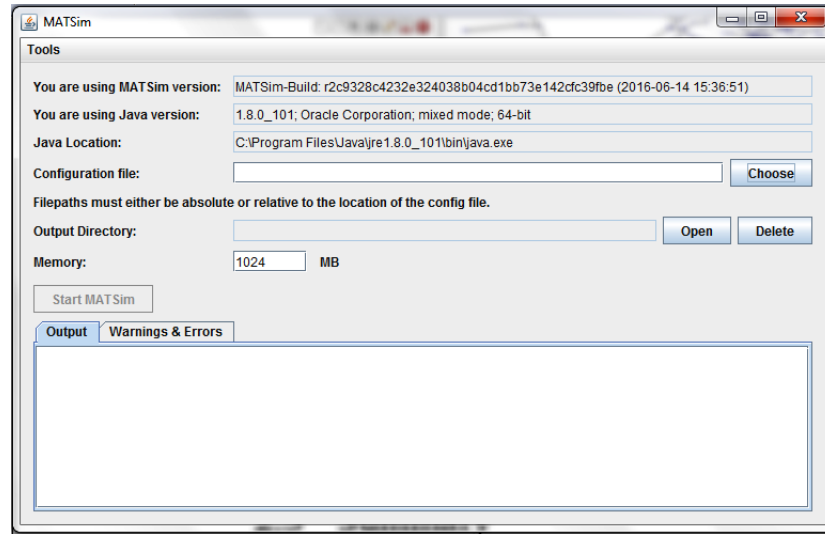
Figure 2.16: Minimal MATSim GUI.

Setting up and running MATSim As input for a simulation, one need three minimal files. They are the following.

1. network.xml. It contains the physical network of the considered transport network along with the network supply and its capacity.

2. population.xml. The file population, shall provides a synthetic population representing the transport demand along with plans of agents. In fact, every user of the being synthetic population, is consider as an agent.

3. config.xml is a configuration file. It configures all the files being used by MATSim. Also it says MATSim modules that shall be used or solicited during the simulation. It says whether re-routing is planning.
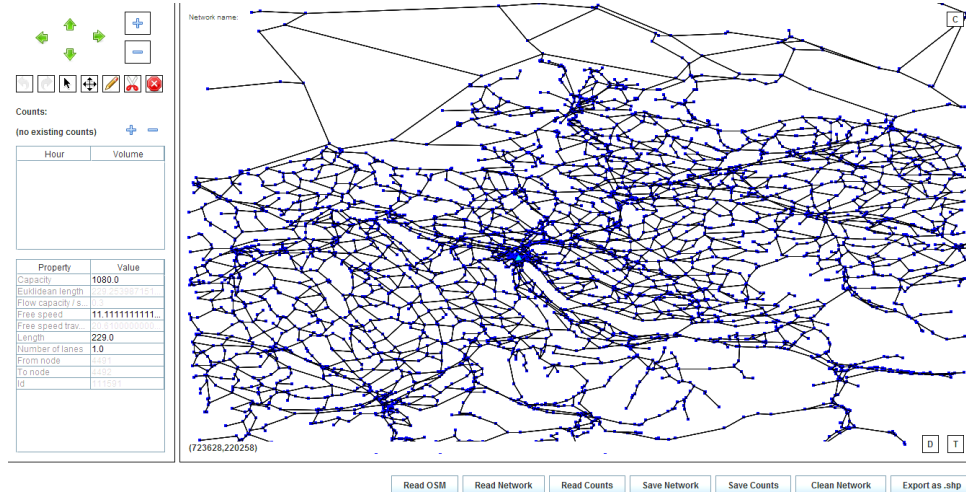
Figure 2.17: Very large road network, seen with the MATSim network editor - the networkEdit.

2.5 Summary

We have so far presented macroscopic models related to transport simulation of vehicles inside surface networks. We have seen that two-dimensional modeling framework is a good way for simulating large networks, without distinction of transport mode. In case one should distinguishes transport modes in a network, it is relevant to use different flow models. Those help to get realistic model of flow for entire multimodal transport network. A microscopic model sometimes is required depending on the type of transport or provided transport services. What shall be the right combination or coupling of models? Shall we build a very new model from scratch? Let see that below in the rest of the manuscript.

Nowadays, many transport simulators allow a good estimation of network flows over time. They even are capable of simulating very large network. However, sometimes the computational complexity is very high, and they are not suited for large networks.

This page is intentionally left blank.

Chapter 3

Bi-dimensional dynamic traffic flow modeling

Macroscopic traffic flow models applied to very large transport networks induces several parameters and variables, and significant computational efforts. In the context of the traffic management and traffic controlling of very large surface networks, new directions in mathematical approaches emerge. We make a focus on one of these directions: the bi-dimensional traffic flow theory. It is an efficient way to mitigate the lack of data in very large surface networks since very large transport networks have a little real data – to the best of our knowledge. We want to be able to simulate traffic on very large networks (urban and motorway) using the minimum of the real data. Thus we can overcome the data gaps on very large networks by applying the bi-dimensional traffic flow theory. Let us see the content of this chapter which is fundamental to our work.

Contents

3.1 Introduction

We introduce in this chapter the theory of the traffic flow at the two-dimensional scale which results in specific approximations. These rely on fluid dynamics in continuous media. We will justify and describe them in the remainder of this chapter.

Related work

The approach used to develop the proposed model in this chapter is known as bi-dimensional dynamic traffic flow modeling or theory. It consists of modeling the area of the large transport network in terms of a continuum anisotropic media where vehicles behave like a two-dimensional fluid. Roads and vehicles will be aggregated respectively in zones of two dimensions and flows. In such traffic zones, some directions of propagation of vehicular flows are dominant (see [93, 77, Wong, Saumtally], and the references therein). The anisotropy of the surface network is due to the dominants directions of propagation. We notice that little research has been performed using this approach in the field of traffic flow management. Let us note the existing researches concerning the traffic flow estimation methodology applied to large-scale network of [93, 74, 77, Wong, Prez and Benitez, Saumtally]. They are undertaken in the static case. Other recent approaches are based on the existence and the concept of the MFD (Macroscopic Fundamental Diagram). The MFD has been firstly introduced by [11, Daganzo], and used by [12, Daganzo and Geroliminis] with a traffic scenario on a congested network which covers about $10km^2$ of Yokohama down town using traffic detectors. Since then, dynamic traffic flow models for large-scale urban networks have been developed with this approach [40, 42, 41, Keyvan-Ekbatani et al.] and certain references therein.

Organization of the chapter

The purpose of this chapter is to introduce the bi-dimensional dynamic traffic flow model and compare it to the MFD-based traffic flow models. In this chapter, we provide methods to manage and evaluate traffic on wide and dense networks with a minimum of available measurements and data, through the modeling of global traffic behaviors of car-flow which are derived from its local traffic behaviors. Local traffic behaviors reflect the properties of the flow seen from a macroscopic viewpoint. As for global traffic behaviors, they correspond to observable traffic dynamics seen from a high altitude after a planar projection of the network graph onto its network domain. These observable dynamics, with some restrictions in addition, represent the traffic flow at the bi-dimensional level. Let us note that the term *network domain* corresponds to the traffic area of the traffic network.

Thereby, the networks we are considering and for which we apply the proposed sample dynamic model are characterized as dense, large-scale, anisotropic and continuous.

In the next section (the section 3.2), it was considered important to address the intersection traffic models [8, Costeseque and Lebacque]. Since traffic zones of two-dimensions are obtained by a high aggregation of road links and road intersections, we shall address road intersections as nodes with internal traffics and external traffics. We will see in the sequel how this aggregation is made, and what we call by traffic zones of two dimensions. We therefore deduce properties of car-flow within urban network modeled from the high level of aggregation of links and intersections. We build in Sec. 3.3 a two-dimensional hyperbolic system of conservation laws. We will see that the hyperbolic system describes the dynamic of car-flow in the corresponding network domain of the surface network. Moreover, we deduce a Godunov-like scheme for a numerical analysis and numerical computations. We have found that the numerical scheme allows easy numerical calculation of the car-flow and car-density over the network domain. We also provide a physical model which is the semidiscretized shape of the former multidimensional hyperbolic system. We will see how the physical model is efficient for dynamic network loading in Sec. 3.4. We will see also that our proposed dynamic bi-dimensional traffic flow model converges very quickly.

3.2 $2d$-**Anisotropic Continuous Network**

Definition 3.1 (Network anisotropy). *In traffic theory, a network is said anisotropic when there are many possible interactions and several directions of propagation of the traffic flow at 'almost' any location of the network.*

For instance, the road network of the city of Paris is anisotropic. It forms a spiderweb, ranking in the type of anisotropic networks. In the United States, cities are new and their networks are rather orthotropic since roads are not gradually constructed as cities grow.

Definition 3.2 (Dense network within a continuum area). *We mean by dense network, a network with very high number of secondary roads that are very close to each other. The density of the network in traffic refers to the plurality of road sections of short length and their closeness's.*

Definition 3.3 (Anisotropic continuous network: ACN). *An ACN is a network whose traffic area can be approached by a continuum media with preferred directions of propagation of the flows.*

In the remainder of the chapter, we discuss on the traffic dynamics of a dense surface network and the bi-dimensional traffic flow theory. We will see that the dynamic bi-dimensional traffic flow (BTF model for short) introduced in the present chapter is particularly timely responding to the issues of the traffic flow estimation over large and dense networks.

Definition 3.4 (Bi-dimensional traffic flow model). *A bi-dimensional traffic flow model is a mathematical traffic model that aggregates a network domain to anisotropic continuous network and formulates the relationships among traffic flow characteristics like density, flow, mean speed per dominant/preferred directions of propagation of the network traffic stream.*

Consequence 3.1 (Bi-dimensional modeling approach). *Traffic streams at the bi-dimensional level are comparable to fluid streams flowing in bounded and euclidian two space dimensions.*

Consequence 3.2. *The bi-dimensional modeling approach shall fit both homogeneous and heterogeneous networks. The interest of this approach is more visible in the case of heterogeneous networks.*

Lemma 3.1. *A continuum approach comes out by the aggregation of the road networks (as it is showed in [93, 74, Wong, Prez and Benitez]) which makes vehicles behave on any 2d-ACN (anisotropic continuous network) like a two-dimensional fluid.*

Let us denote by U the traffic area of a surface network. We assume that the surface network is dense and large. U is also called the network domain. It shall be a bounded and open subspace of the Euclidean space $\mathbb{R}^2$ since any city has a frontier and therefore its urban road network also. Clearly $U \subset \mathbb{R}^2$ and $meas(U) < +\infty$, with $meas$ the Lebesgue measure in two space dimensions. Let $P(x,y)$ be a point of the network domain and (x,y) its coordinates. Four preferred directions of propagation of the flow for the movement of vehicles at the point $P(x,y)$ are distinguished. Figure 3.1(a) depicts these dominant directions: four outflows and four inflows to refer to the directions of propagation of the traffic.
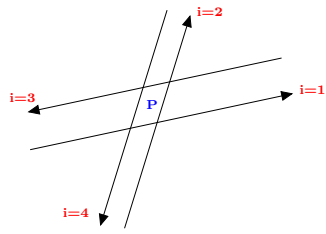
(a) 4 directions of propagation at any point P of a cell of the network domain are considered.
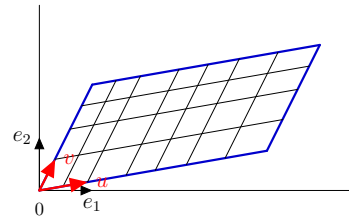
(b) Computing $2d$-cells within each zone from the mesh; every cell has certain number of lanes in considered directions.
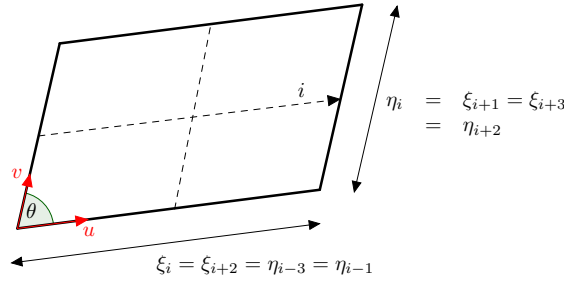
(c) A zoom on a $2d$ computing cell and its dimensions. ξ_i and η_i denote the length and width (according to the clues direction) of the cell.

Figure 3.1: The structure of an $2d$ elementary cell of the network domain.

The network domain U is assumed to be decomposable into traffic zones or sub-network domains U_m, $m = 1, \ldots, M$. Any zone is a sub-domain of the network domain U which follows the below criteria:

i- $U = \bigcup\limits_{m=1}^{M} U_m$

ii- U_m is a polygonal domain of $\mathbb{R}^2$ and the Lebesgue measure of its frontier is strictly positive.

iii- Each zone U_m is meshed in computational cells (often called 2d *elementary cells*) so that the mesh is an admissible mesh in the sense of [16, Definition 5.1 of Eymard et al.].

iv- $\forall m, m' \in M, \left(m \neq m' \Rightarrow U_m \cap U_{m'} \in \{\varnothing, \text{ point, polygonal segment}\} \right)$.

v- $\forall m = 1, \cdots, M, \forall C, C'$ elementary cells of U_m,
$$C \neq C' \Rightarrow C \cap C' \in \{\varnothing, \text{ point, segment}\}.$$

Keeping the anisotropy property of such a large network allows, in an easy way, the dynamical modeling of its traffic flow. It induces a specific dynamic network loading model that we develop in Sec. 3.4.

Flows functions and turning movements

Let $t > 0$ be the time variable, and $P(x, y) \in U$ the position variable. The index $i = 1, 2, 3, 4$ denotes the direction of propagation of the traffic flow.

On a section of U, let us denote by $\tilde{q}_i(P, t)$ the car-flow and $\tilde{\rho}_i(P, t)$ the car-density in the direction $i = 1, 2, 3, 4$ at the time t and at the point P. These quantities can be considered as the flow and density on individual links of the network in the direction i.

We denote for $i \in \{1, 2, 3, 4\}$ by:

• λ_i : the density of streets or arcs in the direction i.

• ν_i : the average number of lanes per street or arc in the direction i.

Consequence 3.3. *For any $i \in \{1, 2, 3, 4\}$, $\lambda_i \nu_i$ defines the density of lanes in the direction i. Let us denote by $f = (f_1, f_2, f_3, f_4)$ the vector density of lanes in the four directions i.e. $\forall i = 1, 2, 3, 4, f_i \overset{def}{=} \lambda_i \nu_i$.*

Lemma 3.2 (Local equilibrium of the traffic)**.** *According to the plain traffic conservation laws, the flow $\tilde{q}_j(P, t)$ in the direction $j = 1, 2, 3, 4$, satisfies the below equation (3.1):*

$$\forall P(x, y), \forall t, \quad \tilde{q}_j(P, t) = \sum_{i=1}^{4} \Gamma_{ij}(P, t)\tilde{q}_i(P, t). \tag{3.1}$$

This Eq. (3.1) is the formula of the traffic at the local equilibrium. $\Gamma = \left(\Gamma_{ij} \right)_{i,j=1}^{4}$ is the matrix of the turning movement coefficients. The matrix form of Eq. (3.1) is:

$$\forall P(x, y), \forall t, \quad \tilde{q}(P, t) = (\tilde{q}.\Gamma)(P, t) \tag{3.2}$$

where $\tilde{q} = \left(\tilde{q}_1 \ \tilde{q}_2 \ \tilde{q}_3 \ \tilde{q}_4 \right)^T$ is the flow-vector of all directions. Further, there is a relationship between the vector lineic traffic flow $\tilde{q}$ and the vector cell traffic flow q. Correspondingly, the vector lineic traffic density $\tilde{\rho}$ and the vector cell traffic density ρ are related by the same relationship. They are stated below:

$$\left[\begin{array}{l} \tilde{\rho}_i(P,t) = \rho_i(P,t)/\lambda_i \nu_i \\ \tilde{q}_i(P,t) = q_i(P,t)/\lambda_i \nu_i \end{array} \right. \quad \forall P(x,y) \in U, \ \forall i \in \{1,2,3,4\}, \ \forall t > 0. \tag{3.3}$$

Let us set $\lambda = (\lambda_1, \lambda_2, \lambda_3, \lambda_4)$ and $\nu = (\nu_1, \nu_2, \nu_3, \nu_4)$.

Remark 3.1. *Let us recall that the function $(P,t) \mapsto \left(\Gamma_{ij}(P,t) \right)_{ij}$ defines the time-dependent turning movement coefficients at the points P of the network domain U. Clearly $\Gamma_{ij}(P,t)$ is the fraction of turning movement coming from lanes of density $\lambda_i \nu_i$ in the directions i, reaching the point P and going to direction j. The matrix Γ expresses the assignment of traffic in the network. We have two obvious relations:*

$$\forall i,j = 1,2,3,4, \quad \forall P(x,y), \forall t, \quad \Gamma_{ij}(P,t) \geqslant 0 \tag{3.4}$$

and

$$\forall i = 1,2,3,4, \quad \forall P(x,y), \forall t, \quad \sum_{j=1}^{4} \Gamma_{ij}(P,t) = 1. \tag{3.5}$$

The equation (3.5) is interpreted as a conservation law, meaning that cars do not appear or disappear on the lanes. The same equation shows clearly that the assignment matrix Γ is stochastic. Hence, the two properties Eq. (3.4) and Eq. (3.5) show that $\Gamma(P,t) = \left(\Gamma_{ij}(P,t) \right)_{ij}$ is a nonnegative and positive stochastic matrix.

Corollary 3.1. *Let us assume that the matrix $\Gamma(P,t)$ is irreducible and consider the remark 3.1. By applying the Theorem of Perron-Frobenius or the theorem of Brouwer of the Fixed Point to Eq. (3.2), we show that Γ has a real maximum positive left eigenvalue $\mu(P,t)$ equal to 1 such that: $\tilde{q}(P,t) = \mu(P,t)U^{\Gamma}(P,t)$. U^{Γ} is the eigenvector at left of Γ associated to the eigenvalue 1.*

This eigenvector U^{Γ} has all its components positive. It can be viewed as yielding the dominant directional components of the traffic at any point P.

Cell internal flow dynamics

Let Δ_j denotes the lineic traffic demand and Ω_j the lineic traffic supply. δ_j denotes the traffic demand per lane, and correspondingly σ_j the traffic supply per lane. We deduce that:

$$\left[\begin{array}{l} \delta_j(P,t) = \lambda_j\, \nu_j\, \Delta_j\big(\tilde{\rho}_j(P,t)\big) \\[2mm] \sigma_j(P,t) = \lambda_j\, \nu_j\, \Omega_j\big(\tilde{\rho}_j(P,t)\big) \end{array}\right. \qquad \forall P(x,y) \in U,\ \forall j \in \{1,2,3,4\},\ \forall t > 0.$$

with $\tilde{\rho}_j$ being the lineic density in the direction j. Let us note that the traffic density per lane ρ_j is defined as below:

$$\rho_j(P,t) = \lambda_j\, \nu_j\, \tilde{\rho}_j(P,t)\big) \quad \forall P(x,y) \in U,\ \forall j \in \{1,2,3,4\},\ \forall t > 0.$$

The function link demand Δ_j and the function link supply Ω_j are respectively shown to be:

$$\left[\begin{array}{l} \Delta_j\big(\tilde{\rho}_j(P,t)\big) = \max_{r \leq \tilde{\rho}_j} Q_{e,j}(r,P) \\[3mm] \Omega_j\big(\tilde{\rho}_j(P,t)\big) = \max_{r \geq \tilde{\rho}_j} Q_{e,j}(r,P) \end{array}\right. \qquad \forall P(x,y) \in U,\ \forall j \in \{1,2,3,4\},\ \forall t > 0. \qquad (3.6)$$

Since every car aims to maximize its own time travel, there is an issue on the flow optimization at the points P of the network domain U. This results in Eq. (3.7) according to the intersection traffic flow model of [8, Costeseque and Lebacque]. We have the below optimization problem:

$$\max_{\tilde{q}} \sum_{j=1}^{4} \Phi_j\big(\tilde{q}_j\big)$$

$$\text{under constraints} \quad \left[\begin{array}{l} \forall j = 1,2,3,4, \quad 0 \leqslant \tilde{q}_j \leqslant \min(\delta_j, \sigma_j), \\[3mm] \forall j = 1,2,3,4, \quad \tilde{q}_j - \sum_{i=1}^{4} \tilde{q}_i \Gamma_{ij} = 0. \end{array}\right. \qquad (3.7)$$

with $\tilde{\rho}_j$ being the lineic density in the direction j and $\tilde{q}_j$ its corresponding lineic flow. The functions $(\Phi_j)_{j=1,2,3,4}$ are assumed increasing and strictly concave with the flow $(\tilde{q}_j)_{j=1,2,3,4}$. Precisely, we can made this assumption in the case of a surface network wherein there is no traffic regulation at the intersections, for instance in a urban and suburb networks. If there are traffic lights, the functions $(\Phi_j)_{j=1,2,3,4}$ are different (for instance linear). We mention that $(\Phi_j)_{j=1,2,3,4}$ are the attributes of the intersection model. In addition, we argue that we should extend macroscopic traffic intersection models to obtain a right bi-dimensional dynamic traffic flow model. Models extended are Lebacque's Intersection model [8, 53, Costeseque and Lebacque, Lebacque and Khoshyaran].

Lemma 3.3. *Under the Karush-Kuhn-Tucker conditions of optimality, we easily find the implicit analytic expression of the flow function $\tilde{q}_i$ for $i \in \{1, 2, 3, 4\}$.*

We have:

$$\forall i = 1, 2, 3, 4, \ \tilde{q}_i = \min\left(\zeta_i; \min\left(\delta_i, \sigma_i\right)\right) \tag{3.8}$$

with $\Phi_i'^{-1}$ the inverse function of the attribute Φ_i and $\ell = (\ell_i)_{i=1,2,3,4}$ the Lagrange multiplier vector associated to the last constraint listed in (3.7).

The function Φ_i is strictly increasing on $[0, k_i]$ and $\Phi_i'(0) > 0$. $\zeta_i = \max\left(0, \Phi_i'^{-1}\left(\ell_i - \sum_{j=1}^{4} \ell_j \Gamma_{ij}\right)\right)$ expresses an implicit traffic supply for the upstream link (i) of the intersection, given that the admissible traffic demand on the link (i) is $\min(\delta_i, \sigma_i)$ for any $i \in \{1, 2, 3, 4\}$.

Eq. (3.8) expresses an implicit intersection charge of the link. Let us specify the functions δ_i and σ_i. $\delta_i(P, t)$ is the users' traffic demand in the direction (i) upstream to the point P at the time t. $\sigma_i(P, t)$ is the traffic supply in the direction (i) downstream to the same point P at the same time t. We provide analytic expressions of $\delta_i(P, t)$ and $\sigma_i(P, t)$ in Eq. (3.6) above. They are depicted by the well-known flow-density FD (fundamental diagram) in Figure 3.2. The flow-density FD emphasizes the equilibrium between the traffic demand and supply per direction of propagation, which we depict by Figure 3.2.
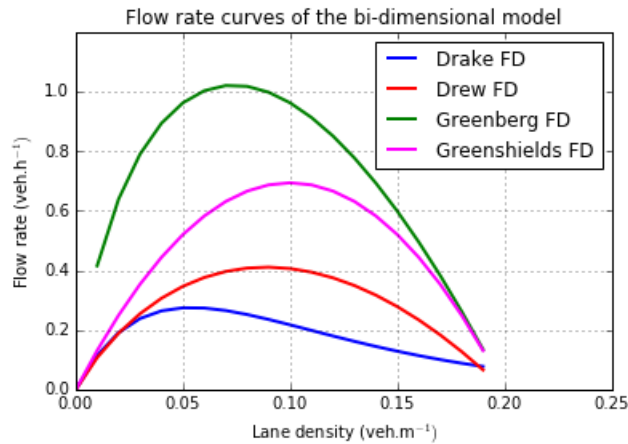
Figure 3.2: Bi-dimensional flow rate curves following a lane and the propagation directions.

For the sake of accuracy in the traffic flow, speed, density computing, we should apply different fundamental diagrams (FDs) with respect to the direction of the propagation, the characteristics of its lanes and the topology of the whole network domain. We assume that the maximal capacity in the directions should also be different. Figure 3.2 depicts the Drake, Drew, Greenber and Greenshields fundamental diagrams.

Lemma 3.4. *Under above assumptions and hypothesis of Corollary 3.1, the following relation holds:*

$$\forall i \in \{1,2,3,4\}, \ \tilde{q}_i = \mu U_i^{\Gamma}, \ with \ \mu = \min_{1 \leq j \leq 4} \left\{ \min(\delta_j, \sigma_j)/U_j^{\Gamma} \right\}. \qquad (3.9)$$

Proof.

$\forall i \in \{1,2,3,4\}$, one has $\mu U_i^{\Gamma} = \tilde{q}_i$ because of Corollary 3.1.

In addition, $\forall i \in \{1,2,3,4\}$, $\tilde{q}_i \leq \min(\delta_i, \sigma_i)$ because of the law of the minimum between the traffic demand and the traffic supply which says that *"the flow could not exceed either the supply or the demand"*.

Hence, $\mu \leq \min_{1 \leq i \leq 4} \left\{ \min(\delta_i, \sigma_i)/U_i^{\Gamma} \right\}$. Besides, μ reaches its upper bound following the optimality condition of the flows, verified by the physics of the traffic. □

The relations (3.3) and (3.9) represent the traffic states of the resulted intersection model. Figure A.1 depicts the attribute function Φ_j according to the lanes' characteristics in the direction j, for $j \in \{1,2,3,4\}$.

3.3 Traffic dynamic within $2d$ Anisotropic continuous network

This section is devoted to the modeling of traffic flow within the network domain U. We assume that U can be disaggregated in M traffic-zones U_m, $m = 1, \ldots, M$. A conservation law of car-flow within each U_m will result. It is stated by the system of hyperbolic conservation laws (3.10).

Vehicles dynamics within $2d$ traffic zone

There is internal conservation of the mass flow in any direction i of propagation. The two flow functions $\tilde{q}_i$ and q_i are related with $q_i = \lambda_i v_i \tilde{q}_i$ formula. As mentioned above, each zone U_m is meshed by a family of $2d$ elementary cells, denoted by $\left(C_m^{\alpha,\beta} \right)_{\alpha,\beta}$ for $m = 1, \ldots, M$. The cells satisfy [16, Definition 5.1 of Eymard et al.]. First we consider regular mesh. It means that the $2d$ elementary cells $C_m^{\alpha,\beta}$ are square or rectangular cells (since besides four directions of propagation of the traffic are considered).

We assume that $\lambda_3 = \lambda_1$ and $\lambda_4 = \lambda_2$, and that $\Gamma_{13} = \Gamma_{31} = \Gamma_{24} = \Gamma_{42} = 0$. The first relationship implies that at any point P there is always four directions which are pairwise side by side. The second expresses that there is no U-turning movement at any point P.

Under these assumptions, the dynamical traffic flow model in [78, Saumtally et al.] is valid

for the topological structure of the network discussed in this study. The model in [78, Saumtally et al.] boils down to a system of conservation laws of car-densities within an elementary cell (3.10). For any fixed zone-index $m = 1, 2, \ldots, M$, the same system shall be valid on U_m, since any cell of U_m has the same values of lane-densities λ_i, $i = 1, 2, 3, 4$ (which may differ from one zone to another). Below, (3.10) is the multidimensional hyperbolic conservation laws that describes the variation of car-density vector ρ in all directions. This holds in the local basis (u, v) related to each elementary cell, and then for the zone containing the cell. We have:

$$\left| \begin{array}{c} \forall m = 1, \ldots, M, \ \forall t \in \mathbb{R}^+, \ \forall P(x, y) \in U_m \subset U \subset \mathbb{R}^2, \\[2mm] \partial_t \rho + \partial_x Q^x(q) + \partial_y Q^y(q) = 0. \end{array} \right. \tag{3.10}$$

with $\rho = \left(\rho_1 \ \rho_2 \ \rho_3 \ \rho_4 \right)^T$ and $q = (q_1, q_2, q_3, q_4)^T$ taking values in $\mathbb{R}^4$, where ρ_i is the car-density and q_i the car-flow in the preferred direction of propagation i, $i \in \{1, 2, 3, 4\}$.

$$Q^x(q) = \left(Q_1^x \ Q_2^x \ Q_3^x \ Q_4^x \right)^T (q) \text{ and } Q^y(q) = \left(Q_1^y \ Q_2^y \ Q_3^y \ Q_4^y \right)^T (q).$$

The vector function $Q : \mathbb{R}^4 \longrightarrow \mathbb{R}^8$, $(q_1, q_2, q_3, q_4)^T \longmapsto \left(Q_1^x \ Q_2^x \ Q_3^x \ Q_4^x \ Q_1^y \ Q_2^y \ Q_3^y \ Q_4^y \right)^T$ takes into account the theory of hydrodynamic and velocity profiles applied in traffic theory.

$$Q^x(q) = \begin{pmatrix} q_1 \\ \frac{1}{2}\left(\Gamma_{12}q_1 - \Gamma_{32}q_3 + \frac{\lambda_1}{\lambda_2}(\Gamma_{21} - \Gamma_{23})q_2 \right) \\ -q_3 \\ \frac{1}{2}\left(\Gamma_{14}q_1 - \Gamma_{34}q_3 + \frac{\lambda_1}{\lambda_2}(\Gamma_{41} - \Gamma_{43})q_4 \right) \end{pmatrix}, \quad Q^y(q) = \begin{pmatrix} \frac{1}{2}\left(\Gamma_{21}q_2 - \Gamma_{41}q_4 + \frac{\lambda_2}{\lambda_1}(\Gamma_{12} - \Gamma_{14})q_1 \right) \\ q_2 \\ \frac{1}{2}\left(\Gamma_{23}q_2 - \Gamma_{43}q_4 + \frac{\lambda_2}{\lambda_1}(\Gamma_{32} - \Gamma_{34})q_3 \right) \\ -q_4 \end{pmatrix}. \tag{3.11}$$

$Q^x(q)$ and $Q^y(q)$ are the flow vector functions for measuring the change in flow in the x-direction and y-direction (see [78, Sautmally et al.]) of cells of the network domain.

To proof Eq. (3.11), one should integrate the laws $q_i(\rho_i)$. By using an affine transformation, the system can be transformed regarding the global basis (e_1, e_2) (Figure 3.1(b)).

We assume for physical reasons, for instance according to the fundamental diagram and the conservation of the traffic in the four directions, that the system (3.10) is hyperbolic. We have not demonstrated this. One possibility would be to calculate:

$$\partial_q Q \times \partial_\rho q = \partial_\rho Q \tag{3.12}$$

Eq. (3.12) is a system of 4 equations of conservation in two space dimensions. Mathematical literature says little about it.

Cell transport demand and cell network supply

Let m be fixed. Let us make a focus on U_m. We recall that $C_m^{\alpha,\beta}$ denotes an $2d$ elementary cell of U_m. For the sake of simplicity we omit the index m. The traffic supply and traffic demand in the cell $C^{\alpha,\beta}$ in the direction $i \in \{1,2,3,4\}$ are defined as follows:

$$\left[\begin{array}{l} \delta_i^{\alpha,\beta} = \lambda_i \nu_i \Delta_i^{\alpha,\beta} \left(\rho_i^{\alpha,\beta} / \lambda_i \nu_i \right) \\[2mm] \sigma_i^{\alpha,\beta} = \lambda_i \nu_i \Omega_i^{\alpha,\beta} \left(\rho_i^{\alpha,\beta} / \lambda_i \nu_i \right) \end{array} \right. \qquad \forall C^{\alpha,\beta}, \ \forall i \in \{1,2,3,4\}, \qquad (3.13)$$

where $\Omega_i^{\alpha,\beta}$ and $\Delta_i^{\alpha,\beta}$ are the supply and demand at a point.

Inflows and outflows of an $2d$ elementary cell

Remark 3.2. *Within the same zone U_m for m fixed, values of λ_i from one cell to the other are the same. Let us mention that, in the two dimensional approach, there is no buffer between cells. Hence, cell outflow rates do not depend upon cell inflow rates. But the cell itself is a buffer between its inflows and outflows.*

Inflow and outflow rates in the four privileged directions with their constraints are expressed as follows. Inflow rates are set in the first column and outflow rates are in the second one of the below equation (3.14).
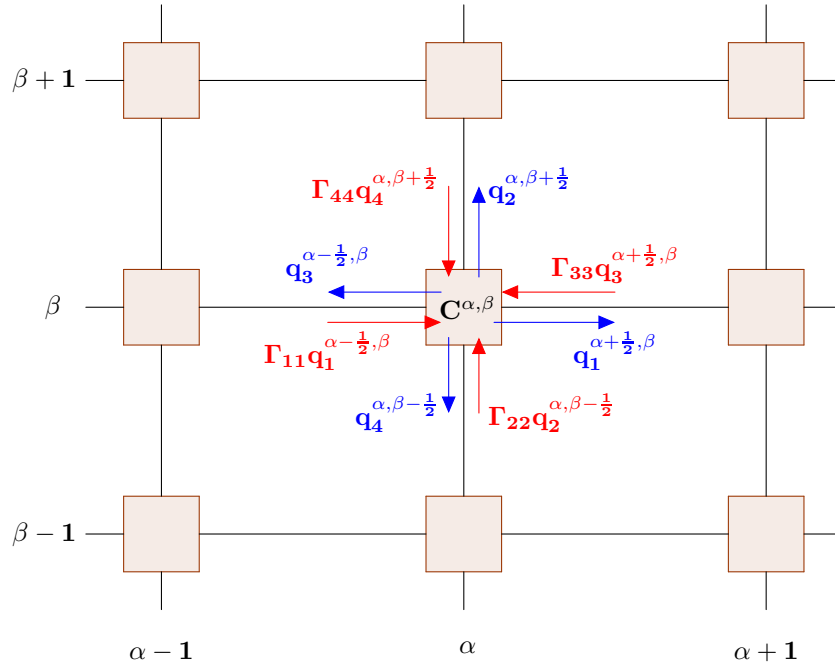

Figure 3.3: Inflows and outflows of 2d computing cells

Other turning flows can be suggested as:

i- $q_1^{\alpha,\beta-\frac{1}{2}}\Gamma_{21}$ and $q_4^{\alpha,\beta+\frac{1}{2}}\Gamma_{41}$ in the direction $i = 1$.

ii- $q_1^{\alpha-\frac{1}{2},\beta}\Gamma_{14}$ and $q_3^{\alpha+\frac{1}{2},\beta}\Gamma_{34}$ in the direction $i = 2$.

iii- $q_2^{\alpha,\beta-\frac{1}{2}}\Gamma_{23}$ and $q_4^{\alpha,\beta+\frac{1}{2}}\Gamma_{43}$ in the direction $i = 3$.

iv- $q_1^{\alpha-\frac{1}{2},\beta}\Gamma_{14}$ and $q_3^{\alpha+\frac{1}{2},\beta}\Gamma_{34}$ in the direction $i = 4$.

We will see how to accommodate them effectively.

The constraints of supply and demand at the 4 interfaces of each cell $C^{(}\alpha,\beta)$ are set below.

$$
\begin{aligned}
&\bullet(\alpha,\beta)\leftarrow(\alpha+1,\beta) : q_3^{\alpha+\frac{1}{2},\beta}\leqslant\sigma_3^{\alpha,\beta} \qquad &&\bullet(\alpha,\beta)\rightarrow(\alpha+1,\beta) : q_1^{\alpha+\frac{1}{2},\beta}\leqslant\delta_1^{\alpha,\beta} \\
&\bullet(\alpha,\beta)\leftarrow(\alpha-1,\beta) : q_1^{\alpha-\frac{1}{2},\beta}\leqslant\sigma_1^{\alpha,\beta} \qquad &&\bullet(\alpha,\beta)\rightarrow(\alpha-1,\beta) : q_3^{\alpha-\frac{1}{2},\beta}\leqslant\delta_3^{\alpha,\beta} \\
&\bullet(\alpha,\beta)\leftarrow(\alpha,\beta-1) : q_4^{\alpha,\beta+\frac{1}{2}}\leqslant\sigma_4^{\alpha,\beta} \qquad &&\bullet(\alpha,\beta)\rightarrow(\alpha,\beta-1) : q_2^{\alpha,\beta+\frac{1}{2}}\leqslant\delta_2^{\alpha,\beta} \\
&\bullet(\alpha,\beta)\leftarrow(\alpha,\beta+1) : q_2^{\alpha,\beta-\frac{1}{2}}\leqslant\sigma_2^{\alpha,\beta} \qquad &&\bullet(\alpha,\beta)\rightarrow(\alpha,\beta+1) : q_4^{\alpha,\beta-\frac{1}{2}}\leqslant\delta_4^{\alpha,\beta}
\end{aligned}
\tag{3.14}
$$

Flows at interfaces are maximal given their constraints and thus:

$$
\begin{aligned}
q_1^{\alpha-\frac{1}{2},\beta} &= \mu^{\alpha,\beta}U_1^{\alpha,\beta,\Gamma} \quad ; \quad q_3^{\alpha+\frac{1}{2},\beta} = \mu^{\alpha,\beta}U_3^{\alpha,\beta,\Gamma} \; ; \\
q_2^{\alpha,\beta-\frac{1}{2}} &= \mu^{\alpha,\beta}U_2^{\alpha,\beta,\Gamma} \quad ; \quad q_4^{\alpha,\beta+\frac{1}{2}} = \mu^{\alpha,\beta}U_4^{\alpha,\beta,\Gamma} \; .
\end{aligned}
\tag{3.15}
$$

where $\mu^{\alpha,\beta} = \min\left(\mu_1^{\alpha,\beta},\mu_2^{\alpha,\beta},\mu_3^{\alpha,\beta},\mu_4^{\alpha,\beta}\right)$ with

$$
\begin{aligned}
\mu_1^{\alpha,\beta} &= \min\left(\delta_1^{\alpha-1,\beta},\sigma_1^{\alpha,\beta}\right)/U_1^{\alpha,\beta,\Gamma} \quad ; \quad \mu_3^{\alpha,\beta} = \min\left(\delta_3^{\alpha+1,\beta},\sigma_3^{\alpha,\beta}\right)/U_3^{\alpha,\beta,\Gamma} \; ; \\
\mu_2^{\alpha,\beta} &= \min\left(\delta_2^{\alpha,\beta-1},\sigma_2^{\alpha,\beta}\right)/U_2^{\alpha,\beta,\Gamma} \quad ; \quad \mu_4^{\alpha,\beta} = \min\left(\delta_4^{\alpha,\beta+1},\sigma_4^{\alpha,\beta}\right)/U_4^{\alpha,\beta,\Gamma} \; .
\end{aligned}
$$

We recall that $\mu^{\alpha,\beta}$ is the real maximum positive left eigenvalue of Eq. (3.2) which we assume valid either at the points $P(x,y)$ of the network domain (local equilibrium) or in each $2d$ elementary cell (global equilibrium). $U^{\alpha,\beta,\Gamma} = \left(U_j^{\alpha,\beta,\Gamma}\right)_{j=1,2,3,4}$ is the eigenvector at left of the assignment matrix Γ related to the cell $C^{\alpha,\beta}$. $U^{\alpha,\beta,\Gamma}$ and $\mu^{\alpha,\beta}$ are time-dependent and different from one cell to another.

3.4   Numerical methods

We provide in this section the spatial domain for Riemann problem with respect to the directions of propagation in the cells. Next, we provide a Godunov-type numerical scheme construction for the system (3.10) - (3.15). The Godunov method that we describe in the following is based on propagating waves normal to each $2d$ cell interface.

Waves propagation in $2d$ elementary cells

Waves should propagate in a multidimensional manner and affect other cell averages besides those adjacent to the interface. Waves are represented by fluctuations they produce. These fluctuations in multidimensional domain are transverse and are splitted into two categories: the up-going transverse fluctuations and the down-going transverse fluctuations. Spatial domain for Riemann problem is thus either half plane or quater plane. Let us zoom in on an internal cell of a network domain. Through each interface of the cell, there are plane waves crossing it. At the corner of the cell, there is interference of such waves. Let assume constants u the traffic velocity in directions 1 and 3 in the one hand, and v the traffic velocity in the direction 2 and 4. In such a case a single wave should propagate in the direction (u, v). There is a triangular portion of the wave originating from the cell $C^{\alpha,\beta}$ which should move into cells $C^{\alpha,\beta+1}$ and $C^{\alpha-1,\beta-1}$, rather than cells $C^{\alpha-1,\beta}$ or $C^{\alpha,\beta}$ (see Fig. 3.4). Between the latter, the first are up-going transverse fluctuations, the second are down going transverse fluctuations.
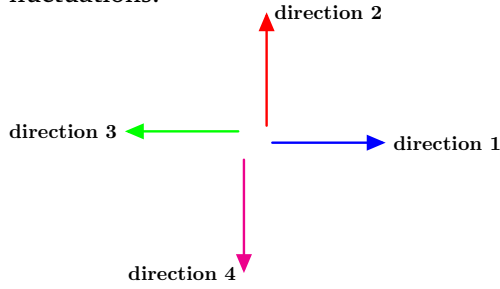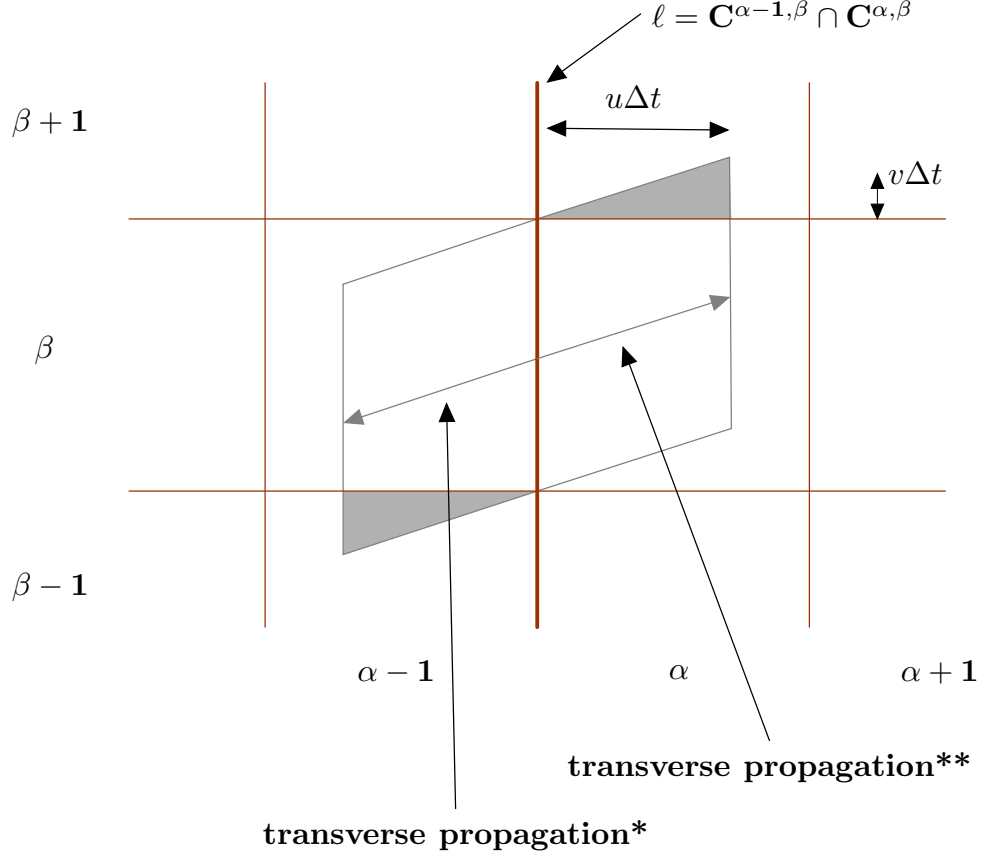
Figure 3.4: Generic two-dimensional waves in $2d$ elementary cells.

Transverse propagation* represents waves originating from the cell $C^{\alpha,\beta}$ passing through the cell interface $\ell = C^{\alpha-1,\beta} \cap C^{\alpha,\beta}$ because of directions 3 and 4 of $C^{\alpha,\beta}$.

Respectively, **transverse propagation**** represents waves originating from the cell $C^{\alpha-1,\beta}$ passing through the same cell interface $\ell = C^{\alpha-1,\beta} \cap C^{\alpha,\beta}$ because of directions 1 and 2 of $C^{\alpha-1,\beta}$.

Waves originating from the cell $C^{\alpha,\beta}$ will intersect as suggested specific waves from neighbor cells. It is a very difficult problem. No analytical solution have been suggested. Therefore, we provide schemes to compute densities and flows without addressing how to treat effectively Riemann problem in the network domain of two space dimensions for the system of hyperbolic PDEs (3.10).

The discretized model

A discretized model is the computational expression of a continuous model. Let us recall that the model is built at the bi-dimensional scale. In a system of axes, α lies on the x-axis and β on the y-axis correspondingly. The average value of the bi-dimensional dynamic traffic state

ρ, at the time t over the cell $C^{\alpha,\beta}$ is defined as

$$\rho^{\alpha,\beta}(t) = \frac{1}{\left|C^{\alpha,\beta}\right|} \int_{C^{\alpha,\beta}} \rho(x,y,t)dxdy. \tag{3.16}$$

The solution at each time step t is described as a piece-wise constant function:

$$\rho(x,y,t) = \sum_{m \in M} \sum_{\substack{\alpha_m \in N_\alpha^m \\ \beta_m \in N_\beta^m}} \rho^{\alpha_m,\beta_m}(t) \, \chi_{\alpha_m,\beta_m}(x,y) \tag{3.17}$$

with

$$\chi_{\alpha_m,\beta_m}(x,y) = \begin{cases} 1 & \text{if } (x,y) \in C^{\alpha_m,\beta_m} \\ 0 & \text{if } (x,y) \notin C^{\alpha_m,\beta_m} \end{cases}$$

N_α^m and N_β^m are sets of cells' indexes of sub-network domain U_m respectively in the x-axis and y-axis.

The following is the first proposal for numerical schemes.

For each cell $C^{\alpha,\beta}$ the density vector at the next time level $(t+1)$ is computed as follows:

$$\begin{cases} \rho_1^{\alpha,\beta}(t+1) = \rho_1^{\alpha,\beta}(t) + \dfrac{\Delta t}{\xi_1 \eta_1} \left(\eta_1 \Gamma_{11} q_1^{\alpha-\frac{1}{2},\beta} + \eta_2 \Gamma_{21} \dfrac{\lambda_1 \nu_1}{\lambda_2 \nu_2} q_2^{\alpha,\beta-\frac{1}{2}} + \eta_4 \Gamma_{41} \dfrac{\lambda_1 \nu_1}{\lambda_4 \nu_4} q_4^{\alpha,\beta+\frac{1}{2}} + \eta_1 q_1^{\alpha+\frac{1}{2},\beta} \right)(t) \\[3mm] \rho_2^{\alpha,\beta}(t+1) = \rho_2^{\alpha,\beta}(t) + \dfrac{\Delta t}{\xi_2 \eta_2} \left(\eta_2 \Gamma_{22} q_2^{\alpha,\beta-\frac{1}{2}} + \eta_3 \Gamma_{32} \dfrac{\lambda_2 \nu_2}{\lambda_3 \nu_3} q_3^{\alpha-\frac{1}{2},\beta} + \eta_1 \Gamma_{12} \dfrac{\lambda_2 \nu_2}{\lambda_1 \nu_1} q_1^{\alpha+\frac{1}{2},\beta} - \eta_2 q_2^{\alpha,\beta+\frac{1}{2}} \right)(t) \\[3mm] \rho_3^{\alpha,\beta}(t+1) = \rho_3^{\alpha,\beta}(t) + \dfrac{\Delta t}{\xi_3 \eta_3} \left(\eta_3 \Gamma_{33} q_3^{\alpha+\frac{1}{2},\beta} - \eta_4 \Gamma_{43} \dfrac{\lambda_3 \nu_3}{\lambda_4 \nu_4} q_4^{\alpha,\beta+\frac{1}{2}} + \eta_2 \Gamma_{23} \dfrac{\lambda_2 \nu_3}{\lambda_2 \nu_2} q_2^{\alpha,\beta-\frac{1}{2}} + \eta_3 q_3^{\alpha-\frac{1}{2},\beta} \right)(t) \\[3mm] \rho_4^{\alpha,\beta}(t+1) = \rho_4^{\alpha,\beta}(t) + \dfrac{\Delta t}{\xi_4 \eta_4} \left(\eta_4 \Gamma_{44} q_4^{\alpha,\beta+\frac{1}{2}} + \eta_3 \Gamma_{34} \dfrac{\lambda_4 \nu_4}{\lambda_3 \nu_3} q_3^{\alpha-\frac{1}{2},\beta} + \eta_1 \Gamma_{14} \dfrac{\lambda_4 \nu_4}{\lambda_1 \nu_1} q_1^{\alpha-\frac{1}{2},\beta} - \eta_4 q_4^{\alpha,\beta-\frac{1}{2}} \right)(t) \end{cases} \tag{3.18}$$

Here we assume the model (3.9) at the behavior level together with the equation of conservation (3.10) and (3.11). We integrate the physical behavior governed by (3.15) in the discretized model (3.18). This latter formulation does not integrate the intersection model but only the assignment $\left(\Gamma_{ij}\right)_{i,j=1,2,3,4}$.

Crossing flows $q_\ell^{\alpha \pm \frac{1}{2},\beta}(t)$ and $q_\ell^{\alpha,\beta \pm \frac{1}{2}}(t)$ from the cell $C^{\alpha,\beta}$ appearing in the above formulation (3.18) are determined by the traffic equilibrium principle at each time step t. It is the traffic equilibrium between the four traffic demands in a cell and the four network supplies of its neighbor cells. This is expressed by Eq. (3.15).

For $i \in \{1,2,3,4\}$, η_i denotes the length of lanes in the direction i and ξ_i denotes the width of lanes in the direction $i+1$ *modulo* 4 (see Fig. 3.1(c)).

Replacing expressions of Eq. (3.15) in Eq. (3.18), we obtain Eq. (3.19) below.

$$
\left\{
\begin{aligned}
&\rho_1^{\alpha,\beta}(t+1) = \rho_1^{\alpha,\beta}(t) + \mu^{\alpha,\beta}\frac{\Delta t}{\xi_1\eta_1}\left(\eta_1\Gamma_{11}U_1^{\alpha,\beta,\Gamma} + \eta_2\Gamma_{21}\frac{\lambda_1\nu_1}{\lambda_2\nu_2}U_2^{\alpha,\beta,\Gamma} + \eta_4\Gamma_{41}\frac{\lambda_1\nu_1}{\lambda_4\nu_4}U_4^{\alpha,\beta,\Gamma}\right)(t) \\
&\qquad\qquad + \mu^{\alpha+1,\beta}\Delta t U_1^{\alpha+1,\beta,\Gamma}(t)/\xi_1 \\[2mm]
&\rho_2^{\alpha,\beta}(t+1) = \rho_2^{\alpha,\beta}(t) + \frac{\Delta t}{\xi_2\eta_2}\left(\mu^{\alpha,\beta}\eta_2\Gamma_{22}U_2^{\alpha,\beta,\Gamma} + \mu^{\alpha-1,\beta}\eta_3\Gamma_{32}\frac{\lambda_2\nu_2}{\lambda_3\nu_3}U_3^{\alpha-1,\beta,\Gamma}\right. \\
&\qquad\qquad \left. + \mu^{\alpha+1,\beta}\eta_1\Gamma_{12}\frac{\lambda_2\nu_2}{\lambda_1\nu_1}U_1^{\alpha+1,\beta,\Gamma} - \eta_2\mu^{\alpha,\beta+1}U_2^{\alpha,\beta+1,\Gamma}\right)(t) \\[2mm]
&\rho_3^{\alpha,\beta}(t+1) = \rho_3^{\alpha,\beta}(t) + \mu^{\alpha,\beta}\frac{\Delta t}{\xi_3\eta_3}\left(\eta_3\Gamma_{33}U_3^{\alpha,\beta,\Gamma} - \eta_4\Gamma_{43}\frac{\lambda_3\nu_3}{\lambda_4\nu_4}U_4^{\alpha,\beta,\Gamma} + \eta_2\Gamma_{23}\frac{\lambda_2\nu_3}{\lambda_2\nu_2}U_2^{\alpha,\beta,\Gamma}\right)(t) \\
&\qquad\qquad + \mu^{\alpha-1,\beta}\Delta t U_3^{\alpha-1,\beta,\Gamma}(t)/\xi_3 \\[2mm]
&\rho_4^{\alpha,\beta}(t+1) = \rho_4^{\alpha,\beta}(t) + \mu^{\alpha,\beta}\frac{\Delta t}{\xi_4\eta_4}\left(\eta_4\Gamma_{44}U_4^{\alpha,\beta,\Gamma} + \eta_1\Gamma_{14}\frac{\lambda_4\nu_4}{\lambda_1\nu_1}U_1^{\alpha,\beta,\Gamma}\right)(t) \\
&\qquad\qquad + \frac{\Delta t}{\xi_4\eta_4}\left(\mu^{\alpha-1,\beta}\eta_3\Gamma_{34}\frac{\lambda_4\nu_4}{\lambda_3\nu_3}U_3^{\alpha-1,\beta,\Gamma} - \mu^{\alpha,\beta-1}\eta_4U_4^{\alpha,\beta-1,\Gamma}\right)(t)
\end{aligned}
\right.
\tag{3.19}
$$

The latter equation really integrate the physical behavior expected which is expressed by the eigenvector $U^{\alpha,\beta,\Gamma}$ and the eigenvalue $\mu^{\alpha,\beta}$.

Remark 3.3. *For any admissible mesh of quadrangular cells, one could apply the method introduced in [90, Vides et al.] where a simple two-dimensional HLL Riemann Solver has been proposed to find approximate solutions to the above system of nonlinear hyperbolic conservation laws. HLL Riemann solver refers to "Upstream Differencing and Godunov-Type Schemes for Hyperbolic Conservation Laws" [27, Harten et al.] 'HLL' is initials of authors of [27]: Harten, Lax and van Leer. Their resulting solver for Riemann problem has been named HLL Riemann Solver. In the case of application of a high-resolution method to the system* (3.10), *we could adapt the works of LeVeque [56, 55, LeVeque and Shyue, LeVeque].*

Algorithms

With regard to the two-dimensional system equations we present a snippet of pseudo-code to compute the values of cell demands and cell supplies, flows across cell interfaces and cell densities. The obtained pseudo-code below derives from [78, Saumtally et al.].

Algorithm 1 Computation of flows of large orthotropic continuous networks

---

Input: ∗ the mesh of the considered network domain

(We use .msh file generated by *GMSH* software).

∗ lane density λ_i in the direction (i)

∗ average number of lanes ν_i per link in the direction (i)

∗ turning movement coefficients Γ_{ij} ⟵ the assignment matrix Γ

∗ boundary conditions: cell supplies $\sigma_i^{t=0}$ and users' demands $\delta_i^{t=0}$ along

network's entry points and exit points

∗ ending time T for the simulation.

∗ empty network initial conditions (at time $t = 0$): $\rho_i^{\alpha,\beta,0} = 0$, $i = 1, 2, 3, 4$, for all the cells' indexes α, β

for $t = 0$ to T **do**

  for $\alpha = 1$ to N_α do

    for $\beta = 1$ to N_β do

    ∗ calculate users' demand $\left(\delta_i^{\alpha,\beta,t}\right)_{1\leq i \leq 4}$ with (3.13)(a)

    ∗ calculate cell supply $\left(\sigma_i^{\alpha,\beta,t}\right)_{1\leq i \leq 4}$ with (3.13)(b)

    ∗ compute $\left(U_i^{\alpha,\beta,\Gamma}\right)_{1\leq i \leq 4}$ and $\mu^{\alpha,\beta}$

    end for

  end for

  for $\alpha = 1$ to N_α do

    for $\beta = 1$ to N_β do

    ∗ calculate the flows $q_i^{\alpha,\beta,t}$ across cell interfaces with the min-formula (3.15)

    ∗ calculate densities $\rho_i^{\alpha,\beta,t}$ within each cell with the expressions of (3.18)

    end for

  end for

end for

Output: ∗ the flows $q_i^{\alpha,\beta,t}$, $t = 0 \ldots, T$ and the densities $\rho_i^{\alpha,\beta,t}$, $t = 0 \ldots, T$.

Table 3.1: Large orthotropic continuous networks Algorithm.

Computational aspects

Let us consider a large urban transportation network like the surface network of the city of Paris. Let us see a map of such road network (see Fig. 3.5(a)). Let us extract specific geodesic coordinates of boundaries of the city of Paris and the lake the "Seine". External boundary of the considered network domain is comprised with the "Boulevard Périphérique". Geodesic coordinates have been converted in Euclidean coordinates. We obtain an Euclidean subspace of $\mathbb{R}^2$ which defines the network domain of the the real road map of such city. This domain is meshed with *GMSH* software for the Godunov numerical scheme. The result is depicted by Fig. 3.5(b). Input parameters or data are the vectors lane density $\lambda = (\lambda_1\ \lambda_2\ \lambda_3\ \lambda_4)^T$ specific to each cell, the average number of lanes per link in the directions $\nu = (\nu_1\ \nu_2\ \nu_3\ \nu_4)^T$, the cell capacity $\kappa = (\kappa_1\ \kappa_2\ \kappa_3\ \kappa_4)^T$. κ is the maximal or residual capacity to absorb transport

demand in a cell with respect to the directions of the flow.
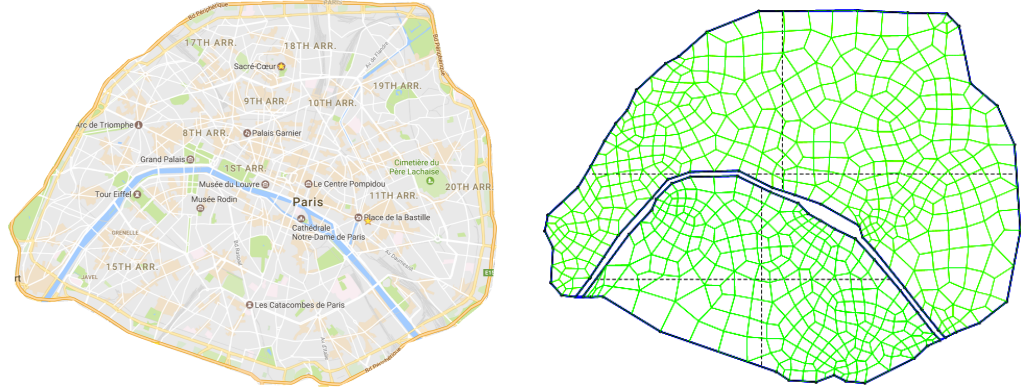
(a) Map of the Paris's road network

(b) Mesh of the network domain by the Gmsh software

Figure 3.5: Mesh of surface network of the city of Paris in $2d$ elementary cells.

Gmsh is a finite element mesh generator developed by Christophe Geuzaine and Jean-François Remacle. Released under the GNU General Public License (with an exception to allow linking with other specific mesh generators), Gmsh is free software. Gmsh contains 4 modules, for geometry description, meshing, solving and post-processing. Gmsh supports parametric input, and has advanced visualization mechanisms [20, Geuzaine and Remacle].

We find that according to the outline border of the considered network, the obtained cells are very small and do not satisfy the minimum length and width of $2d$ elementary cells according to the bi-dimensional modeling approaches of traffic flow. The bi-dimensional traffic flow theory estimate $2d$ elementary cells being of length and width between 1.5 km and 4 km, and comprising more than 20 as lane density in each direction of propagation. To respond to these criteria we shall cleverly force the mesh of the network domain by Gmsh in order to obtain convenient elementary cells. Let us propose how to do that by a specific dynamic network loading (DNL) model. This DNL model covers also the case where $\lambda_i \neq \lambda_{i+2}$ for $i = 1, 2$; what we have not previously considered so far. The DNL model loads a semidiscretized shape of the dynamic BTF model. We discuss this in the following.

Let us suppose a very large surface network which network domain is meshed by GMSH in cells in two-dimensions. Let us mention that the directions of propagation of the flow ventilate the generated traffic demands, from cell to cell.

Notation: We use following parameters and variables.

- $a, b, c, d, e, f, g, h, k$: indexes of computing cells. The cells are quadrangular surfaces. We refer to Figure 3.6.

- δt : the time step.

- $N_{c,i}(t)$: the number of vehicles of the cell (c) at the time t in the direction (i).

- $Q_{fc}(t)$: the incoming flow of the cell (c) from the cell (f) at the time t.

- $R_{cg}(t)$: the outgoing flow of the cell (c) to the cell (g) at the time t.

- $q_{c,i}(t^+)$: the internal inflow in the direction (i) of the cell (c) at the time t^+.

- $r_{c,i}(t^+)$: the internal outflow in the direction (i) of the cell (c) at the time t^+.

- t^+ : refers to $t+1/2$. That is, from the discrete time t to the next discrete time $t+1 = t+\delta t$, internal traffic states $q_{\text{cell},i}(t^+)$ and $r_{\text{cell},i}(t^+)$ are calculated at $t + \delta t/2$. It comes to the construction of flux splitting scheme.

- $\mathfrak{C}$: set of all cells or nodes of the network domain.

Let us highlight some correspondences between cells $\left(C^{\alpha,\beta}\right)_{\alpha,\beta}$ in the rigid square or rectangular network and quadrangular cells of $\mathfrak{C}$ in any anisotropic network: $f = (\alpha-1,\beta)$ or $f = (\alpha, \beta-1)$, $c = (\alpha, \beta)$ and $g = (\alpha+1, \beta)$ or $g = (\alpha, \beta+1)$ (see Fig. 3.6). So here, in the proposed specific DNL model, we free ourselves from the rigid square network and consider any anisotropic network.

Semidiscretized shape of the bi-dimensional flow model

The traffic flow theory applied to highways and urban networks on the one side and the analogy with fluids flowing within two-dimensional domain on the other side suggest the below equation (3.20) as the physical traffic conservation model for the estimation of the number of vehicles in each $2d$ elementary cell.

$$N_{c,i}(t + \delta t) = N_{c,i}(t) + \left(Q_{fc}(t) - R_{cg}(t) + r_{c,i}(t^+) - q_{c,i}(t^+)\right)\delta t \qquad (3.20)$$

i is the direction of propagation of flow inside the cell (c). (f) and (g) are respectively the indexes of the cells located at the left and right of the cell (c).
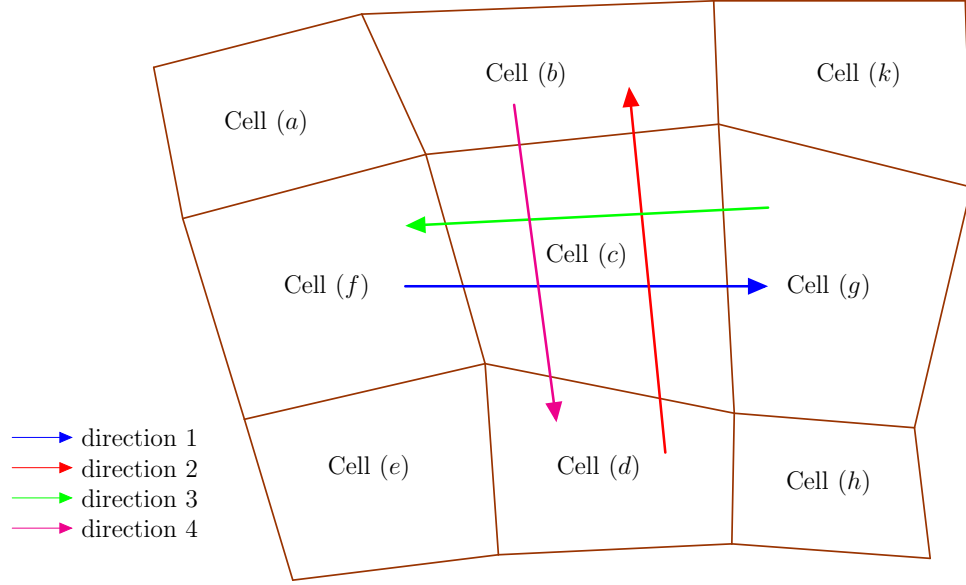
Figure 3.6: Considered directions within $2d$ elementary cells with its neighbor cells.

Cell internal flows control   Using intersection traffic flow model rules following [52, Lebacque and Khoshyaran], we find out that these functions (or variables $r_{c,i}(t^+)$ and $q_{c,i}(t^+)$) are solution of the the below linear-quadratic optimization problem (3.21). We recall that $r_{c,i}$ and $q_{c,i}$ are respectively the outgoing vehicles flow and the incoming vehicles flow of the cell (c) in the direction i.

$$\max_{(q,r)} \left(\sum_{i=1}^{4} \Phi_i(q_i) + \sum_{j=1}^{4} \Psi_j(r_j) \right)$$

$$\text{s.t.} \quad \left|
\begin{array}{ll}
0 \leq q_i \leq \Delta_{ci}^{t+1/2}, & \forall i \in \{1,2,3,4\}, \\
0 \leq r_j \leq \Sigma_{cj}^{t+1/2}, & \forall j \in \{1,2,3,4\}, \\
-r_j + \sum_{i=1}^{4} q_i \Gamma_{c,ij}^{t} = 0, & \forall j \in \{1,2,3,4\}.
\end{array}
\right.
\qquad (3.21)$$

with $q = (q_1, q_2, q_3, q_4)$ and $r = (r_1, r_2, r_3, r_4)$ internal vectors flows which express traffic states inside the cells. Functions $\Psi_\ell(\vartheta_\ell) \doteq \Phi_\ell(\vartheta_\ell)$ are defined by (3.22). They are assumed of the same quadratic concave, increasing form. They describe interactions of vehicles inside each cell. Functions (3.22) are used in intersection theory. They imply that higher capacity directions ($\vartheta_{\ell,max}$ higher) are privileged. The optimization problem (3.21) results in an intersection model similar to the intersection models of [24, 86, Haj-Salem et al., Tampère et al.].

$$\Psi_\ell(\vartheta_\ell) \stackrel{\text{def}}{=} -\frac{1}{2}\vartheta_\ell^2 + \vartheta_\ell.\vartheta_{\ell,max}. \qquad (3.22)$$
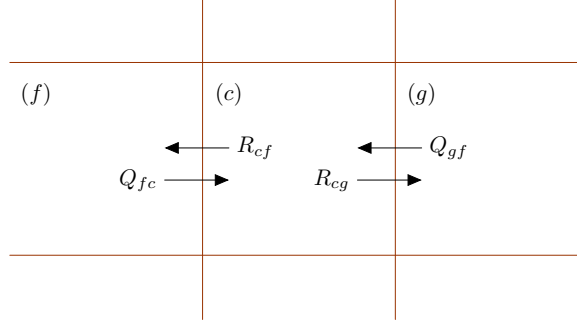
Notations and definitions are the following.

- $\forall i \in \{1,2,3,4\}$, q_i : the incoming vehicles flow in the direction i.

- $\forall j \in \{1,2,3,4\}$, r_j : the outgoing vehicles flow in the direction j.

- $\ell = i, j \in \{1,2,3,4\}$, ϑ_ℓ : refers to q_i or r_j; $\vartheta_{\ell,max}$ denotes $q_{i,max}$ or $r_{j,max}$ which is the maximum flow constraint in the direction i or j.

- $\Gamma_{c,ij}^t$: the assignment coefficients of flows within the cell (c), from the direction i to the direction j, at the time step t.

- μ_{ci} : the number of lanes in the cell (c) in the direction i.

- ν_{ci} : the number of exiting lanes in the cell (c) with respect to the direction i.

- $\delta_i = \Delta_{ci}(\rho_{ci}^t)$: the traffic demand per lane in the direction i of the cell (c).

- $\sigma_j = \Sigma_{cj}(\rho_{cj}^t)$: the traffic supply per lane in the direction j of the cell (c).

- $\Delta_{ci}^{t+1/2} = \mu_{ci}\delta_i$: the traffic demand of (c) in the direction i, at the time $t^+ = t + 1/2$.

- $\Sigma_{cj}^{t+1/2} = \mu_{cj}\sigma_j$: the traffic supply of (c) in the direction (j), at the time $t^+ = t + 1/2$.

- $\left(q_{ci}^{t+1/2}, r_{cj}^{t+1/2}\right)_{i,j=1,2,3,4}$: denote the solution of the above convex optimization problem (3.21). Its resolution is discussed in Appendix A.1.

Cell inflows and cell outflows   Let (c) be a cell. The incoming flows and outgoing flows through the cell (c) are denoted respectively by $Q_{\ell c}$ and $R_{c\ell}$ for $\ell \in \mathcal{V}(c)$, see Figure 3.6 and the figure below. These crossing flows are governed by the law of the minimum between the traffic demand at upstream of the cell (c) and the traffic supply at downstream of the same cell (c). They are defined as follows (Eq. (3.23)). $\mathcal{V}(c)$ denotes the set of neighbors of the cell (c) comprising the only adjacent cells that share together only one interface with the cell (c).

We have:

$$\left[\begin{array}{l} Q_{\ell c}(t) = \min\left(\delta_{\ell,\ell->c}(t), \sigma_{c,\ell->c}(t)\right) \\ R_{c\ell}(t) = \min\left(\delta_{c,c->\ell}(t), \sigma_{\ell,c->\ell}(t)\right) \end{array} \right. \quad \forall \ell \in \mathcal{V}(c). \quad (3.23)$$

For instance neighbors of (c) are $\mathcal{V}(c) = \{(f),(d),(g),(b)\}$ according to Fig. 3.6. For all elements ℓ of $\mathcal{V}(c)$, the directions $\ell-> c$ and $c-> \ell$ are the directions $1,2,3,4$ of the cell (c).

Consequence 3.4. • *Notations $Q_{\ell c}(t)$ and $R_{c\ell}(t)$ generalize $q_\ell^{\alpha\pm\frac{1}{2},\beta}(t)$ and $q_\ell^{\alpha,\beta\pm\frac{1}{2}}(t)$ used in the rigid square network.*

• *Equations (3.21) - (3.22) and (3.23) discretize the phenomenological model (3.9).*

COMPUTATIONAL ASPECTS

Using a finite volume mesh of a transportation network area (which can be obtained easily by any mesh software for finite volume methods), we deduce a graph of the simplified network obtained at the bi-dimensional scale.

Let us discretize the system of equations (3.10) and (3.11). Let t be fixed. N_{ci}^t for $c \in \mathfrak{C}$ is the number of vehicles of cell c, at time t in the direction i. We supposed we know $N_c^t = (N_{c1}^t, N_{c2}^t, N_{c3}^t, N_{c4}^t)$ at time t in all its 4 directions.

The question is how to compute N_c^{t+1} at the next time step $t+1$.?

Let us propose a consistent time-split numerical scheme consisting by schemes 3.24 and 3.25. First, we solve the linear-quadratic optimization problem (3.21) for the internal flow optimization model. It results r_c^t and q_c^t. The reader is referred to Appendix A for details of the resolution.

After, we use the scheme 3.24 and get an intermediate value of the number of vehicle in each cell, and this at time step $t+1/2$ which we denote by $N_c^{t+1/2}$.

$$\forall t \geqslant 0, \forall c \in \mathfrak{C}, \quad N_c^{t+1/2} = N_c^t + \left(r_c^t - q_c^t\right)\delta t \tag{3.24}$$

Further, we propose the discretization of equations (3.10) and (3.11) as follows (scheme 3.25).

$$\forall t \geqslant 0, \forall c \in \mathfrak{C}, \quad N_c^{t+1} = N_c^{t+1/2} + \sum_{g \in Neighbor(c)} \left(Q_{fc}^t - R_{cg}^t \right) \delta t \qquad (3.25)$$

Hence, to compute bi-dimensional cells flows, the general structure of the algorithm is shown schematically in Fig. 3.7.

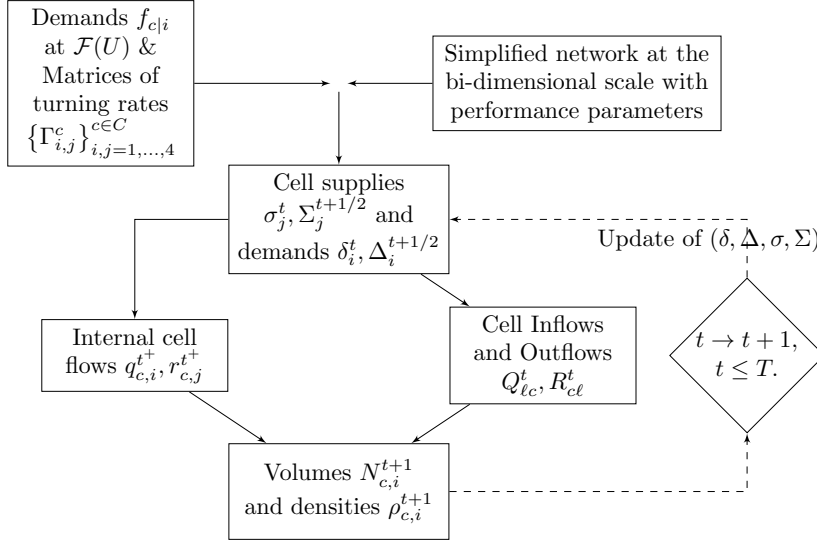Figure 3.7: Bi-dimensional network flows computing engine.

At each time step in the computation, the number of vehicles $N_{c,i}(t+1)$ in cell $c \in \mathfrak{C}$ is calculated by applying successively the scheme 3.24 and the scheme 3.25. $\mathscr{F}(U)$ denotes the cell interfaces at the entry and exit points of the network domain U. We summarrize these with this large anisotropic Algorithm 3.2.

Algorithm 2 Computation of flows of large anisotropic continuous networks

---

Step 1.   Mesh surface network domain in $2d$ elementary cells. Calibrate

parameters of the network domain within cells: residual

capacity in the directions of each cell, density in the cells

at the initial time (network is it empty ?).

Step 2.   Load the demand profile $f_{c|i}$ at the entries $\mathscr{F}(U)$ of the network

domain U and the matrices of turning rates $\left\{ \Gamma_{i,j}^{c} \right\}_{i,j=1,2,3,4}^{c \in \mathfrak{C}}$.

Step 3.   Time iteration: Do the items below.

• Iterate through interfaces ℓ of each cell $(c) \in \mathfrak{C}$ and calculate Inflows

$QI_{\ell|i}^{t}$ and Outflows $QO_{\ell|i}^{t}$, taking into account the lane density $\lambda_{c|i}$.

• Resolve the linear-quadratic optimization problem (3.21) and get

the 4 cell internal inflows $QIint_{\ell|i}^{t}$ and 4 cell internal ouflows

$QOint_{\ell|i}^{t}$, for all interfaces ℓ of each cell $(c) \in \mathfrak{C}$.

• Apply the conservation law to calculate the number of vehicles $N_{c|i}^{t}$

for $c \in \mathfrak{C}$ and for $i \in \{1, 2, 3, 4\}$.

• Compute the densities $\rho_{c|i}^{t}$ for $c \in \mathfrak{C}$ and for $i \in \{1, 2, 3, 4\}$.

Table 3.2: Large anisotropic continuous networks Algorithm.

Numerical experiments are provided in the next section 3.5.

3.5   Validation

We provide in this section some numerical results and numerical analysis in order to validate
the proposed semi-discretized shape of the dynamic BTF model.

Case Studies

For the sake of simplicity we take a triangular FD (see Fig. 3.8) in all the case studies.
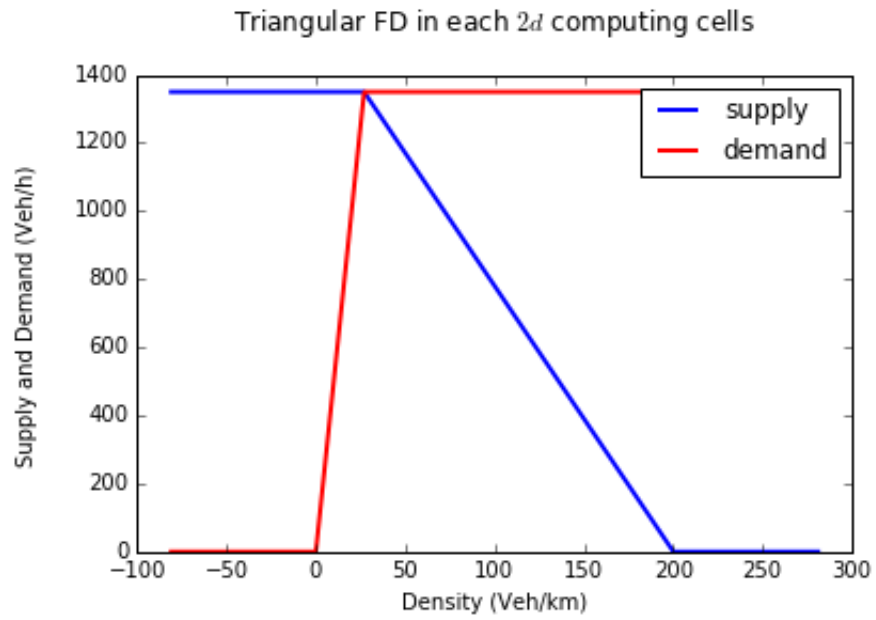
Figure 3.8: Lane FD in each 2d elementary cell.

Let us mention that we do not address queues containing bulk traffic flow generated by the profile traffic demand.

Case study 1

Let us take a surface network whose network domain is meshed in 4 rectangular cells. It is depicted by Fig. 3.21.
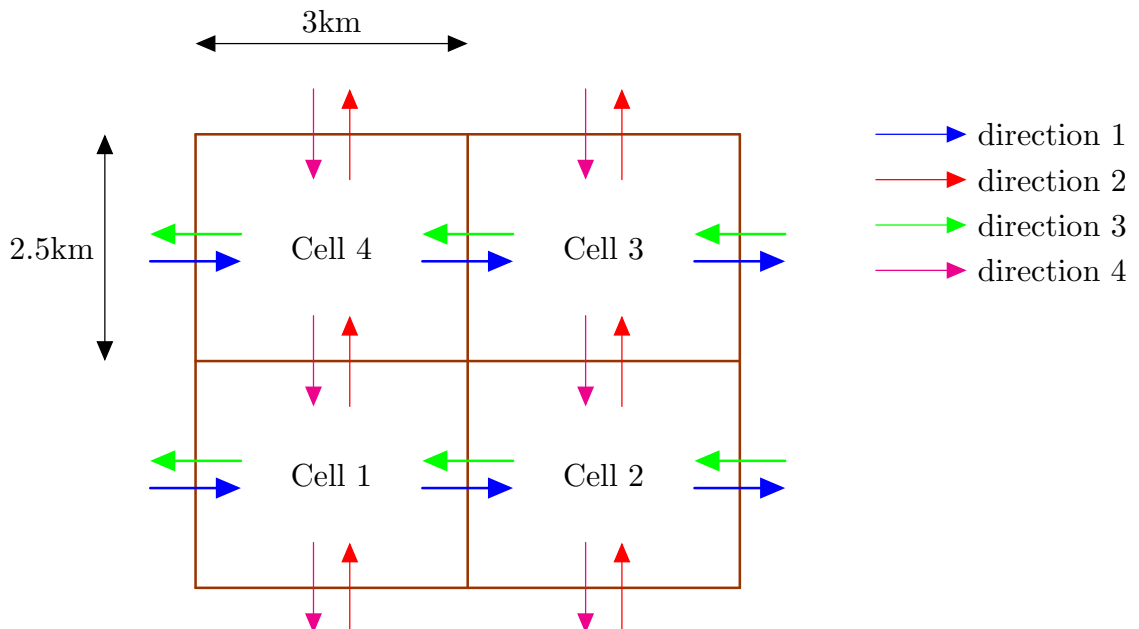
Figure 3.9: Mesh of the Network domain 1 in four 2d elementary cells.

The area of the network is 30 km^2. In the following we set the characteristics of the four cells which comprise the network domain.

	Cell 1, 2, 3, 4
Length	3 km
Width	2.5 km
$\mu_{c,1}$	26
$\mu_{c,2}$	25
$\mu_{c,3}$	23
$\mu_{c,4}$	21

	Cell 1, 2, 3, 4
maximal density	720 Veh/km/lane
critical density	97.2 Veh/km/lane
maximal velocity	50 km/h/lane

Table 3.3: Characteristics of the surface network (network domain): case study 1.

The testing results. First we set the traffic demand constant and equal to 1080 Veh/h/lane at the entry points of the network while the traffic supply at the exit points of the network is equal to 1350 Veh/h/lane. The testing results are the following.

Figure 3.10: Inflows of the 2d elementary cells.

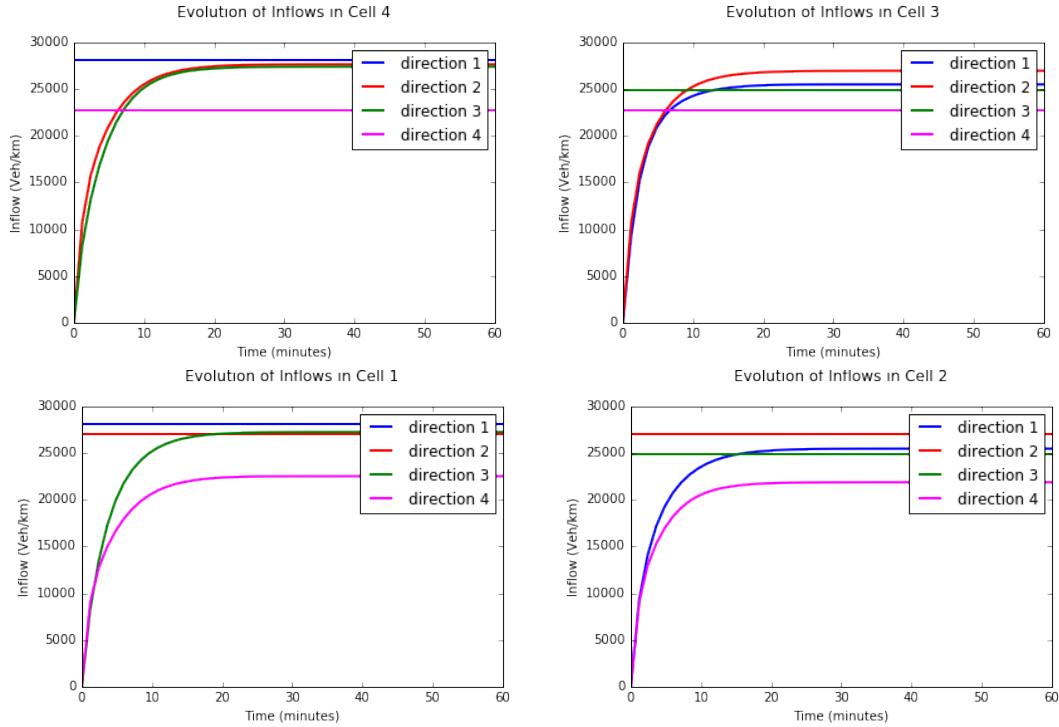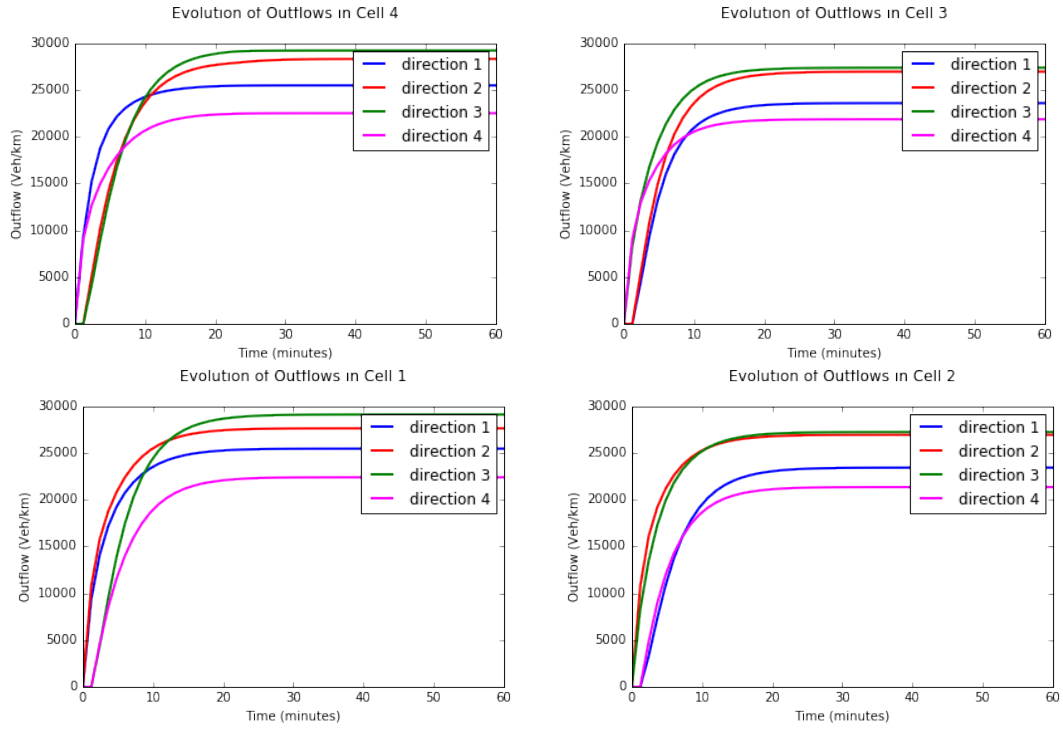Figure 3.11: Outflows from the 2*d* elementary cells.

Figure 3.12: Internal Inflows in the 2*d* elementary cells.
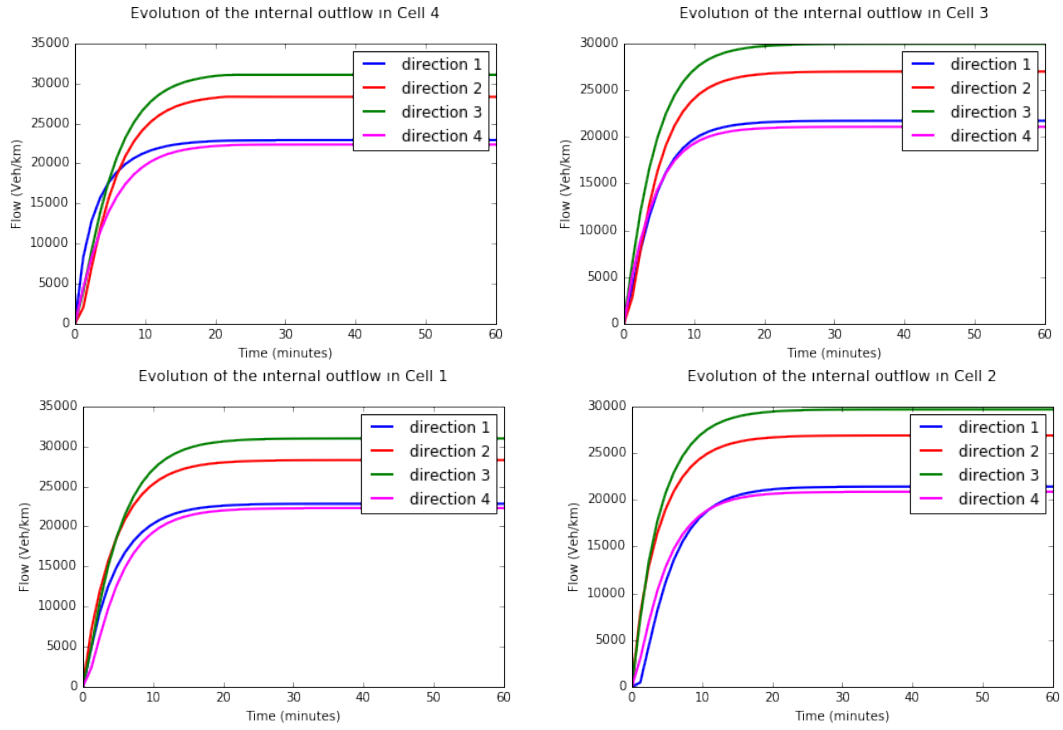
Figure 3.13: Internal Outflows in the $2d$ elementary cells.
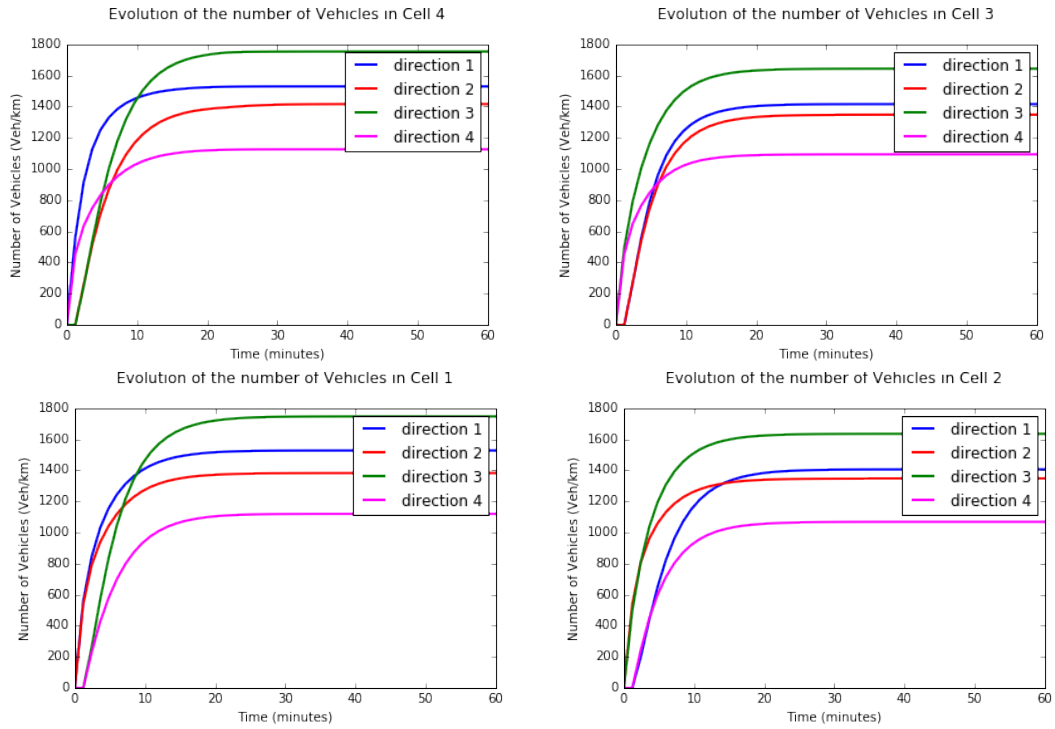
Figure 3.14: Number of Vehicles in the $2d$ elementary cells.
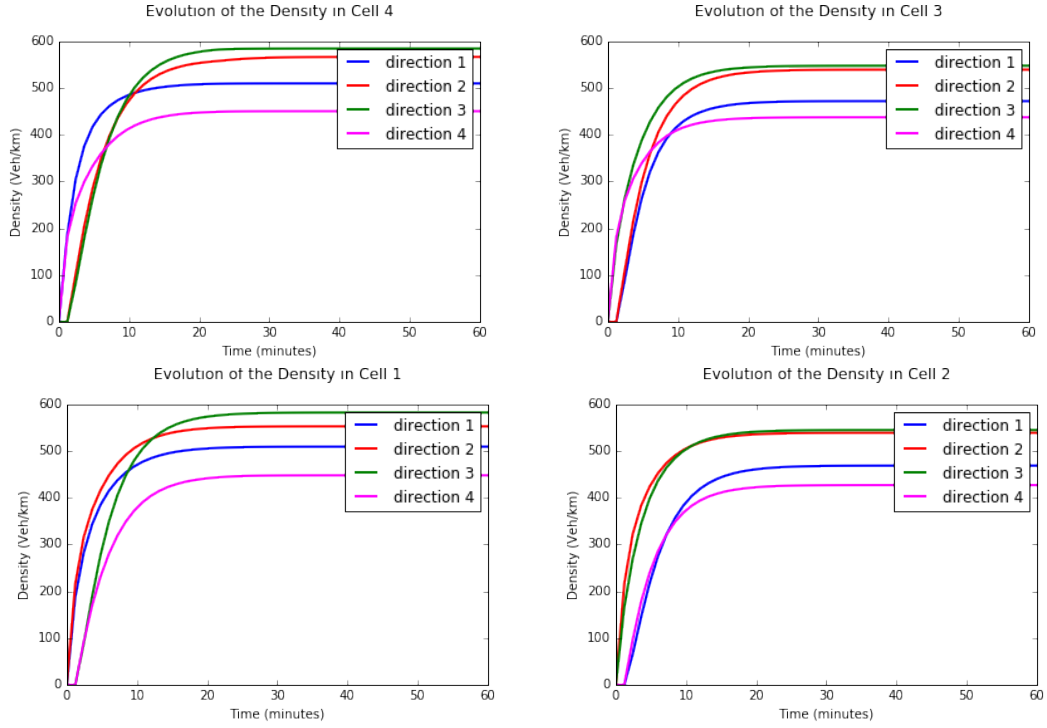
Figure 3.15: Density of the $2d$ elementary cells.

We consider the hypothetical network empty at the initial time of the simulation. In this first case where the demand for travel is constant and less than the supply of the network during the entire simulation, the hypothetical network fills up fast when running the two-dimensional simulator. We reach the equilibrium of the traffic fairly quickly, in the order of 10 to 20 minutes.

Let us simulate again the traffic in the considered hypothetical network with some restrictions: we reduce the residual capacity/supply to 720 Veh/km/lane on the exits of the cells 1 and 3, respectively in the directions 3 and 2, at the time $t = \dfrac{\text{number of time steps}}{4}$. Below are the testing results.
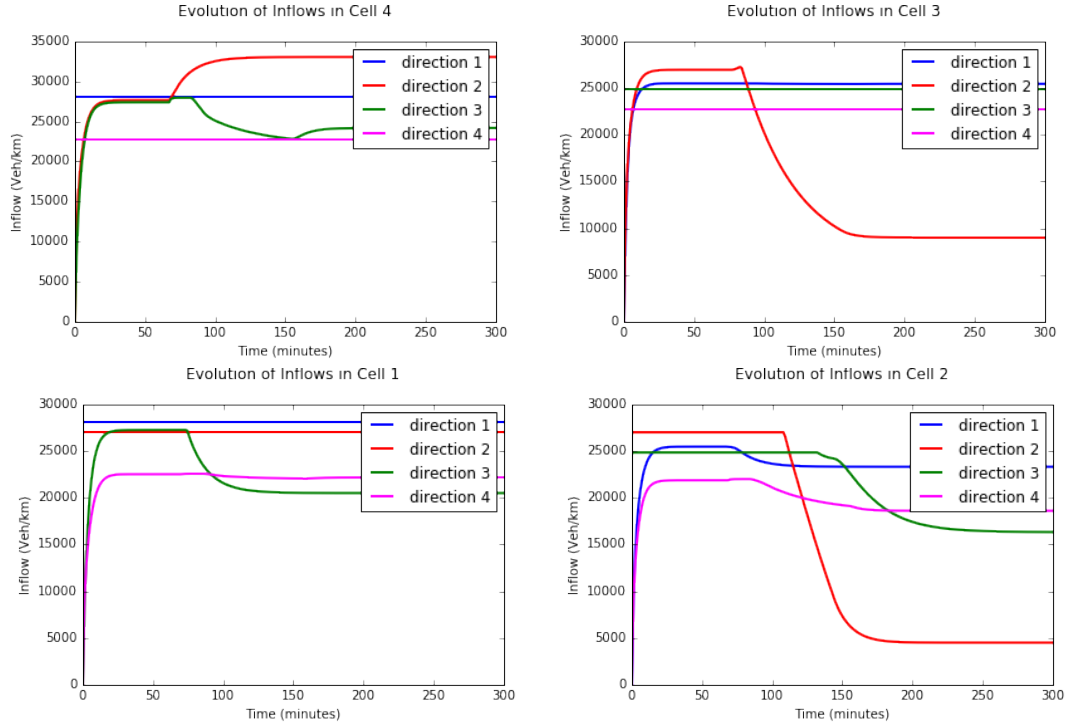
Figure 3.16: Inflows of the 2d elementary cells.
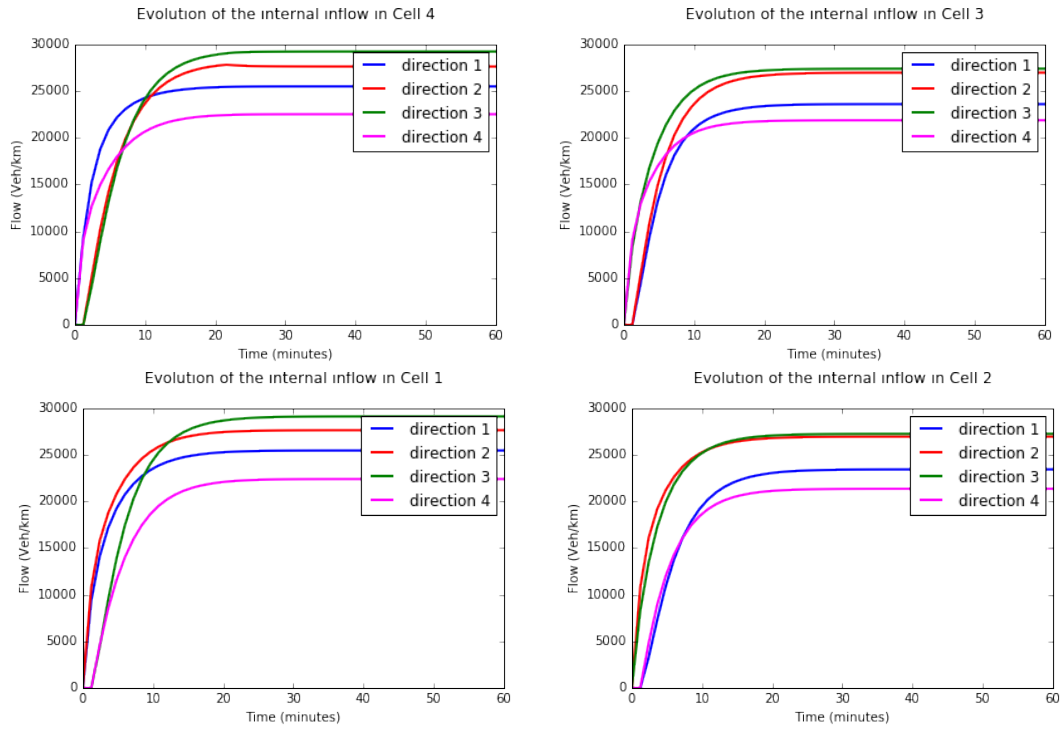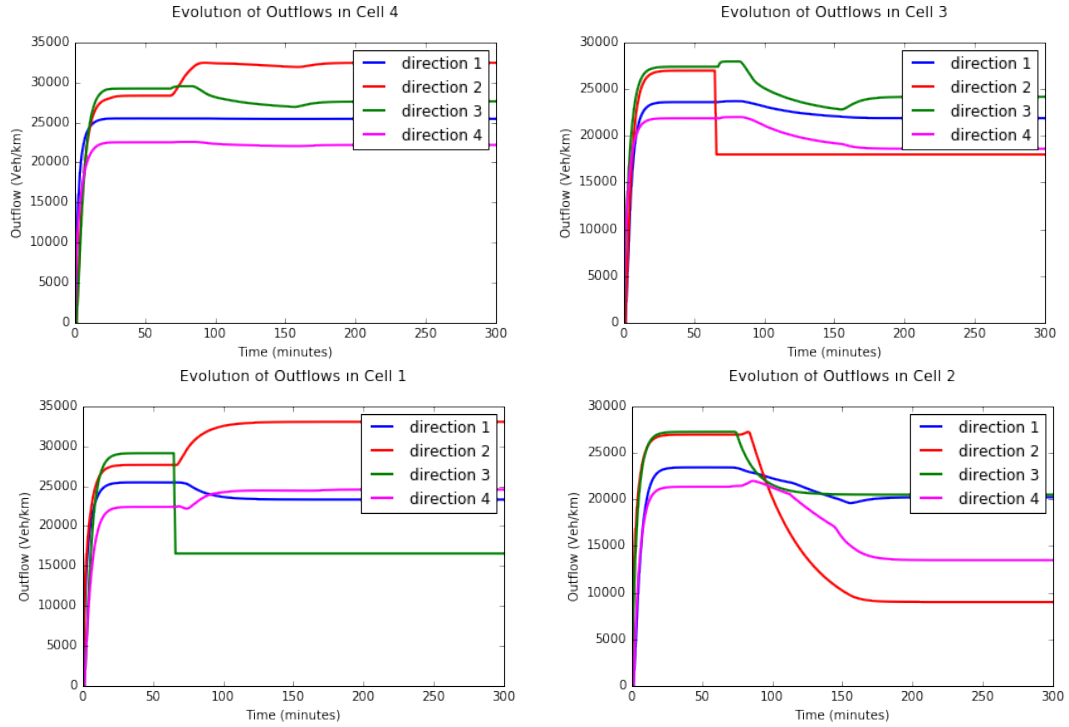

Figure 3.17: Outflows from the 2d elementary cells.

99
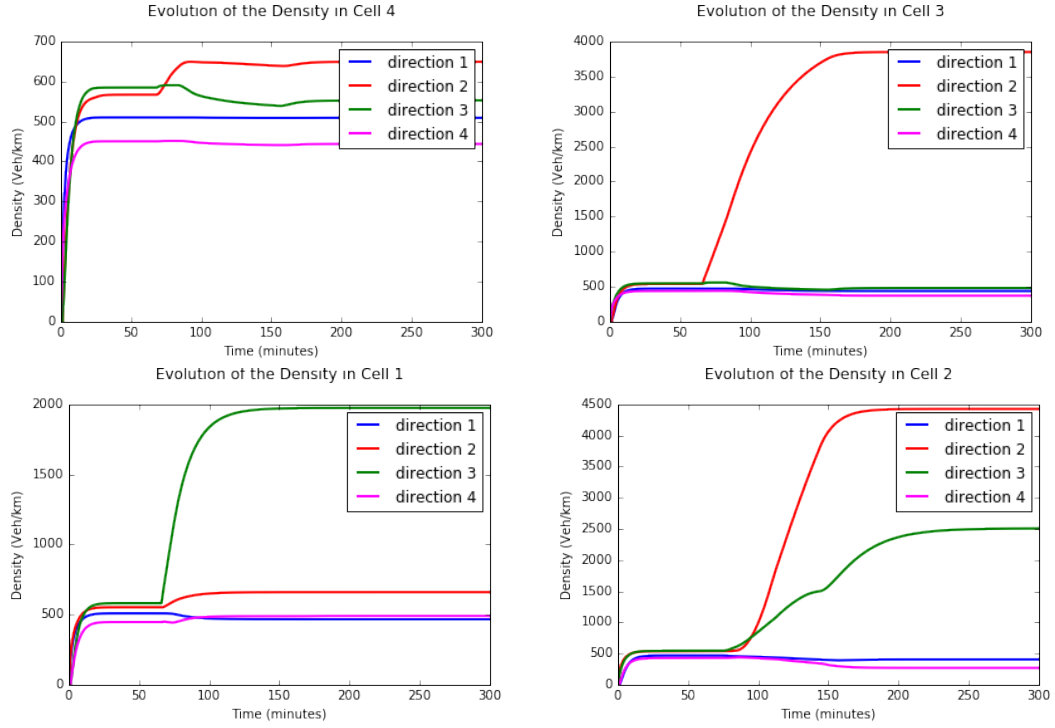
Figure 3.18: Density of the 2*d* elementary cells.

As we expected, before the special time where the capacity of the network in some directions is restricted, inflows and outflows have evolved exactly as in the first case scenario. In the direction 2 of the cell 3 and direction 3 of the cell 1, in and out flows have significantly decreased from the time of the network capacity-restriction. That explains the fact that the density has become important in such directions from this time, as shown by Fig. 3.18 above.

Another case scenario is an input demand profile and without any restriction, depicted by Fig. 3.19 as below.
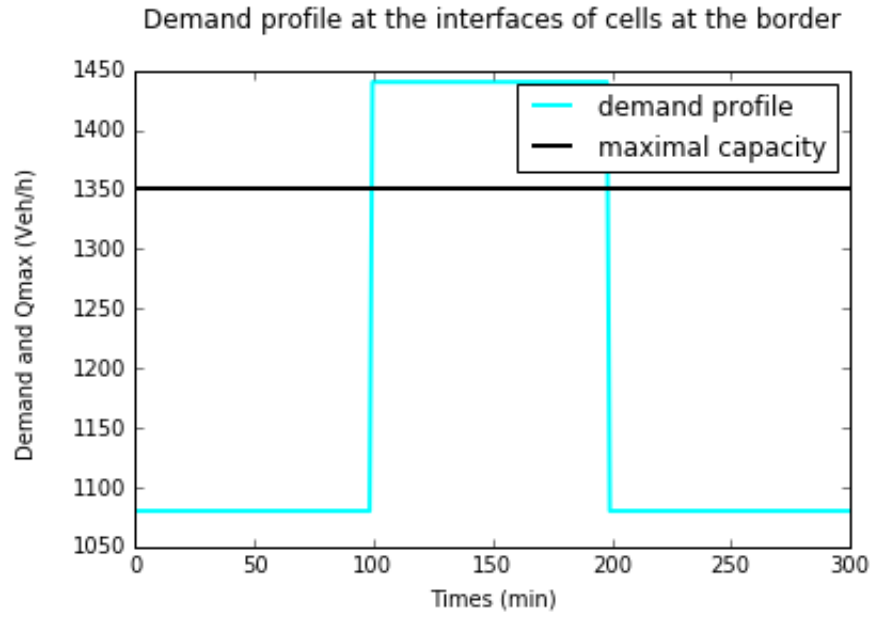
Figure 3.19: Demand profile at the entry of the network 1

Figure 3.20 shows the evolution of the density with such a transport demand profile.
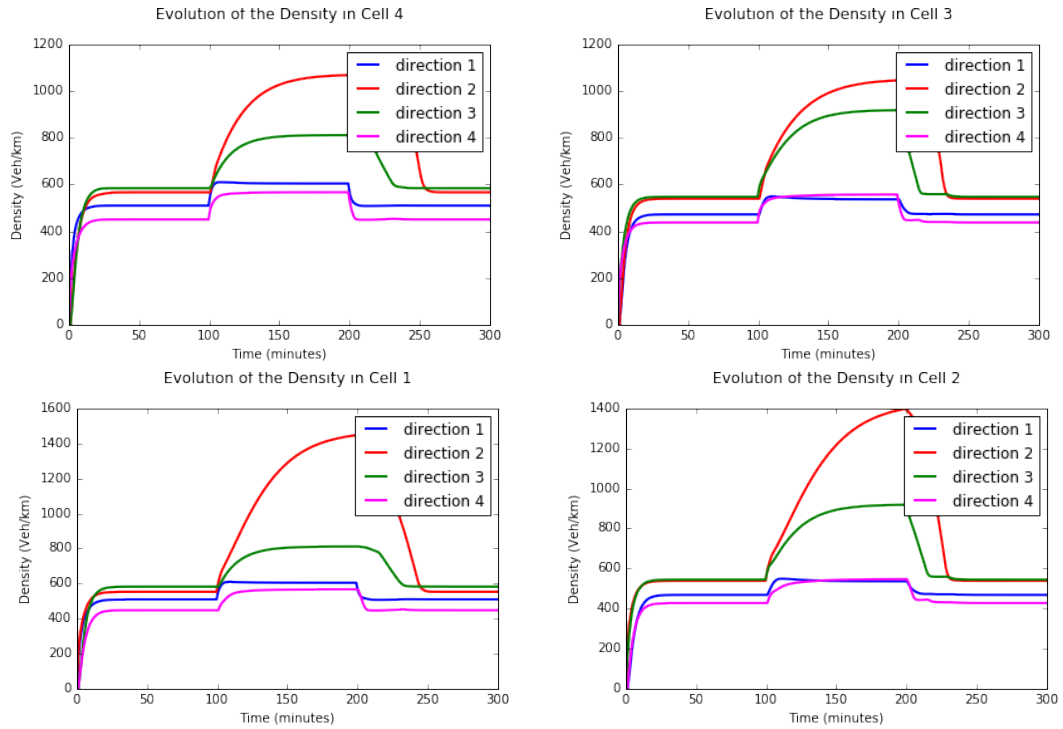
Figure 3.20: Density of the $2d$ elementary cells with non constant demand at the entry of the network.

This result suggests a combination of the results of the two previous scenarios. It explains

that the dynamic bi-dimensional traffic flow model handles efficiently a dynamic transport demand, even during times the transport demand is greater than the network supply.

Case study 2: A greater surface network

Let us take some very large surface network of $12 \, \text{km} \times 11.04 \, \text{km} = 132.48 \, \text{km}^2$. Its network domain is meshed in 20 $2d$ elementary cells. Below Fig. 3.21 shows the mesh of such surface network and its graph representation.
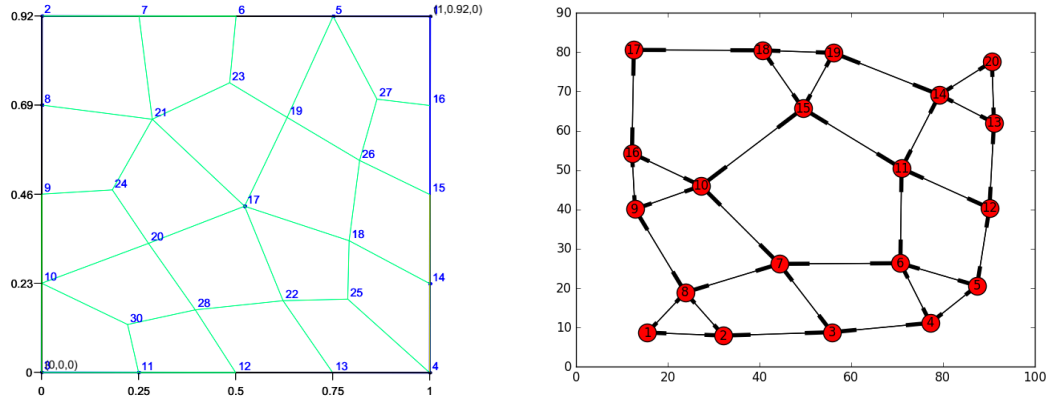
Figure 3.21: Mesh to a Network domain

At the left, a non-uniform mesh of the network domain and at the right, its corresponding weighted directed graph. Every node at the right represents the center of a quadrangular cell at the left. In each quadrangular cell the considered directions of propagation of vehicles flow are the same.

The testing results   We run the bi-dimensional simulation engine using the network domain of Figure 3.21 shown above. Let us remind that there are 6 significant variables: the internal flow and the internal outflow, the inflow and the outflow, the number of vehicles and the density, all following the dominant directions of propagation of each bi-dimensional cell. Since there are 20 cells, there is a total of $6 \times 20 = 120$ figures to shown. We choose to show the results concerning some cells, for instance cells 4, 5, 14 and 20. Cells 4 and 5 on the one hand, and cells 14 and 20 on the other hand have a certain peculiarity. We see that the dominant outgoing direction 1 of cell 4 and the dominant outgoing direction 4 of cell 5 cross the interface $1, 25$. It is a peculiarity since 1 and 4 are not usual pairwise opposite directions of propagation. In the same way, the outgoing directions 2 and 3 of cells 14 and 20 (respectively) through the interface $5, 27$ are not usual pairwise opposite directions of

propagation since the common pairwise opposite directions of propagation are i and $i+2$ for $i = 1, 2$.

First, we take a constant demand equal to 1080 Veh/h/lane at the entries of the network domain like in the case study 1. Let us see certain results below.
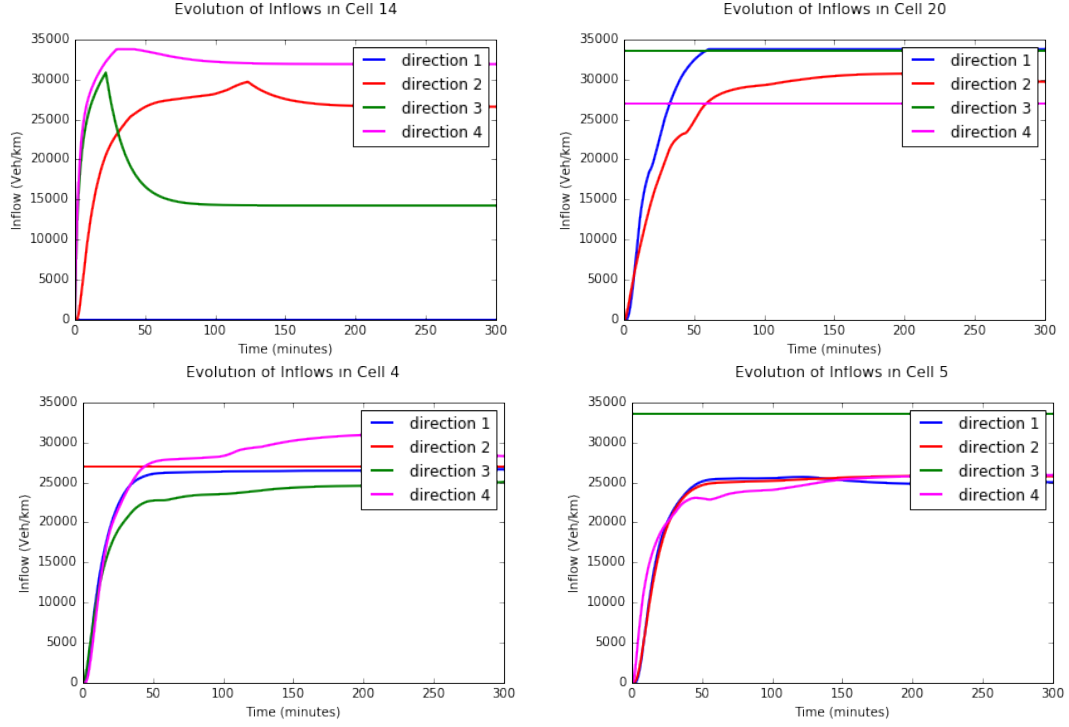
Figure 3.22: Inflows of the cells 4, 5, 14, 20.
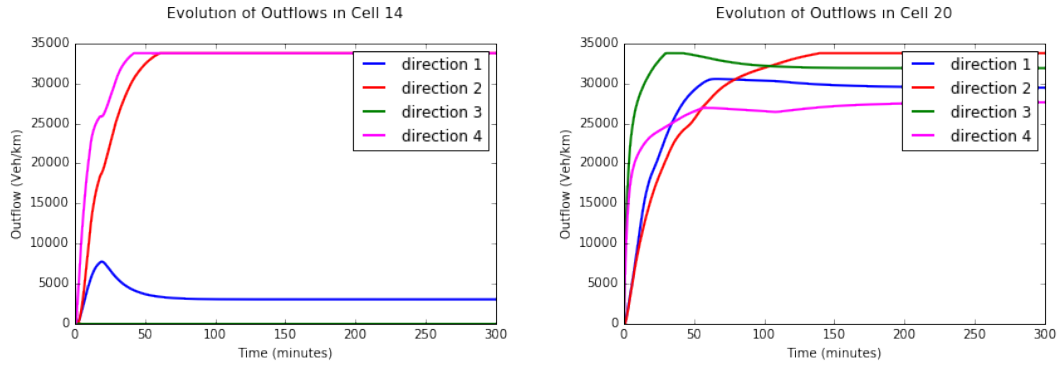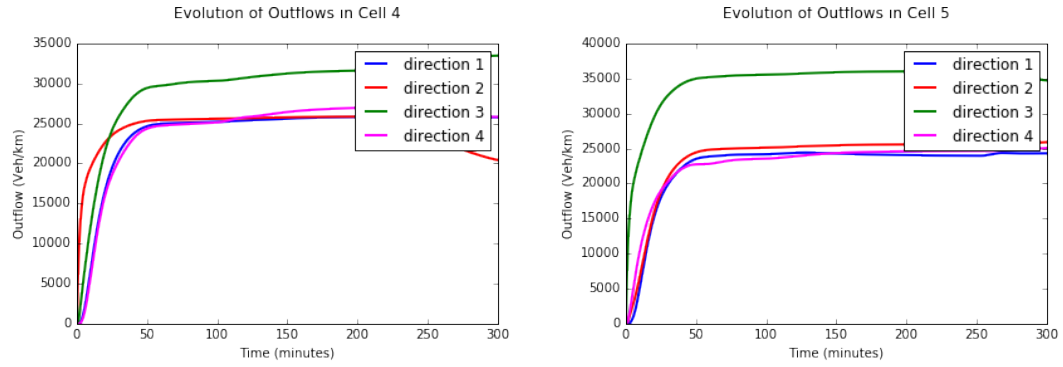
Figure 3.23: Outflows of the cells 4, 5, 14, 20.
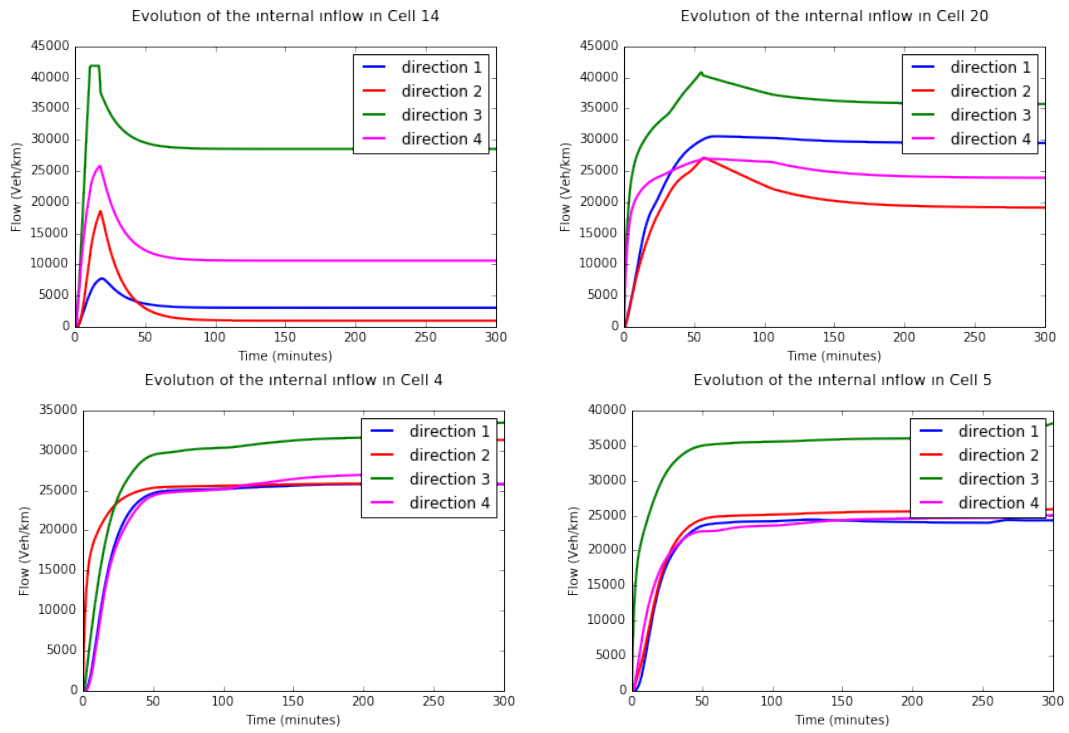
Figure 3.24: Internal Inflows of the cells 4, 5, 14, 20.
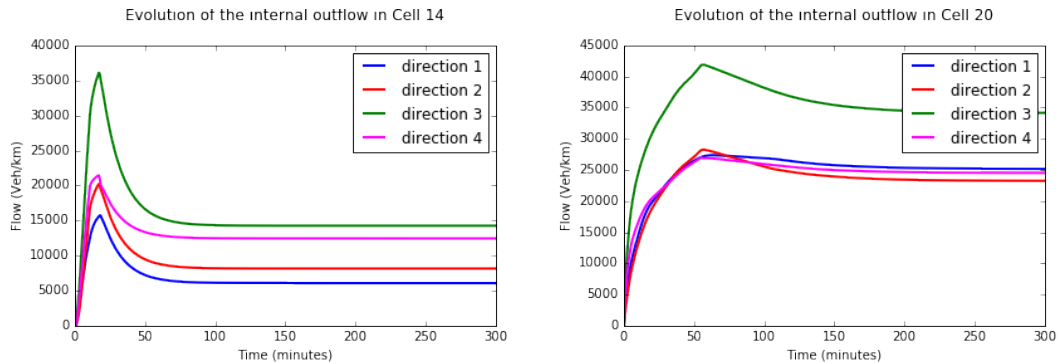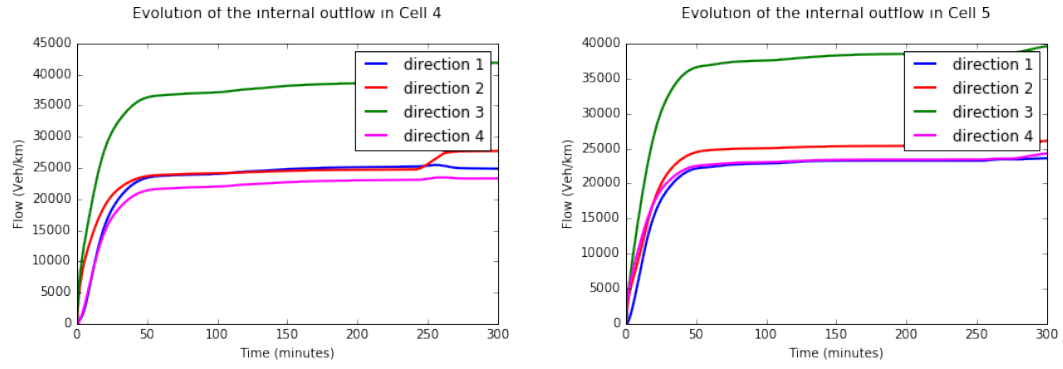
Figure 3.25: Internal Outflows of the cells 4, 5, 14, 20.
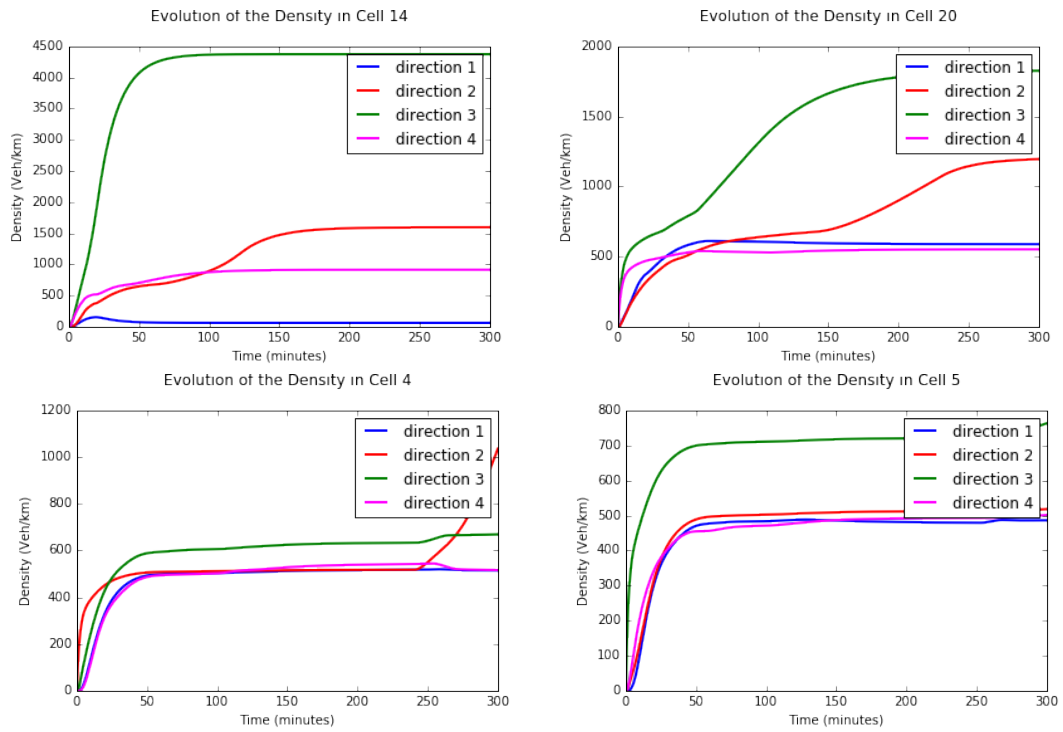
Figure 3.26: Density of the cells 4, 5, 14, 20.

Using the same profile demand at the entries of the network, we get below results.
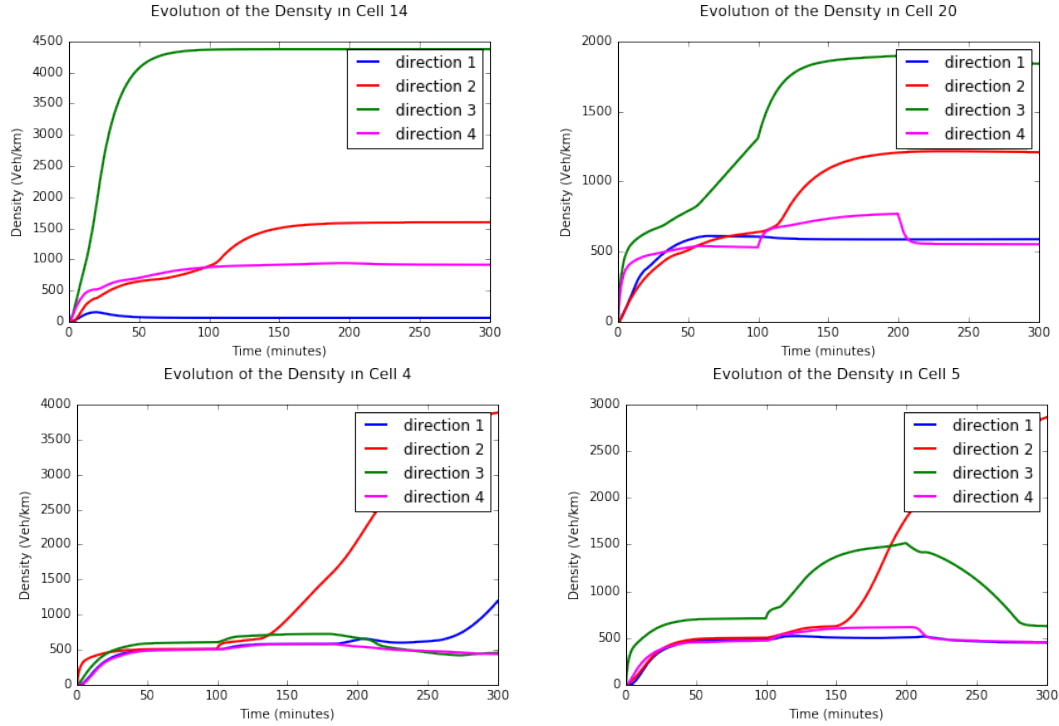
Figure 3.27: Density of the cells 4, 5, 14, 20 with non constant demand at the entry of the network.

Convergence of the dynamic bi-dimensional traffic flow model

In all illustrations, the variables of $\rho_{c,i}^t$ are scaled by ρ_{max}. The Courant-Friedrichs-Lewy (CFL) number is defined by $\text{CFL} = \dfrac{\ell_{xy}}{2 * V_{max}}$ with ℓ_{xy} the minimal length of all lengths of the $2d$ elementary cells, and V_{max} being the maximal velocity in all the four directions of cells. The time step δt is set to be $\delta t = 80\%\text{CFL}$.

In the case scenarios, the dynamic BTF model allows to reach the equilibrium of the traffic fairly quickly, in the order of 10 to 20 minutes. It is a great advantage compared to microscopic or macroscopic simulation traffic flow models.

Summary and perspectives

To summarize, large transportation networks management requires specific traffic flow simulation model. We have developed mathematical and physical approaches in this framework. We comes that we could simulate and regulate very large transport surface networks just using scarce traffic data. In addition, the BTF model is efficient applied to any large scale orthotropic or anisotropic surface networks for which their traffic is assumed homogeneous

or even heterogeneous. That is not the case when MFD based dynamic traffic flow models are used [11, 12, 6, 10, Daganzo, Daganzo and Geroliminis, Cassidy, Courbon and Leclercq]. The MFD is more right for Freeways networks. It is the case of MFD applied to large surface networks which traffic is supposed to be homogeneous. The thing is that in a zone the MFD approach defines its traffic states from an assumption of homogenization of traffic. In the bi-dimensional traffic theory, as many fundamental diagrams as number of dominant directions (or privileged directions) of propagation of flows need. Moreover, from any cell to another, the BTF theory is right also when the dominant directions are different.

3.6   Conclusion

In the field of traffic flow modeling of large scale urban networks, a bi-dimensional model of traffic flow within large-scale transportation networks is proposed for dynamic network loading. In discrete-continuous network the coupling of GSOM macroscopic flow model with the bi-dimensional traffic flow model is a key for modeling several cities (road) networks. Such a transport model has the capability to reduce the cumbersome calculations involved when traditional macroscopic flow models are applied to large, dense and inhomogeneous networks. We have found that the dynamic BTF model is also suitable for networks with few traffic detectors.

Mostly dynamic assignment is essential for efficient traffic controlling. We then proposed an assignment methodology based on this bi-dimensional network loading model (refer to the Chapter 6). The bi-dimensional model is completely achieved by the development of *BidiTSim* (Bi-dimensional Transport Simulator) [80, Sossoe and Lebacque].

This page is intentionally left blank.

Chapter 4

Vehicular multimodal traffic flow modeling

Contents

4.1 Introduction

Several transportation systems (of road or rail types) have been progressively built so far, since the recent century, to limit traffic congestion issues in industrialized cities. Since travel demand grows exponentially contrary to physical transport networks, many transportation issues occur.

Motivation

We are witnessing the renewing of existing transport systems and services to mobility in order to respond to daily travel demands of mass transportation in reliable and efficient ways. These are renewing and reinforcements of transport infrastructures and deployments of rapid buses for mass transit. They are complying with the regulation of the reduction of carbon emissions since it use natural gas instead of fuel. Besides, as the technology increases considerably, automatic and autonomous vehicles are designed for efficient Intelligent Transportation Systems (ITS). It is in the context of creating smart network infrastructures for smart territories. One notes the case of Vehicle-to-Vehicle communication (V2V) and Vehicle-to-Infrastructure (V2I) communication technologies. Personal Rapid Transit (PRT) system falls within the framework of these so called intelligent transportation systems, and the scopes for getting smart territories.

(a) skyTran routes designed through buildings   (b) skyTran City-scape

Figure 4.1: skyTran PRT transporters for public transportation (Image courtesy of: www.skytran.com)

A special intelligent transportation system is the skyTran system. It consists of skyTran vehicles operating autonomously in the style of demand-responsive system, equipped with maglev technologies. SkyTran vehicles are also named personal rapid maglev-transporters or sky-podcars. The physical network of the skyTran system is built in the air-space, and the routes are sky-railways.

The skyTran system or technology is designed to respond to transportation issues in the framework of smart transportation for smart cities. skyTran vehicles are high-speed, low-cost, green, elevated and personal rapid transit. These are their advantages: they are fast and they do not operate in the same physical network space as the other ground transport vehicles modes (such public traditional transit vehicles, buses for rapid transit, taxis for particular

services, car-sharing vehicles, private vehicles, etc). Thus, the traffic space is considerably increased in the cities where skyTran is constructed and in operation. The maglev-transporters have the ability to be reliable and they contribute to alleviate traffic congestion.

Meanwhile, traditional modes of transport are also of great importance for the movement of users. We consider that it is essential to combine the traditional modes with new modes and uses. This should allow a greater possibility of choice of users in a multimodal transportation system.

In this situation, what would be an efficient transport simulation model for the prediction and the estimation of vehicles and/or passengers flow within multimodal transportation systems comprising traditional transport modes and theirs uses and by taking also into account the skyTran system and its transport services ? Further issue is that, this transportation pattern can it actually and considerably contribute to an optimal control of the skyTran transit system to an highly optimized traffic monitoring and regulation ?

Organization of the chapter

Since this dissertation particularly focuses on the traffic modeling, we describe in the next section (4.2) dynamics of maglev-personal rapid transporters. We provide a travel demand pattern taking into account the sykTran transit network's supply. Assumptions and analysis for effective operation of this type of personal rapid transit (PRT) systems are carried out. Dynamics of users getting in and out of skyTran vehicles at stations are addressed and modeled. The reactive dynamic traffic assignment in such PRT system is further described. It turns out that the transport model we develop (in the section 4.2) and applied to the skyTran transit system is a traffic pattern for the skyTran system and an archetype for autonomous demand responsive systems.

Theories of multi-graph and multicommodity traffic flow modeling are timely responding to the issues of finding comprehensive solutions to multimodal transport network flows modeling. We hence look forward to improve traffic flow models which implementation could easily induce performances evaluation of multimodal transport road network while providing traffic flow forecasting and estimation (discussed in section 4.4). To achieve this, transport attributes have been used. The reader is referred to multiclass, multilane and multiclass multilane traffic flow models [5, 69, 39, 82]. The multi-attribute model mentions the traffic on highways (which is consisting in several lanes) and the traffic on public network

transit. It corresponds to a macroscopic traffic flow model for main roads and for network public transit lines of a heterogeneous transport network.

The two systems studied in this chapter are archetypes of non general transportation systems.

4.2 Modeling skyTran network

It is assumed that the PRT system is designed to operate autonomously, and that it is equipped with an adaptive cruise control maneuvering for a smooth traffic controlling, to ensure safety, reliability and security of the system. Let us recall that this system is an archetype for autonomous demand responsive systems.

The corresponding graph

In connection with transport graph as well, a maglev-graph includes few different components. Denoted by $\mathscr{G}_{\mathcal{M}}$, it is a quadruple of sets $(\mathscr{N}_{\mathcal{M}}, \mathscr{A}_{\mathcal{M}}, \mathscr{L}_{\mathcal{M}}, \mathscr{P}_{\mathcal{M}})$. $\mathscr{N}_{\mathcal{M}}$ is the set of all nodes. These are intersections and poles of stations (departures and arrivals portals of sky-station) of the maglev system. $\mathscr{A}_{\mathcal{M}}$ is the set of arcs connecting two nodes of same maglev-lanes. Maglev-lanes are deceleration lanes, non-stop guide-ways, acceleration non-stop guide-ways (or simply called acceleration lanes) which are vertically set up above the former. $\mathscr{L}_{\mathcal{M}}$ denotes the set of all lanes. $\mathscr{P}_{\mathcal{M}}$ denotes the set of all pairs of portals (departure and arrival portals) that physically represent the stations. At any station, there is an "off line guide-way" which keeps sky-podcars that are at rest waiting for passengers to board. Intersections allow sky-podcars to switch from "acceleration lane" onto "low non-stop guide-way", and inversely.

Model of the system

This section provides a fluid model for the dynamic of skyTran vehicles in Lagrangian coordinates. Afterwards, the passengers travel demand, constrained by the supply of the syTran transit system, is optimized. Moreover, we analyze spatial interactions of skyTran transit system with existing systems of other transport modes.

Sky-podcar motion formulation

To set ideas on the dynamic of sky-podcars along sky-railways, the following assumptions have made on the functioning of the skyTran transit system.

i- The number of sky-podcar stations in the system can be as high as desired to reach all transport demands.

ii- Sky-podcars do not takeover each other except at internal intersections (where they can switch from vertical lines that are connected via specific intersection dedicated to switching).

iii- The capacity of a sky-podcar is limited, taking a finite number of passengers of "similar profile", for instance of same origin and destination.

iv- A sky-podcar is available for only one transport demand.

v- For each transport demand in the system, more than one passenger can enter in the sky-podcar at the starter station from departure portal to the arrival portal of the target destination station.

vi- Maglev-lines at the same elevation cannot intersect with each other at a station; maglev-lines of different levels interconnect together at station poles. This allows avoidance of collisions. Exchange of traffic between two maglev-lines of different levels is carried out through the poles at the station levels.

vii- Generally, we assume that the considered demand-responsive transportation system is equipped with an adaptive cruise control that increases the driving comfort, reducing traffic accidents and increasing the traffic flow throughput.

viii- In the context of skyTran transit system energy consumption, it is assumed that acceleration of sky-podcar does not cost anything while it is offset by deceleration. However, this aspect which concerns the control of the energy consumption of the system is not addressed in this dissertation.

Let S be the set of all stations $s \in$ S of the maglev-system. Let x denote the position of sky-podcar, $t \geqslant 0$ the time and a the podcar index. $\{x_a(t), \ t \in \mathbb{R}^+\}$ refers to the trajectory of the sky-podcar $a \in \Lambda$, Λ being the total number of sky-podcars that is operating in the skyTran transit system, and $x_a^j(t)$ is referring to the position of a on the arc $(j) \in \mathscr{A}_{\mathscr{M}}$. Let $u_a(t)$ be the speed of the sky-podcar a at the time t, and $w_a(t)$ the acceleration-deceleration of the pod a at the time t. Assuming that vehicles are labeled according to a snapshot of line from downstream to upstream, the sky-podcar labels will increase with the position x. Therefore, $r_a(t) = x_{a-1}(t) - x_a(t)$ is the spacing between vehicle a and its leader $a-1$ at time t, and $v_a(t) = \dot{r}_a(t) = \dot{x}_{a-1}(t) - \dot{x}_a(t) = u_{a-1}(t) - u_a(t)$ is its relative velocity at the same time t.

Motion of skyTran vehicles along sky-ways stretches Let us describe the dynamic of the vehicles along the sky transit network. Along the same lane, and on a section without intersection and without switch pole, the dynamic of sky-podcar is governed by the following system of equations (as one can observe it in several car-following transport models in the literature, also known as time-continuous models):

$\forall t \geq 0, \forall a \in \Lambda, \exists!(j) \in \mathscr{A}_{\mathcal{M}}$ such that:

$$\begin{cases} x_a^j(t+1) = x_a^j(t) + \delta t u_a^j(t) \\ u_a^j(t) = \min\left(U_e\left(r_a^j(t)\right), u_{p_a}\left(x_a^j(t)\right)\right). \end{cases} \tag{4.1}$$

$U_e\left(r_a^j(t)\right)$ is the speed equilibrium relationship between followers skyTran vehicles on same sky-lane. It is depicted by Fig. 4.2.
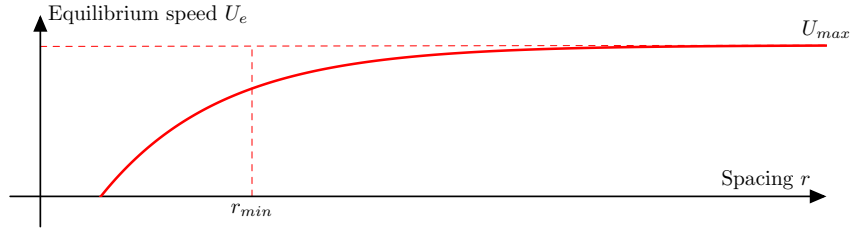
Figure 4.2: Spacing-equilibrium speed fundamental diagram of sky-podcar motion

During high traffic interruption on sky-lane, we argue that sky-podcar speed should also depend on what it is called the velocity profile of sky-podcar which depends on its mission, position on the sky-lane and spacing r_a between its followers sky-podcars. We denote $u_{p_a}\left(x_a^j(t)\right)$ the sky-podcar velocity profile of the pod-car a. It depends on its mission and the charge of the current link (j). In the sake of capturing all cases, one may applied a following dynamic system (4.2) instead of the system of governing equations (4.1):

$\forall t \geq 0, \forall a \in \Lambda, \exists!(j) \in A_M$ such that,

$$\begin{cases} x_a^j(t+1) = x_a^j(t) + \delta t u_a^j(t) \\ u_a^j(t+1) = \min\left(u_a^j(t) + \delta t w_a^j(t), U_e\left(r_a^j(t)\right), u_{p_a}\left(x_a^j(t)\right)\right) \\ w_a^j(t) = f_a\left(r_a^j(t), u_a^j(t)\right). \end{cases} \tag{4.2}$$

where f_a captures deceleration and acceleration constraints of the podcar a during interrupted traffic or traffic breakdowns.
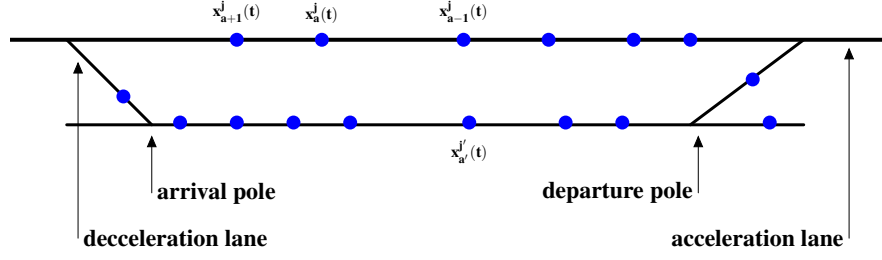
Figure 4.3: Notations of sky-podcar following model.

Motion of sky-podcars across intersections In this paragraph is briefly described how merges and diverges work in the proposed Lagrangian transport model for maglev PRT network. It is clear that diverges are trivial. Merges are then analyzed in the following. Let a be the first podcar on an upstream link (j). Let (d_1) be the next link pertaining to the mission of the podcar a, and nd_1 be the last podcar on this lane. Then the motion of the podcar a is given by Eq. (4.2) with $r_a^j(t)$ being the sum of the distance from a to the intersection plus the distance from the intersection (I) to the podcar nd_1. This can be stated as:

$$r_a^j(t) = |x_a(t) - x_I|_{(j)} + |x_I - x_{nd_1}|_{(d_1)}.$$

Let us now consider a merge with two upstream links (u_1) and (u_2), and (d) the downstream link, a_1 and a_2 the first podcars on links (u_1) and (u_2) respectively, and a_d the last podcar on the downstream link. The two upstream podcars are liable to compete for passage through the intersection (I). The first issue to be solved is to determine which podcar will cross first the intersection (I). For each podcar a_i, $i = 1, 2$, we calculate for $i = 1, 2$, time $\Delta t_i = |x_{a_i}(t) - x_I|_{(u_i)}/u_{a_i}^{u_i}(t)$, required to reach the intersection (I) according to the incoming line (i). The velocity $u_{a_i}^{u_i}(t)$ is calculated following Eq. (4.2), with the distance $r_{a_i}^j(t)$ being the sum of the distance from a_i to the intersection plus the distance from the intersection to the podcar $a_d : r_{a_i}^j(t) = |x_{a_i}^j(t) - x_I|_{(u_i)} + |x_I - x_{a_d}(t)|_{(d)}$.

115
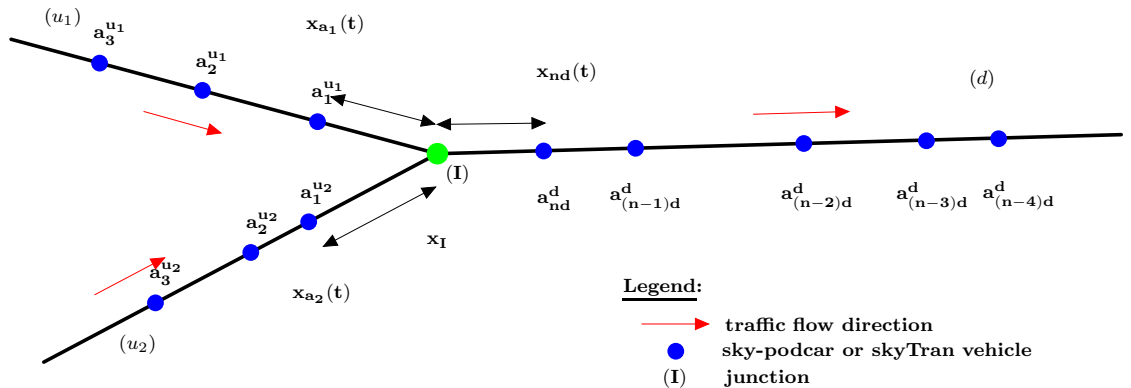
Figure 4.4: Merge node model

Once the order of passage is decided, it is not changed. The trajectory of the first podcar to pass is calculated by Eq. 4.2 with respect to the podcar a_d. Let a_1 be this podcar. The trajectory of the second podcar is calculated with respect to the podcar a_d but with an additional term forcing passage as second. This term is applied as long as the podcar a_1 has not exited link (a_1). Thus, the velocity of the podcar a_2 at the next instant time $t + 1$ being $u_{a_2}^{u_2}(t+1)$ is calculated by:

$$u_{a_2}^{u_2}(t+1) = \min\left(u_{a_2}^{u_2}(t) + \delta t w_{a_2}^{u_2}(t),\ U_e\left(r_{a_2}^{u_2}(t)\right),\ u_{p_a}\left(x_{a_2}^{u_2}(t)\right),\ \alpha \times u_{a_2 \neg a_1}^*(t)\right) \qquad (4.3)$$

where

$$u_{a_2 \neg a_1}^*(t) = \frac{|x_{a_2}(t) - x_I|_{(a_2)}}{|x_{a_1}(t) - x_I|_{(a_1)}} u_{a_1}^{u_1}(t) \qquad (4.4)$$

is the velocity constraint for a_2 to be the second podcar to pass across the merge intersection (I), from the time t to the time $t + \delta t_2 \leqslant t + |x_{a_2}(t) - x_I|_{(a_2)} \times u_{a_2 \neg a_1}^*(t)$, and where the coefficient α is a sensitivity parameter for the calibration.

Travelers' demand optimization pattern

Notations and definitions are the following.

- k, ℓ, m : the indexes of stations (destinations or origin points of the trips).

- $T_{m\ell}(t)$: the demand of displacement from the station ℓ to the station m : $(\ell \rightarrow m)$ between the instants times t and $t + \delta t$. There is $T_{m\ell}(t)\delta t$ passengers that want to travel from the station ℓ to the station m.

- $N_\ell(t)$: the number of sky-podcars at the station ℓ.

- $K_\ell(t)$: the maximal capacity in term of number of travelers that can board at the station ℓ, and at the time t.
  The following relation holds : $N_\ell(t) * K_R = K_\ell(t)$, with K_R the residual capacity of any sky-podcar, with $K_\ell(t) \leqslant \overline{K}_\ell\ \forall t$ and $\mathbb{N}^* \ni \overline{K}_\ell$ being the maximal number of sky-podcars handle-able in the station ℓ.

- $K_\sigma(t)$: the capacity of the sky-podcar σ at time t. This variable changes only at stations due to the passengers boarding in σ and the passengers exiting the σ. So K_R constrains $K_\sigma(t)$ such that $K_\sigma(t) \leqslant K_R, \forall t$.

- $S_W(\ell, t)$: the ordered set of sky-podcars waiting at station ℓ to board passengers at the time t.

- $D_\ell(t)$: the demand at the station ℓ and at the time t.

- $N_{\ell m}(t)$: the number of sky-podcars that want to go to the stop (station) m from the station ℓ at time t. This number represents the total demand at time t and at ℓ of travelers that are going to m.

- $U_\ell(\sigma, t)$: the set of stations for-which the sky-podcar σ can reach from the station ℓ. It refers to the pointed neighborhood of the station ℓ. This set is assumed to contain information on time-dependent shortest paths between the station ℓ and the other stations m of the skyTran system.

- $\tau_{\ell m}$: the travel time from ℓ to the achievable-station $m \in U_\ell(\sigma, t)$.

- $v_{\ell m \sigma}$: the number of travelers from ℓ to m using the sky-podcar σ at the instant time t. That is to say the satisfied demand from ℓ in order to reach m taking σ. This is the number of travelers that is transferring exactly from the stop ℓ to m. This number represents a packet of passengers in the sens of dealing with macroscopic dynamic of travelers. That is to say the performed travelers' demand by the system and from the stop ℓ to m.

- $n_{\ell m}(t)$: the performed travel demand. Hence, the following holds :
$n_{\ell m}(t) = \min(N_{\ell m}(t), K_{\ell m}(t))$ with the equality $K_{\ell m}(t) = \sum_{\sigma \in S(\ell, t) \,;\, m \in U_\ell(\sigma, t)} K_\sigma(t)$.

- $\sigma \in S(\ell, t)$ means that σ is at the station ℓ at time t.

- $m \in U_\ell(\sigma, .)$ means that the station m is in the neighborhood of the station ℓ and that it is easily reachable from ℓ using the sky-podcar σ, when departing at time t from ℓ.

At the station ℓ, the demand $D_\ell(t)$ at time t reduces to: $D_\ell(t) = \sum_m \left\{ \left\lfloor \frac{T_{\ell m}(t) \delta t}{K_R} \right\rfloor + 1 \right\}$ where $\lfloor z \rfloor$ denotes the integer part of the number z. The real volume of traffic departs at the station ℓ at the time t is the following sum $\sum_{m \in U_\ell(\sigma, t)} n_{\ell m}(t)$, where the $n_{\ell m}(t)$ value is calculated as follow by this analytical expression $\sum_{\sigma / m \in U_\ell(\sigma, t)} v_{\ell m \sigma}(t)$.

The estimation of the travel time $\tau_{\ell m}(\sigma, t)$ from ℓ to m of the sky-podcar σ, starting from

the station ℓ at the time t, is suggested to follow the below integer programming problem (4.5):

$$\min \sum_{\sigma \in S(\ell,t)\,;\,m \in U_\ell(\sigma,t)} v_{\ell m \sigma}(t) * \tau_{\ell m}(\sigma,t)$$

$$\text{s.t.} \left| \begin{array}{ll} \displaystyle\sum_{m \in U_\ell(\sigma,t)} v_{\ell m \sigma}(t) \leqslant K_\sigma & \forall \sigma \\[3mm] v_{\ell m \sigma}(t) \in \mathbb{N}^* & \forall \ell, m, \forall \sigma, \forall t \end{array} \right. \tag{4.5}$$

We recall that the demand assigned to any sky-podcar σ cannot exceed its residual capacity K_σ. We assume, for the sake of simplicity, that $K_\sigma = K_R, \forall \sigma$. That is to say that all sky-podcars have the same residual capacity to transport the same maximum number of travelers (users). The unperformed demand in the station ℓ to a station m, is simply the difference $r_{\ell m}(t) = N_{\ell m}(t) - n_{\ell m}(t)$. This value, added to the arrival of sky-podcars at the next time $t + 1$, denoted by $a_{\ell m}(t + 1)$ reduces to $N_{\ell m}(t + 1)$: $N_{\ell m}(t + 1) = r_{\ell m}(t) + a_{\ell m}(t + 1)$.

Numerical resolution of the integer programming (4.5)

We generate a travel demand data as input data of the integer programming problem (4.5) and for the skyTran transport simulation, by implementing these equations and relations (4.2)–(4.5). This profile of travelers' demand depicted by the Figure 4.5 refers to the mean volume of demand at the skyTran stations. We need to disaggregate such demand in time-dependent origin-destination matrices, for successively calculating in time, the skyTran system supply and the performed-travel demand.
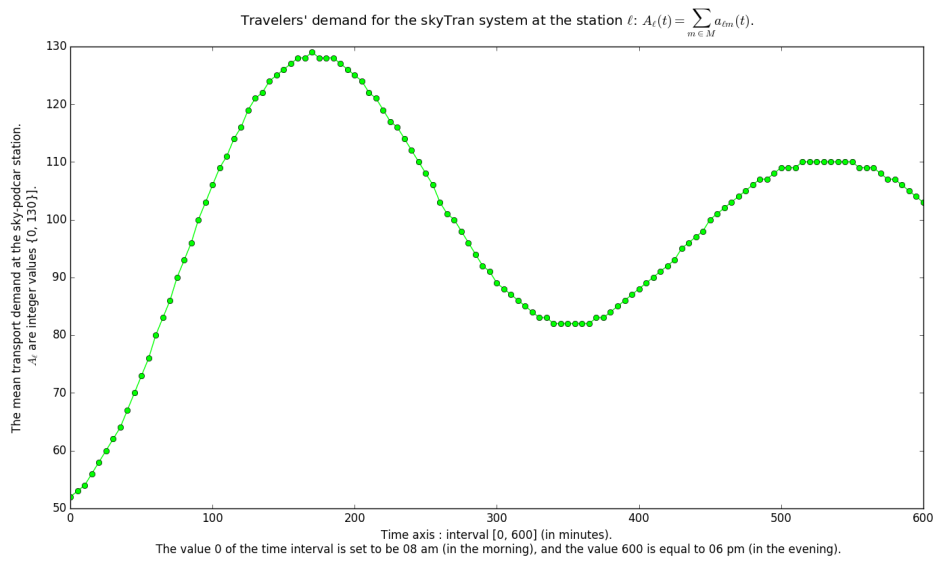
Figure 4.5: The profile of the skyTran passengers' transport demand.

A first implementation of this new demand responsive and personal rapid transit system will be held in the city of Tel-Aviv (see Figure 4.6).
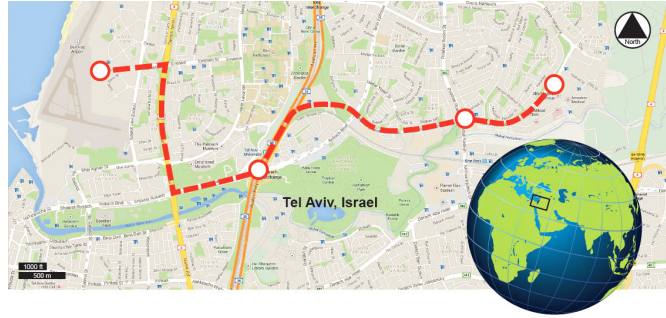
Figure 4.6: Illustrated possible route and street view in a typical city deployment - skyTran route in Tel-Aviv (Image courtesy of: www.skytran.com)

We take as direct weighted graph that of the transit network upon the Figure 4.6. Travel times used in the script are listed in the table below as well as the graph of the transport system.

To solve the optimization problem we use Pyomo. Pyomo is a collection of Python software packages for formulating optimization models [25, 26]. It is an open source algebraic modeling language.Since its introduction, Pyomo has undergone major restructuring and extension, such that Pyomo is now stable, flexible, and widely used. An overview of the current features of Pyomo is shown in Figure 4.7. Pyomo supports a wide range of problem types including Linear Programming (LP), Mixed-Integer Programming (MIP), Nonlinear Programming (NLP), and Mixed-Integer Nonlinear Programming (MINLP) introduced in the literature of mathematical programming computation. Pyomo also provides interfaces to a variety of optimization solvers and provides automatic differentiation (AD) for NLP problems via the open source AMPL Solver Library (ASL).

One of Pyomo's main advantages over other algebraic modeling languages is that it is written in a high- level programming language, Python. Consequently, a user does not have to learn a specialized modeling language in order to formulate and solve optimization problems; a basic understanding of Python is all that is required. Models are represented using Python objects and can be formulated and manipulated in sophisticated ways using simple scripts. Furthermore, Pyomo users have access to a large collection of other Python packages which include tools for plotting, numerical and statistical analysis, and input/output. These

capabilities enable the development of novel algorithms, complicated model formulations, and general model transformations. All of these features make Pyomo a promising platform for implementing extensions for problem classes such as dynamic optimization.
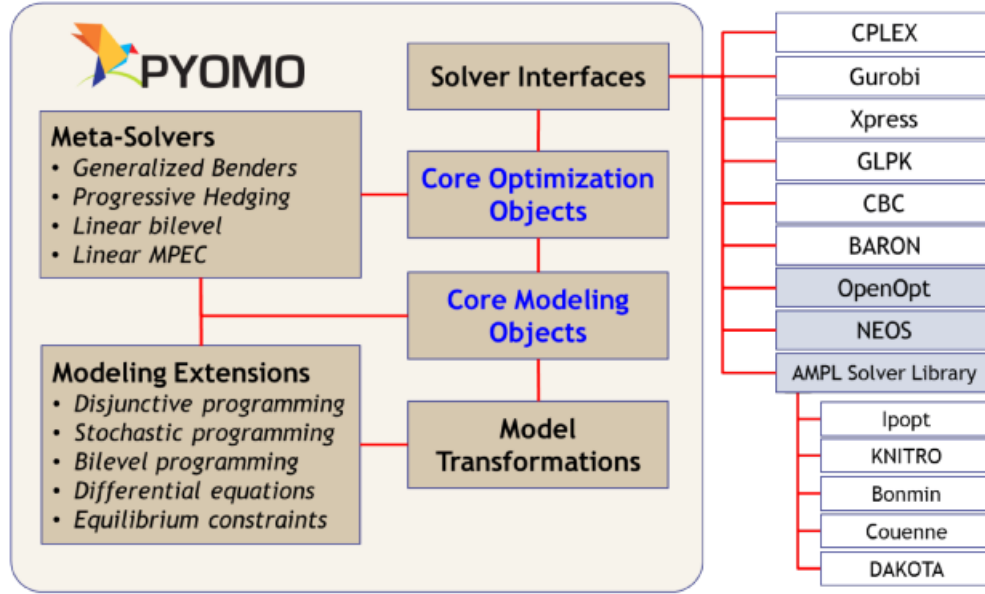
Figure 4.7: Summary of Pyomo features [70].

4.3 Towards vehicular multimodality

Spatial interactions between different transport modes

Let us consider a multimodal transport system with the sky-podcar transit system. We assume that the whole multimodal system is semi-computerized, that is to say there is advanced information for travelers about traffic conditions, for each network mode. For the sky-podcar transit system, there is dynamic allocation of podcars on stations with respect to the following:

- the known cumulative demands,

- the stocks of sky-podcars at stations on the off line guide-way, and

- the foreseeable demands induced by passengers travel orders for some future times.

We propose a logit model for the modal choice in general, and user paths choice. In the case of this PRT system, it is only up to the system manager to make the path choice according to the origin, the destination and the traffic state of system itself. We assume only three choices

for users in our considered multimodal system comprising only road network (by referring to private vehicles) and personal maglev network. Any OD pair could be joined with respect to following choices:

- choice c_1 : the use of road vehicle, then parking search availability to park and parking, and pedestrian walk for attending final destination, or

- choice c_2 : the use of sky-podcar and pedestrian walk, or

- choice c_3 : the use of both modes m_1 and m_2.

For $p \in \{1, 2, 3\}$ and a pair $(o, d) = w \in W$ (origin-destination), the Logit-based route allocation is deduced as [59]:

$$\pi_w^p = P\left(c_p \mid w = (o, d)\right) = \frac{\exp\left(-\theta C_w^{c_p}\right)}{\sum_{p' \in \{1,2,3\}} \exp\left(-\theta C_w^{c_{p'}}\right)} \tag{4.6}$$

θ is a parameter of sensitivity.

The probability of choosing the mode p, $p = 1, 2, 3$ from an origin o to a destination d is set by:

$$\left[\begin{array}{l} 0 \leq \pi_w^p \leq 1, \quad \forall p = 1, 2, 3 \,, \forall w = (o, d) \in W \\[2mm] \sum_{p=1}^{3} P\left(c_p \mid w = (o, d)\right) = 1 \,, \forall w = (o, d) \in W \end{array} \right. \tag{4.7}$$

and by the above formulation (4.6). $C_w^{c_p}$ is the cost of using c_p to reach destination d from origin o; this cost depends on the monetary cost, the predicted travel time that will be spent in the system, given by an ATIS information (advanced traveler information system). It also depends on the the walking time and the search time for parking-car (in the case of taking partially a car mode).

Experimental setup

We shall introduce the sky-podcars system in existing multimodal transport network in order to evaluate its impact and its performance compared to other transport modes. Skypod could be an intermediate "feeding system" for mass transportation such as the RER. Let us consider the below transport infrastructure and transport services.

i- Lines A and B of the RER (Réseau Express Régional - the commuter rail service serving Paris and its suburbs).

ii- The network domain comprising these two lines RER A and RER B.

iii- The proposed line of the skyTran system (depicted by the Figure 4.8). Skypod-lines are design as transverse lines with respect to RER A and RER B radial lines.

It compels to take into account only the OD matrices of commuters which will take routes by lines A and B, and road ways with respect to all the existing modes and transport services in the "Ile de France transport network". For sake of simplicity, we aggregated the lines A and B of the RER that we are considering in this case scenario. The RER (A and B) lines are aggregated respectively in 9 and 7 undirected and valued nodes. We assume the existence of skyTran lines passing through the nine nodes on the brink of the 2-RER lines networks, that is depicted by the Figure 4.8. We then obtain a multigraph from the multimodal transport system forming by skyTran lines and the aggregated RER (A and B) lines. skyTran lines are designed to be transverse with respect to the 2-radials RER lines.
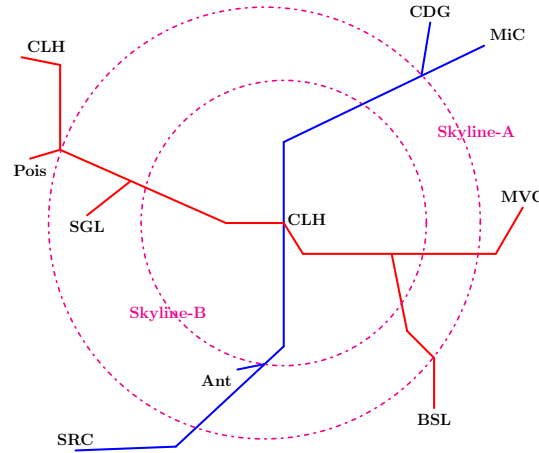
Figure 4.8: Two skyTran lines could be integrated with the existing RER A and RER B lines. Correspondences between the two different railways systems should take place via the corridors between RER hubs and skyTran portals.

We assume that passengers arrive exogeneously at the stop-stations of the skyTran system. Most of the time, these passengers do not come from other modes of transport, that is to say the correspondences. Passengers from other modes in their multimodal mobility arriving at skyTran poles should be more/or less deterministic. That is to say their arrivals are deterministic. Besides, the skyTran lines could be timely used as feeder of airports and centroids

of the city. For example, passengers going to "Charles De Gaulle airport" from "Saint Rémi les-Chevreuse" neighborhood could instead take RER-B and SkyLine-A and RER-B to reach quickly the airport.

Model summary and perspectives

The skyTran system lines could be implemented in a city in such a way that it contributes to traffic services' regularity and reliability between airports and centroids of the city. Probable choice of users in such multimodal system comprising skyTran system, RER system and road network for private vehicles traffic is the following.

1/ Private vehicle + RER vehicle.

2/ Private vehicle + skyTran transporter.

We assume that people do not take both RER vehicle and skyTran transporter along their multimodal trips in such network domain. Since just few routes are possible to take, during travel, it would be easy the computation of instantaneous travel time. The reactive assignment on such designed (or proposed) multimodal transportation system is fast and reliable.

The implementation of the model and the sky-podcar demand responsive system shall show its real performance. The proposed system of equations is a queue approach with adaptive cruise control on the dynamic of sky-podcars. The model proposed in this paper focused on Lagrangian coordinates of the motion of sky-podcars in the whole PRT system. We discuss about multimodal trips that take into account the new responsive autonomous transport system. The relocation of sky-podcars shall be addressed to respond to extra transport demands at stations where there are no available sky-podcars to board passengers, and then from where re-routing of other sky-podcars which are at rest in other stop-points is relevant.

4.4   Multiclass traffic flow modeling

Traffic is heterogeneous both in composition (depending on various types of vehicles and classes of users) and spatially (with respect to lanes, etc.). This section analyses how to adapt macroscopic models to such diversity. We therefore analyse multilane/multiclass model as an archetype for macroscopic multimodal model.

Multiclass multilane vehicular traffic flow model

ρ, q and v denote respectively the total density, flow and mean velocity variables for macroscopic traffic flow models. Let us consider that vehicles are dis-aggregated by class, denoted by $k \in K$ (K being the set of all vehicle classes), and that each class $k \in K$ is dis-aggregated by same destination $d \in D$. We denote by ρ^k, q^k and v^k the class specific densities, flows and mean velocities of the vehicle class $k \in K$; and by $\rho^{k,d}$ and $q^{k,d}$ the class specific densities and class specific flows of vehicles indexed by class $k \in K$ which are going to destination $d \in D$. The class specific densities and flows, and the class-destination specific densities and flows are partial quantities, and particularly $\rho^k, \forall k \in K$ are weighed according to the "passenger car unit" [39]. The mean velocity v and the class specific velocity v^k are defined respectively by the following relationships $q = \rho v$ and $q^k = \rho^k v^k$ thanks to the hydrodynamic approach applied in *Traffic Theory*. We can also add new traffic attribute, that of driving behavior (see works in [53]). Since roads network considered may have several lanes, the traffic attributes considered in the model are related to transport mode, lanes on the roads and destinations [18].

Traffic dynamic on shared roads

It is well known that the total density is a conservative physical quantity (according to the well known LWR model of [57] and [76]). According to conservation law of density and flow, class specific densities related to vehicle modes at any location and time are also conserved along a homogeneous shared multilane highway stretches without entrances and exits. These two properties are expressed by the following hyperbolic system of conservation laws:

$$\begin{cases} \partial_t \rho + \partial_x (\rho v) = 0 \\ \partial_t \rho^k + \partial_x \left(\rho^k v^k \right) = 0, \ \forall k \in K. \end{cases} \tag{4.8}$$

The relationship between the total and the class specific densities adopted in this paper is: $\rho v = \sum_k \rho^k v^k$ [39]. The latter relation implies that $v = \sum_k \chi^k v^k$ and $\chi^k \rho = \rho^k$, with $\chi^k \geq 0$ the class specific vehicles fraction. Obviously the fractions χ^k verify $\sum_k \chi^k = 1$. Class densities depend on class-destination densities, and their relationships can be expressed as below:

$$\rho^k \overset{def}{=} \sum_d \rho^{k,d}, \forall k \in K. \tag{4.9}$$

Introducing variables such as the lane densities ρ_ℓ and the fraction of density indexed by the class k and the lane ℓ that we denote η_ℓ^k, $\forall k$, $\forall \ell$, one has the following relation:

$$\rho_\ell \overset{def}{=} \sum_k \eta_\ell^k \rho^k, \forall \ell \in \text{L}. \tag{4.10}$$

A multiclass lane fundamental diagram for each lane is easily deduced. Class specific velocities are expressed at time t and location x as follow:

$$v^k = \sum_\ell \eta_\ell^k v_\ell = \sum_\ell \eta_\ell^k V_\ell(\rho_\ell), \ \forall k \in \text{K}. \tag{4.11}$$

with V_ℓ the lane-velocity field. This is the maximum velocity of vehicles flowing on the lane ℓ. It is expressed below:

$$V_\ell(\rho_\ell) = \alpha_{K_\ell} \max_k V_\ell^k(\rho_\ell), \ \forall \ell \in \text{L}. \tag{4.12}$$

α_{K_ℓ} The composition of the types (classes) of vehicle allowed to access the road by the lane ℓ, according to the road infrastructure and traffic signs. It also depends on density-speed fundamental diagrams on the lane ℓ.

The phenomenological behavior of class specific vehicles moving through lanes are formulated thanks to *Wageningen-Kessels'* thesis works [39] such below:

$$V_\ell^k(\rho_\ell) = \begin{cases} v^{k,max} - \dfrac{(v^{k,max} - v_{\ell,crit})\rho_\ell}{\rho_{\ell,crit}} \text{ for } 0 \leq \rho_\ell < \rho_{\ell,crit} \\[2mm] \dfrac{v_{\ell,crit}\rho_{\ell,crit}}{\rho_{\ell,jam} - \rho_{\ell,crit}} \left(\dfrac{\rho_{\ell,jam}}{\rho_\ell} - 1 \right) \text{ for } \rho_{\ell,crit} \leq \rho_\ell \leq \rho_{\ell,jam} \end{cases} \tag{4.13}$$

giving the multiclass lane fundamental diagram of the traffic in terms of speeds-densities diagrams. $v^{k,max}$ and $v_{\ell,crit}$ respectively denote maximal velocity of class k and critical velocity on lane l; $\rho_{\ell,crit}$ and $\rho_{\ell,jam}$ denote critical and jam densities on lane ℓ. The first is the limit value under which the traffic is assumed fluid and the second a quantity beyond which the density is nil meaning that over this limit vehicles on road can not move. It is assumed that all vehicle classes move at the same speed during congestion phase while at free phase, vehicle velocity is more depending on the class than the density. In the congested phase traffic dynamics respect the LWR [57, 76] model on each lane, whereas in the fluid phase density-speed relationship from transport data depend exclusively on the different vehicle classes that are traveling on the roads. For a class of vehicles such as buses for public transportation, the maximal velocity is the commercial speed and the critical one is a function of the mean headway between two followers buses. For each lane, the multiclass fundamental diagram is depicted by the Figure 4.9.
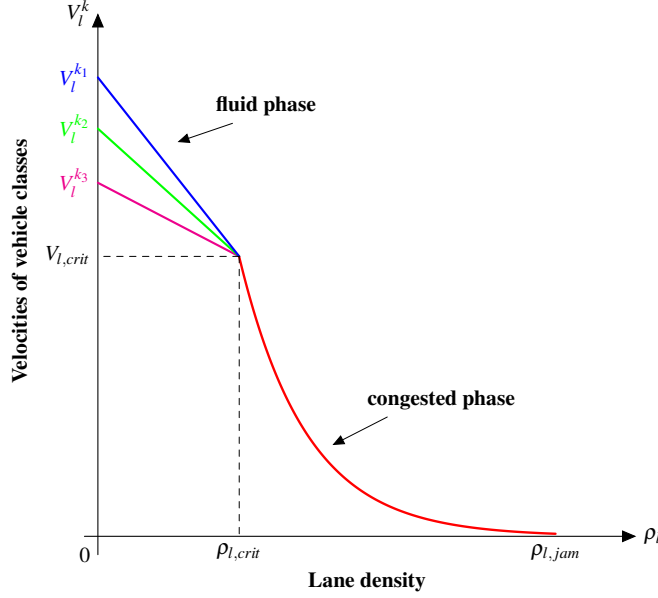
Figure 4.9: Multiclass lane fundamental diagram.

There are $K \times L$ free-flows velocities and L congested phases that can occur due to the total number of lanes on the considered section; many transport demands occur on the section with a unique transport supply.

In the sequel, a Logit model for traffic assignment through lanes [18, 37] will be discussed. This is to determine the rate of total density per vehicle class $k \in K$ on lane $\ell \in L$.

A Logit assignment model for vehicle classes The variable η_ℓ^k is a function of position x and time t for determining the number of vehicles of class k on lane ℓ based on the lane density and lane and class specific velocities. It is also depending on local travel time of class k on the lane ℓ. The local travel time is defined as the inverse of the local velocity as follow: $t_\ell^k \overset{def}{=} 1/V_\ell^k(\rho_\ell)$. We review the Logit assignment model per destination [18] and the model of [37]

on multiclass assignment of users and vehicles. We formulate η_ℓ^k as follows:

$$\eta_\ell^k = \exp(-\theta_k \rho^k / V_\ell^k(\rho_\ell) + c_{k\ell})/p^k \tag{4.14}$$

where $p^k = \sum_r \exp\left(-\theta_k \rho^k / V^k(\rho_r) + c_{kr}\right)$, with ℓ and r indexes of lanes. The parameters $c_{k\ell}$ indicate the preference of lane ℓ for a vehicle class k. These parameters depend on the position x and somewhat on the time t. Here we assume that $\forall k, \forall \ell$, $c_{k\ell}$ is independent from the location x and the time t once the concerned vehicles enter the lane ℓ, due to the fact that, some lanes are imposed to the traffic. For the same token, $\eta_\ell^k = 0$ for certain vehicle

126

classes with respect of specific(s) lane(s). Particularly, $c_{k\ell}$ is more explicit for buses for public transportation where their routes and the real-time schedules are well known.

Let us mention that, in the formulation (4.14), $\{\eta_\ell^k\}_{k,\ell}$ really result from the following optimization problem:

$$\max_{(\eta_\ell^k)_{k,\ell}} \sum_\ell \int_0^{\rho_\ell = \sum_k \eta_\ell^k \rho^k} \frac{ds}{V_\ell^k(s)} - \sum_{k,\ell} \frac{1}{\theta_k}(H(\eta_\ell^k) - c_{k\ell}\eta_\ell^k)$$
$$\left| \sum_\ell \eta_\ell^k = 1, \forall k \right. \tag{4.15}$$

where $H(x) = x(\log(x) - 1)$ is the negentropy function. By Karush-Kuhn- Tucker conditions, we find that formulations (4.14) and (4.15) are equivalent. The focusing problem of car users is the optimization of their global travel time which mainly depends on the routes they will use during their trips and general traffic conditions of these routes. The global travel time depends in turn on the successive local travel times which are increasing functions of the density in correspondent locations. The first term of the objective function of the optimizing problem (4.15) defines the local travel time of vehicle of class k along the lane ℓ in terms of the inverse of specific lane and class velocity in local location. The second term is part of the description of how users behave on the road regarding the competition between keep safe spacing and react more flexibly for filling available gaps in order to optimize travel times.

Numerical schemes for multiclass traffic flow on arcs

Considering a long road section that is shared with a private and public vehicles, we use a split Lagrange-remap scheme based on a finite volume discretization of the road section in control volume for calculating numerically multiclass car-flows. The scheme consists in two steps (a Lagrangian step and a Remapping step) for integrating the system 4.8 between successive time instants t^n and $t^{n+1} = t^n + \Delta t$; Δt being the time-step. We introduce two grids: Lagrangian grid $\{X_{i+\frac{1}{2}}\}$ and Eulerian grid $\{x_{i+\frac{1}{2}}\}$, and the $(x,t) \rightarrow (X,t)$ variable change such that $\rho dx = \rho_0 dX$ where $\rho_0(x)$ denotes $\rho(x,t^n)$ the car-density at time t^n. With this variable change, we rewrite the system 4.8 in Lagrangian form 4.16 as follows:

$$\begin{cases} \partial_t (\rho_0 s) - \partial_X u = 0 \\ \partial_t (\rho_0^k s^k) - \partial_X u^k = 0, \ \forall k \in K \end{cases} \tag{4.16}$$

where $s = 1/\rho$ is the spacing without distinction of vehicle classes, $s^k = 1/\rho^k$, $k \in K$ are spacing between vehicles of class $k \in K$, $u(s(X,t),t) \overset{def}{=} \partial_t x(X,t)$ and $u^k(s(X,t),t) \overset{def}{=} \partial_t x^k(X,t)$

are respectively the correspondent (in Lagrangian system) specific car-speed and specific class car-speeds. Let us note $\rho_0^k(x) = \rho^k(x, t^n)$ the class car-densities at time t^n and location x. Setting $\rho_0(x) = \rho(x, t^n)$ we assume that Eulerian grids $\{x_{i-\frac{1}{2}}\}$ and Lagrangian grids $\{X_{i-\frac{1}{2}}\}$ coincide at time t^n. The trick is the calculation of the Lagrangian conservative variables, notably by a discretization of the system (4.8) at time t^{n+1} on a non-regular grid, and afterwards to remap them on the initial Eulerian grid. The two steps are described in the following.

Lagrangian step Discretizing the system (4.16), we have the following formulation:

$$
\begin{cases}
(\rho_0 s)_i^{n+1} = (\rho_0 s)_i^n + \frac{\Delta t}{\Delta X}\left(u_{i+\frac{1}{2}}^n - u_{i-\frac{1}{2}}^n\right) \\
(\rho_0^k s^k)_i^{n+1} = (\rho_0^k s^k)_i^n + \frac{\Delta t}{\Delta X}\left(u_{i+\frac{1}{2}}^{k,n} - u_{i-\frac{1}{2}}^{k,n}\right)
\end{cases}
\tag{4.17}
$$

while the moving of the Eulerian coordinates x located at $x_{i+\frac{1}{2}}$ is governed by $x_{i+\frac{1}{2}}^{n+1} = x_{i+\frac{1}{2}} + \Delta t(u^*)_{i+\frac{1}{2}}^n$, with $x_{i+\frac{1}{2}}^{n+1}$ the new position of vehicles that exited the boundary $x_{i+\frac{1}{2}}$ at time t^n after the during time-step Δt and where $(u^*)_{i+\frac{1}{2}}^n$ is the speed of vehicles located at $X_{i+\frac{1}{2}}$ with respect to the Lagrangian system. Therefore, a third grid $\{x_{i+\frac{1}{2}}^{n+1}\}$ results which is not regular due to the fact that the speeds are not constants between two consecutive time instants.

Remapping step After the Lagrangian step, we remap $s_{i+\frac{1}{2}}^n$ and $(s^k)_{i+\frac{1}{2}}^n$ values on the Eulerian grid $\{x_{i+\frac{1}{2}}\}$ by splitting and we obtain the densities at time t^{n+1} (and then the flows crossing the boundary $x_{i+\frac{1}{2}}$):

$$
\begin{cases}
\rho_i^{n+1} = \rho_{0,i}^{n+1} - \frac{\Delta t}{\Delta x}\left((u^*)_{i+\frac{1}{2}}^n (\rho^*)_{i+\frac{1}{2}}^n - (u^*)_{i-\frac{1}{2}}^n (\rho^*)_{i-\frac{1}{2}}^n\right) \\
\rho_i^{k,n+1} = \rho_{0,i}^{k,n+1} - \frac{\Delta t}{\Delta x}\left((u^{k,*})_{i+\frac{1}{2}}^n (\rho^{k,*})_{i+\frac{1}{2}}^n - (u^{k,*})_{i-\frac{1}{2}}^n (\rho^{k,*})_{i-\frac{1}{2}}^n\right) \quad k \in \text{K}.
\end{cases}
\tag{4.18}
$$

The variables $(\rho^*)_{i+\frac{1}{2}}^n$ and $(\rho^{k,*})_{i+\frac{1}{2}}^n$ are obtained from the output of the first step of the scheme, using relations between car-densities ρ, ρ^k and spacing s, s^k, (for $k \in \text{K}$). Besides, the discrete unknowns $(u^*)_{i+\frac{1}{2}}^n$ and $(u^{k,*})_{i+\frac{1}{2}}^n$ are obtained thanks to the calculus of the class specific rate $\{\eta_\ell^k\}_{k \in \text{K}, \ell \in \text{L}}$ of vehicles on any lane by a fixed point method regarding the equation (4.14). They could be solve by the concave optimizing problem (4.15). Following speed-spacing lane class fundamental diagram obtained by introducing $s_{\ell, crit} = 1/\rho_{\ell, crit}$ and $s_{\ell, jam} = 1/\rho_{\ell, jam}$ respectively the critical lane-spacing and the jam lane-spacing are hence used.

The Figure 4.10 below depicts the process of computation of the class specific flows and class specific densities in cells.
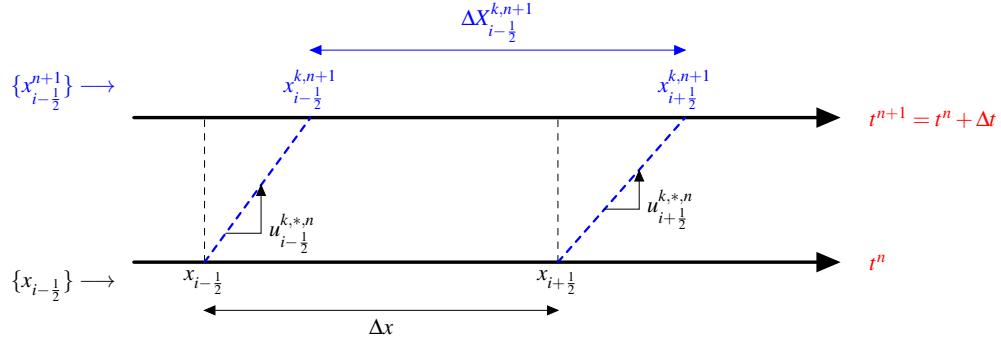
Figure 4.10: Euler-Lagrange remap scheme

Numerical results We implement the multiclass scheme within Matlab software to get total and partial densities over the time along a long shared road section. We take $K = L = 2$ as number of lanes and vehicle classes. Each lane is 8 kilometers long. The time step $\Delta t = 1$ second (in Lagrangian step) and $\Delta x = 200$ meters (in Eulerian step). With artificial initial condition, we show the partial ρ_1, ρ_2, ρ^1, ρ^2 densities at two different times $t = 10$ seconds and $t = 25$ seconds. The later are depicted by Figure 4.11 and Figure 4.12.

Figure 4.11: Total density, lane densities and class densities at a time $t = 10$s.

Figure 4.12: Total density, lane densities and class densities at a time $t = 25$s.

Intersection model with driver-specific attribute

Let us consider a multiclass node denoted by (Z). The term multiclass node, is used to specify the fact that different class of vehicles are allowed to pass through the node (Z).
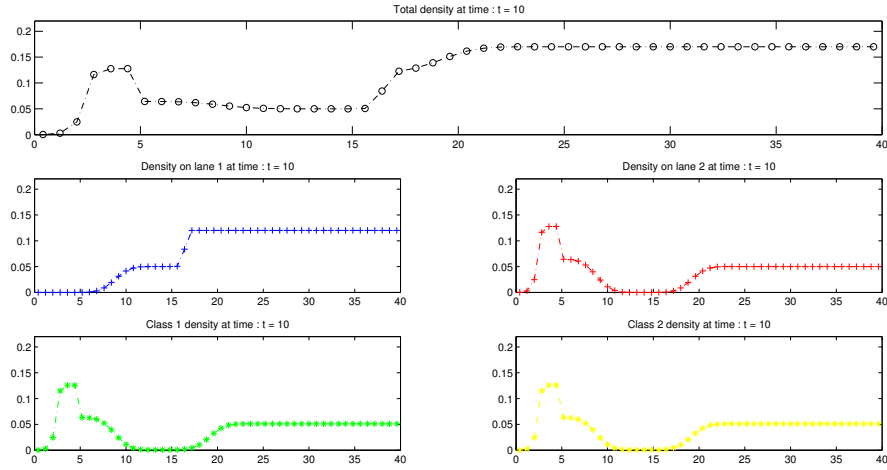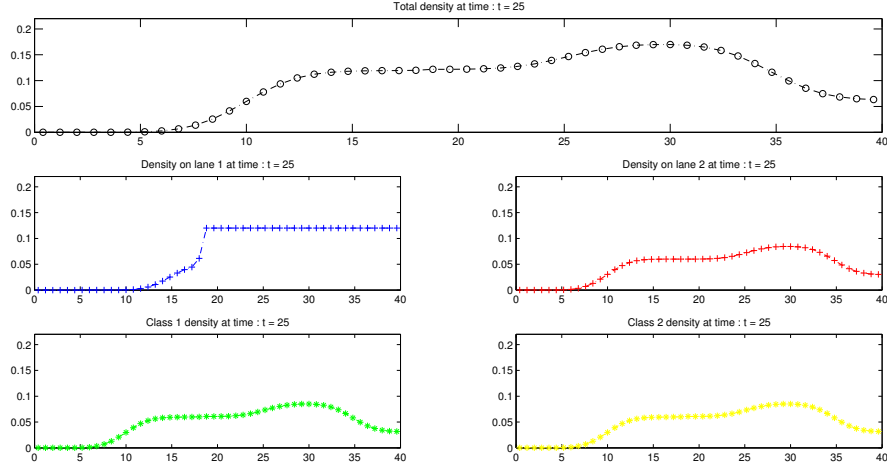
Notations and definitions are the following. I is the set of incoming links or arcs (i), and the notation $\ell \in i$ means that the lane ℓ is part of the link (i); J is the set of outgoing links or arcs (j), and the notation $\lambda \in j$ means that the lane λ is part of the link (j).

It is known that a network, approached by a graph, is a collection in good manner of arcs and nodes. In the sequel, we are going to discuss formulations of the dynamic of traffic flow through intersections represented by nodes. The scope will be the design of an intersection model which will easily calibrate with the model adopted for arcs. First of all, we add a new parameter $d_{j\ell}$ in the formulation of η_ℓ^k (traffic rate per class and lane) for arcs. This new parameter represent the preference of users going to (j) via $\ell \in i$. We assume that $d_{j\ell}$ is a continuous and convex function with respect to the position x. More precisely, $d_{j\ell}$ is almost certainly nil on $\ell \in i$, except in the admissible region of (Z), at the side of the end of the lane ℓ. It is revealed that $d_{j\ell}$ is an increasing and strongly convex function of the position x. Therefore, at the upstream of the node (Z) $\forall i \in I$, the fraction of vehicle flows indexed by k and $\ell \in i$, has a similar expressions as in (4.14):

$$\eta_{ij\ell}^k = \frac{exp(-\theta_k \rho^k / V_\ell^k(\rho_{i\ell}) + c_{k\ell} + d_{j\ell})}{\sum\limits_{h \in i} exp\left(-\theta_k \rho^k / V_h^k(\rho_{ih}) + c_{kh} + d_{j\ell}\right)} \tag{4.19}$$

with $d_{j\ell}$ is the preference of users located on the lane $\ell \in i$ and which are going to the lane

$j \in J$; $d_{j\ell}$ is a deterministic utility parameter.

The new formulation leads to: $\rho_{i\ell} = \sum\limits_{k,j} \rho_i^k \gamma_{i,j}^k \eta_{ij\ell}^k$, $\forall i \in I$, $\forall \ell \in i$.

The term $\rho_i^k \gamma_{i,j}^k$ in the latter expression gives the exact traffic rate of users k coming from i and going to j.

As mentioned before for the equation (4.14), for $j \in J$ fixed, $\left(\eta_{ij\ell}^k\right)_{i,\ell,k}$ are solutions of the below concave optimization problem:

$$\max_{\left(\eta_{ij\ell}^k\right)_{k,j,\ell}} \sum_{\ell \in i} \int_0^{\rho_{i\ell}=\sum\limits_{k,j}\rho^k\gamma_{i,j}^k\eta_{ij\ell}^k} \frac{dr}{V_\ell^k(r)} - \sum_{k,\ell \in i} \frac{1}{\theta_k} H(\eta_\ell^k) + \sum_{k,j,\ell \in i} (c_{kl} + d_{jl})\eta_{ij\ell}^k, \tag{4.20}$$

under the constraints $\sum\limits_{l \in i} \eta_{ijl}^k = 1, \forall k \in \mathrm{K}$.
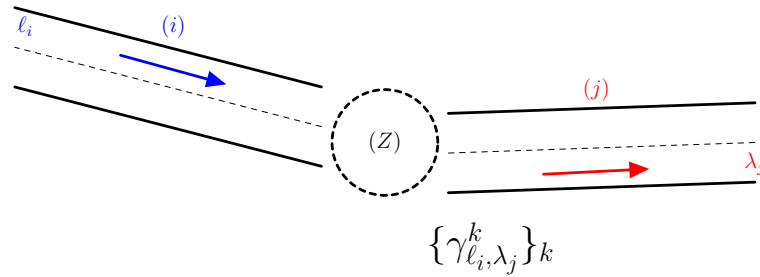

Figure 4.13: A multiclass node with incoming links and outgoing links.
The node is (Z) with incoming links $(i), i \in I$ and outgoing links $(j), j \in J$.

The arrows indicate the sens of propagation of the flows, and then specify the incoming and outgoing links of any node (Z) of the network. $\{\gamma_{\ell_i,\lambda_j}^k\}_{k \in \mathrm{K}}$ denote the turning coefficient movements of users indexed by k and who are leaving the lane ℓ_i of (i) to reach the lane λ_j of (j). Below variables for specific volumes passing through intersections.

- N_{ij}^k: the number of users of class k going to (j) from (i);

- $N_i = \sum\limits_{j,k} N_{ij}^k$: the total number of users coming from lanes of (i);

- $N^j = \sum\limits_{i,k} N_{ij}^k$: the number of users of class k who have left lanes of (i) and are currently on lanes of (j).

Traffic fraction of class k at node (Z) of type $\ell_i \in i \to \lambda_j \in j$ is defined and expressed by $\gamma_{Z,\ell_i,\lambda_j}^k = \exp(-\alpha d_{\ell_i,\lambda_j})/\sum\limits_{\mu_j \in j} \exp(-\alpha d_{\ell_i,\mu_j})$, with d_{ℓ_i,μ_j} "the local time distance" between the end of ℓ_i and the beginning of μ_j.

From the total demand from lane $\ell \in i$, one question arises: "Should one takes into account the composition in class k of incoming vehicles on lanes with respect to $\ell \in i$? Firstly, on prorata by the number of class, one has: $\Delta_{i\ell}(\rho_{i\ell}) = \sum_k \Delta_{i\ell}^k(\rho_{i\ell}) \times \frac{\eta_{\ell_i}^k \rho^k}{\rho_{i\ell}}$ with $\Delta_{i\ell}^k(\rho_{i\ell})$ a demand function. Therefore, the lane supply of $\ell \in (i)$ is expressed as $\sigma_{Z,i\ell}(N_i) = \sum_i (N_i)/\#(\ell \in i)$. The exiting flow of (i), from lane ℓ is $q_{i\ell} = \min(\Delta_{i\ell}(\rho_{i\ell}), \sigma_{Z,i\ell}(N_i))$. Entering on (j), the lane $\lambda \in j$ has one supply: $\sigma_{j\lambda} \overset{not.}{=} \sum_{j,\lambda}(\rho_{j,\lambda})$ is the supply of the lane λ of the arc (j); which depends on $\rho_{j,\lambda}$ of the lane $\lambda \in j$. Traffic fraction of class k inside the node (Z) coming from lane $\ell \in i$ and going to j is following $\sum_k \eta_{Z,j,\ell}^k$.

The demand of (Z) for the arc (j) is deduced as

$$\Delta_{Z,j}(N^j) = \sum_{\ell \in i} \left(\sum_k \eta_{Z,j,\ell}^k \right) \Delta_{Z,j\ell}(N^j). \tag{4.21}$$

where $\eta_{Z,j,\ell}^k$ denotes the traffic fraction of class k inside the node (Z) coming from lane $\ell \in i$ and going to j. Hence, the exiting flow from (Z) towards the lane λ of (j) is equaled to $\Omega_{Z,j\ell} = \min(\Delta_{Z,jl}(N^j), \sigma_{j\ell})$.

Dynamics of vehicles within a generic node (Z) are governed by the below equation:

$$\frac{d}{dt} N_{ij}^k = \sum_{\ell \in i, \lambda \in j, k} q_{i\ell} * \gamma_{Z,\ell,\lambda}^k - \sum_{\lambda \in j} \Omega_{Z,j,\lambda} * \eta_{Z,j,\lambda}^k. \tag{4.22}$$

4.5 Conclusion

We introduce an approach for modeling multimodal vehicular within transportation road networks. The proposed multiclass traffic flow model for the multimodal road traffic simulation is more flexible to capture macroscopic mixed traffic flow, notably the proposed numerical scheme well reduces growing discontinuities of outputs traffic data during a simulation, by introducing an arbitrary Euler-Lagrange method. Even though, one can use a high-order split method of [15] for more accuracy in the numerical approximation of the multiclass model. Within a multimodal transport system, the multiclass model allows to determine travel time of users depending on what transport modes are used during trips, and describe interactions between existing type of vehicles in the traffic. The multiclass model is evaluated and validated with artificial traffic data. Furthermore, the model is suitable to estimate vehicles flow from time-dependent OD matrices and from some classes of driving behavior. This model is applied (with some modifications) in Chap. **??** along with other traffic flow models of type two-dimensional. The choice of transport attributes and application of the model on a small

urban network are setting during which numerical analysis of the multiclass node model is investigated.

This page is intentionally left blank.

Chapter 5

Multiscale traffic flow simulation

Contents

5.1 Introduction

In this chapter, we propose an hybridization and a multiscale coupling of the three models we develop in this Report. Let us recall the developed models. They are (i) the resulted integrated microscopic transport model which we instantiate on a proposed skyTran-lines and a compressed form of the RER-lines, (ii) the multiclass macroscopic traffic flow model for specific multimodal road networks, and (iii) the developed dynamic bi-dimensional traffic flow model for large (homogeneous and heterogeneous) surface networks.

Motivation

We argue that a vehicular multimodal traffic flow model shall handle traffic interactions between its different transport modes or transportation systems. We consider a large multi-modal transportation system comprising road networks and railways networks. For instance we assume that road networks comprise highways and urban area, and mass transportation lines (for example the bus-lines). We suppose that railways networks comprise the skyTran demand responsive system, and the system of RER lines under its compressed form (see Figure 4.8). Let us recall that this is stated in Sec. 4.2, and that the model applied to the skyTran network is considered as a generic dynamic transport model for the travel demand in rail transportation systems. In parallel, for a surface network which comprises main arteries/highways and secondary roads, it is obvious to think about an hybridization of the macroscopic and bi-dimensional models which are applicable and adequate respectively to a network of main arteries/highways and a network of secondary roads.

Organization of the chapter

This chapter is organized as follows. The section 5.2 presents how the traffic exchange is due between the macroscopic model and the bidimensional model along and through specific curve lines ($i.e.$ $2d$ cell interfaces) where $2d$-elementary cells and $1d$-elementary cells intersect. The former are computing cells of the network domain of surface network. Since in this chapter the surface network is assumed to comprise secondary roads and main arteries, its network domain shall also contain $1d$-elementary cells. We derive a *specific mesh* of the network domain. The *specific mesh* is the mesh of the area of the network in $2d$ traffic zones (and then in $2d$-elementary cells), but also the mesh of main arteries in $1d$ discrete cells. We present an algorithm for the estimation of the traffic from the hybrid model and multiscale model introduced in Sec. 5.2 and Sec. 5.3. Our key contributions are efficient techniques for the dynamic coupling of individual vehicles traffic (from a rail system, public transport bus service, skyTran demand transportation system, etc.) with aggregate behavior of the macroscopic traffic and bi-dimensional traffic (from main arteries and secondary roads). We demonstrate the flexibility and scalability of our interactive visual simulation techniques on extensive road networks using synthetic scenarios.

5.2 Hybrid traffic flow modeling

Transport networks in this section are assumed discrete-continuous networks. It is the case of road network consisting of urban area (comprising a high number of secondary roads) with highways which refer to principal or main roads. For such networks, it is convenient to develop hybrid model to compute their traffic states. Many hybrid traffic flow models have been developed in the literature. We note hybridization of different microscopic models with macroscopic models. In this chapter, hybridization refers to $2d \leftrightarrow 1d$ hybridization, specifically it is about the hybridization of the *BidiTSim* model which is applicable to traffic area of secondary roads and the GSOM model which is convenient for principal roads.

Interaction between bi-dimensional cells and artery links

Let us consider the situation depicted in figure 5.1. This is the simplest interaction situation between a $2d$ cell (c) (dense surface network) and a major artery (a), with the artery constituting a border element of the $2d$ cell. More complicated situations would be: major artery crossing a $2d$ cell; or a major artery with one $2d$ cell on each side. The major elements of the model are the following.
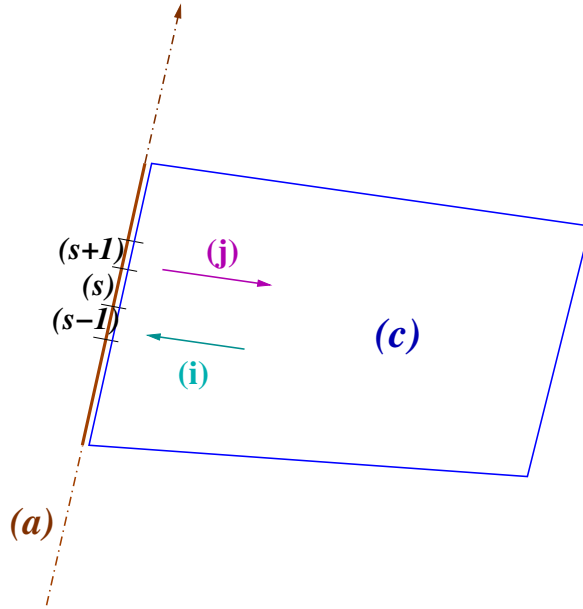

Figure 5.1: Interaction between $2d$ cells and artery links.

- The artery denoted by (a) is divided into $1d$ cells (s) (typically much smaller than $2d$ cells (c));

- Since the cells (s) are much smaller than the cells (c), their time-step is much smaller, actually a divider of the time step of bi-dimensional cells. But this difference will not be stressed in the sequel and we will just loosely invoke the "time" t which is the time-step of artery cells;

- Supply and demand functions of the artery per lane in cell (s) are $\Delta_{a,s}()$ and $\Sigma_{a,s}()$;

- The number of lanes of (a) in (s) is $\nu_{a,s}$;

- The number of lanes devoted to the outflow $(s) \rightarrow (c)$ is $\nu_{a,s}^{s \rightarrow c}$;

- The number of lanes devoted to the outflow $(c) \rightarrow (s)$ is $\nu_{a,s}^{c \rightarrow s}$;

- The density of cell (s) at time t is $\rho_{a,s}^{t}$, its inflow $q_{a,s-1}^{t}$, its outflow $q_{a,s}^{t}$;

- These quantities are liable to be disaggregated with respect to destination d: $\rho_{a,s}^{d,t}$, its inflow $q_{a,s-1}^{d,t}$, its outflow $q_{a,s}^{d,t}$;

- $\gamma_{a,s \rightarrow c}^{d}$ the assignment coefficient of users in cell (s) with destination d who choose the cell (c) to reach this destination and $\gamma_{a,s \rightarrow s+1}^{d} = 1 - \gamma_{a,s \rightarrow c}^{d}$; In an artery cell (s), there is only two directions of propagation of its outflow: the movement (s) to (c) and the movement (s) to $(s+1)$.

- The number of lanes devoted to the outflow $(c) \rightarrow (s)$ is $\nu_{c,i}^{c \rightarrow s}$, follows direction (i);

- The number of lanes devoted to the inflow $(s) \rightarrow (c)$ is $\nu_{c,j}^{s \rightarrow c}$, follows direction (j); This number is the outgoing lanes of the artery cell (s) following the direction (j) of the cell (c).

- Supply and demand functions of the cell (c) per lane are $\Delta_{c,i}()$ and $\Sigma_{c,j}()$;

- $\Gamma_{c,i \rightarrow a}^{d}$ the assignment coefficient of users in direction (i) with destination d who choose the artery (a) to reach this destination;

- $N_{c,i}^{d,t}$ the number of users in direction (i) with destination d with $\rho_{c,i}^{d,t}$ their mean density per lane (obtained by dividing $N_{c,i}^{d,t}$ by the total length of lanes in direction (i) in cell (c)).

Since the densities (of cells (s)) and number of vehicles (of the cell (c)) are calculated from one time-step to the next according to conservation of vehicles, the main difficulty is to calculate the flows. Typically the Godunov scheme [51] will apply for the cells (s) and a scheme extending the model developed in section 3.4 will apply for the cells (c). This is the question we are addressing here. It is also necessary to take into account the fact that there are several artery time-steps in one bi-dimensional cell time-step. For the sake of simplicity, we set the bi-dimensional cell time-step to be a multiple of the artery cell time-step. Let us mention that the two time-steps (the bi-dimensional cell time-step and the artery cell time-step) respect the Courant-Friedrichs-Lewy condition of stability. The cell supplies and demands are the following for the artery.

- the demand from (s) to $(s+1)$: $\delta_{a,s}^t = \left(\nu_{a,s} - \nu_{a,s}^{s\to c} \right) \Delta_{a,s}(\rho_{a,s}^{s\to s+1,t})$, with $\rho_{a,s}^{s\to s+1,t} = \sum_d \gamma_{a,s\to s+1}^d \rho_{a,s}^{d,t} = \sum_d (1-\gamma_{a,s\to c}^d)\rho_{a,s}^{d,t}$; Here we consider concentration on the lanes used and on the link $(s) \to (s+1)$.

- the demand from (s) to (c): $\delta_{a,s}^{s\to c,t} = \left(\nu_{a,s}^{s\to c} \right) \Delta_{a,s}(\rho_{a,s}^{s\to c,t})$, with $\rho_{a,s}^{s\to c,t} = \sum_d \gamma_{a,s\to c}^d \rho_{a,s}^{d,t}$;

- the supply for flow from $(s-1)$: $\varsigma_{a,s}^t = \left(\nu_{a,s} - \nu_{a,s}^{s\to c} \right) \Sigma_{a,s}(\rho_{a,s}^t)$;

- the supply for flow from (c): $\varsigma_{a,s}^{c\to s,t} = \left(\nu_{a,s}^{s\to c} \right) \Sigma_{a,s}(\rho_{a,s}^t)$.

Figure 5.2 below depicts some variables of interactions between cell (c) and artery link (a). The cell supplies and demands are the following for (c) with respect to (s).

- Demand of cell (c) for cell (s): $\delta_{c,i}^{c\to s,t} = \nu_{c,i}^{c\to s}\Delta_{c,i}(\rho_{c,i}^{c\to a,t})$ with $\rho_{c,i}^{c\to a,t} = \sum_d \Gamma_{c,i\to a}^d \rho_{c,i}^{d,t}$;

- Supply of cell (c) for cell (s): $\varsigma_{c,j}^{s\to c,t} = \nu_{c,j}^{s\to c}\Sigma_{c,j}(\rho_{c,j}^t)$.

The flows result from the min formula [51], and driver attributes as in the GSOM model could easily be accomodated following [24], [53]. We obtain the following flows:

- Flow between sections of the artery: $q_{a,s}^t = \min\left[\delta_{a,s}^t, \varsigma_{a,s+1}^t \right]$;

- Flow from (s) to (c): $q_{c,j}^{s\to c,t} = \min\left[\delta_{a,s}^{s\to c,t}, \varsigma_{c,j}^{s\to c,t} \right]$;

- Flow from (c) to (s): $q_{c,i}^{c\to s,t} = \min\left[\delta_{c,i}^{c\to s,t}, \varsigma_{a,s}^{c\to s,t} \right]$.
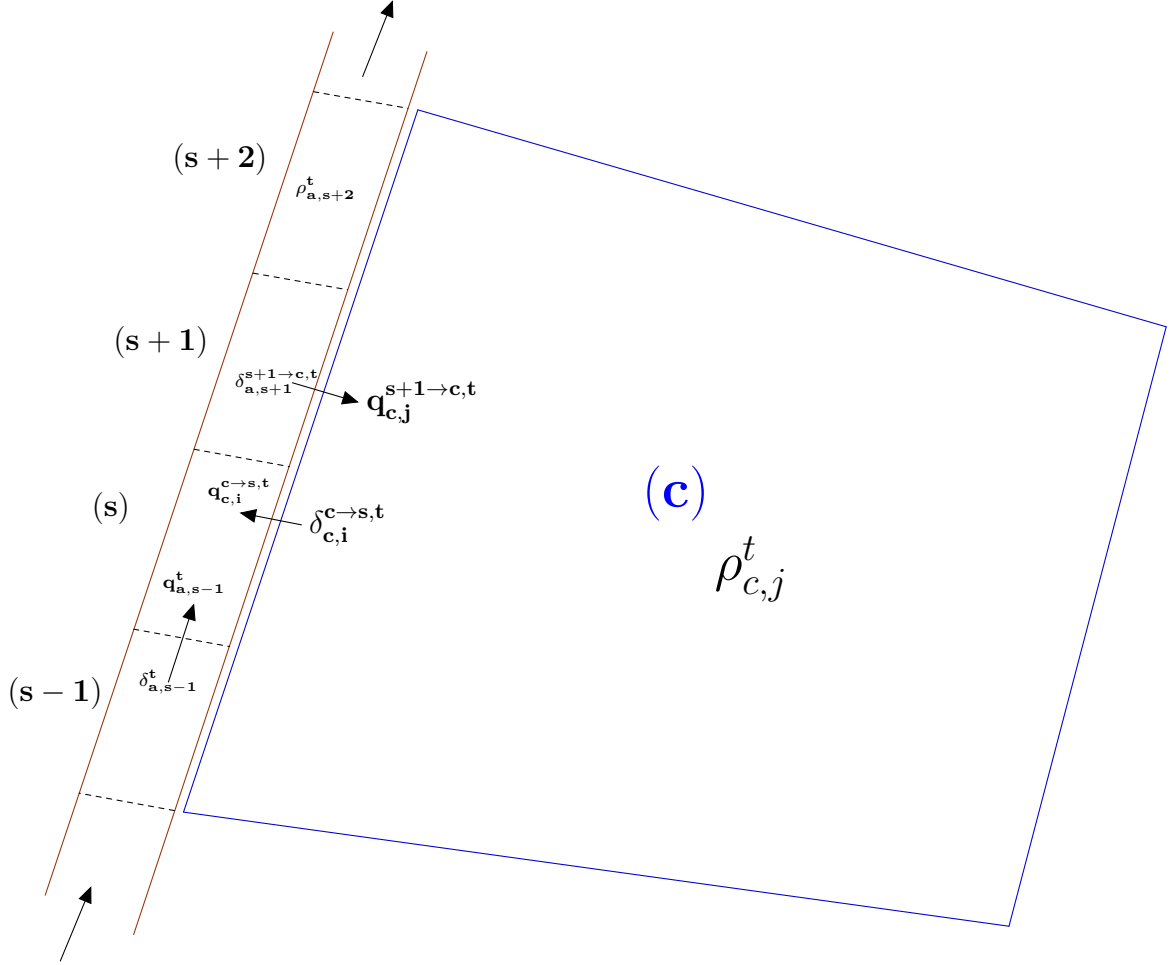
Figure 5.2: Traffic from cell (c) to artery link (a), and conversely.

If needed it is possible to disaggregate these flows per destination. The rule is simple: the flow per destination equals the total flow times the fraction of users with the considered destination. It can for instance be argued that destinations are passive driver attributes and we apply the GSOM model calculation [53].

For instance the composition of the flow from artery to cell, $q_{c,j}^{s \to c,t}$, is

$$\chi_{c,j}^{s \to c,d,t} = \gamma_{a,s \to c}^{d} \rho_{a,s}^{d,t} / \rho_{a,s}^{s \to c,t} , \tag{5.1}$$

and thus the partial flow from artery to cell with destination d is given by

$$q_{c,j}^{s \to c,d,t} = \chi_{c,j}^{s \to c,d,t} q_{c,j}^{s \to c,t} . \tag{5.2}$$

The conservation laws

Let us provide the governing equations for the evolution of densities of the links and bi-dimensional cells in the case of a considered mixed-network.

The density of an artery cell follows the below conservation law.

$\forall t > 0$, for any artery cell (s), we have:

$$\rho_{a,s}^{s\to s+1,t+1} = \rho_{a,s}^{s\to s+1,t} + \delta t \big(q_{a,s-1}^t - q_{a,s}^t\big)/L_a^{s\to s+1} \, . \tag{5.3}$$

where $\rho_{a,s}^{s\to s+1,t}$ is the density of (s) with respect to the direction $(s) \to (s+1)$, and $L_a^{s\to s+1}$ is the length of lanes from the cell (s) to the cell $(s+1)$. The density $\rho_{a,s}^{s\to s+1,t}$ is defined as

$$\rho_{a,s}^{s\to s+1,t} \stackrel{def}{=} \gamma_{a,s\to s+1}\, \rho_{a,s}^t = (1 - \gamma_{a,s\to c})\, \rho_{a,s}^t \, . \tag{5.4}$$

In addition, we have:

$$\rho_{a,s}^{s\to c,t} \stackrel{def}{=} \gamma_{a,s\to c}\, \rho_{a,s}^t \, . \tag{5.5}$$

Let us mention that, for a bi-dimensional cell (c), we found that the density in dominant direction $j = 1, 2, 3, 4$ follows different conservation law which takes into account internal flows inside cell (c).

$\forall t > 0, \ \forall c \in \mathfrak{C}, \ \forall j = 1, 2, 3, 4$, we have:

$$\rho_{c,j}^{t+1} = \rho_{c,j}^t + \Delta t \big(Q_{\underline{c},j}^t - Q_{c,j}^t + r_{c,j}^t - q_{c,j}^t\big)/L_{c,j} \, . \tag{5.6}$$

with

- $L_{c,j}$ is the length of lanes inside the cell (c) in the direction j;
- $Q_{\underline{c},j}^t$ is inflow, follows direction (j), from neighbor cell of cell (c), at time t;
- $Q_{c,j}^t$ is outflow of (c) follows direction (j) at time t;
- $r_{c,j}^t$ is internal inflow of cell (c) at time t;
- $q_{c,j}^t$ is internal outflow of cell (c) at time t.

Let us give the governing equation of the density of cell (c), with respect to dominant directions $j = 1, 2, 3, 4$ and interactions between artery cells (s) and cell (c). These traffic interactions are depicted in Fig. 5.2.

For a cell (c) at a border of the artery, it exists a direction (j) corresponding to $(s) \to (c)$, and at any time $t > 0$, we have:

$$\rho_{c,j}^{t+1} = \rho_{c,j}^t + \Delta t \big(F_{a,s}^{s\to c,t} - Q_{c,j}^t + r_{c,j}^t - q_{c,j}^t\big)/L_{c,j} \tag{5.7}$$

with

$$F_{a,s}^{s\to c,t} = \sum_{y=1}^{n} q_{a,s}^{s\to c,t-\Delta t+y(\delta t)} \, . \tag{5.8}$$

Let us recall that $t + 1 := t + \Delta t$; and $\Delta t = n(\delta t)$ where δt is the artery time-step and Δt is the bi-dimensional time-step. n is a fixed integer number determined such that Δt and δt follow the Courant-Friedrichs-Lewy condition of stability.

$F_{a,s}^{s \to c,t}$ is an accumulate traffic flow from (s) to (c) during Δt. It is taken into account at the next iteration t to $t + 1 = t + \Delta t$ in order to correctly compute traffic flows and traffic densities in the four dominant directions of all bi-dimensional cells.

Experiences on a large mixed road network

We apply and validate in this section the multiscale modeling theory we propose in the previous section. We will see through this section that the coupling of the GSOM family applied to highways and the dynamical bi-dimensional traffic flow model applied to surface network of secondary roads rightly resolves the issues of cumbersome calculations which we discussed in Chapter 3.

Considered road network

We consider a surface network comprising a principal road or highway and a great number of secondary roads. For instance we take the network domain represented by Figure 3.21 of the case study 1. We assume the existence of a principal road such like depicted by the below Figure 5.3. The highway (in gray color) comprises 6 lanes: 3 lanes in each direction of traffic (the direction 2 and 4 according to the four dominant directions in a $2d$ elementary cell). Theirs characteristics are set in the Table 5.1 below. We assume some intersections/junctions on such a multi-lane highway that allow traffic change between the urban area and itself. For instance the traffic change is due between Cell 2 and Cell 3 of the surface network and the highway, all depicted by Fig. 5.3. We mesh the highway in twelve (12) $1d$ cells/links of 0.500 km: $s = 0$; $s = 1$; $\dots$; $s = 11$. a_1 denotes the lanes of the highway in the direction 2 of propagation; and a_2 denotes the lanes in the direction 4 of propagation.

The characteristics of the principal artery are set below in the table 5.1.

maximal density	236.25 Veh/km/lane
critical density	33.75 Veh/km/lane
maximal velocity	80 km/h/lane
maximal flow	2700 Veh/h/lane

Table 5.1: Characteristics of the principal artery for GSOM flow computing.
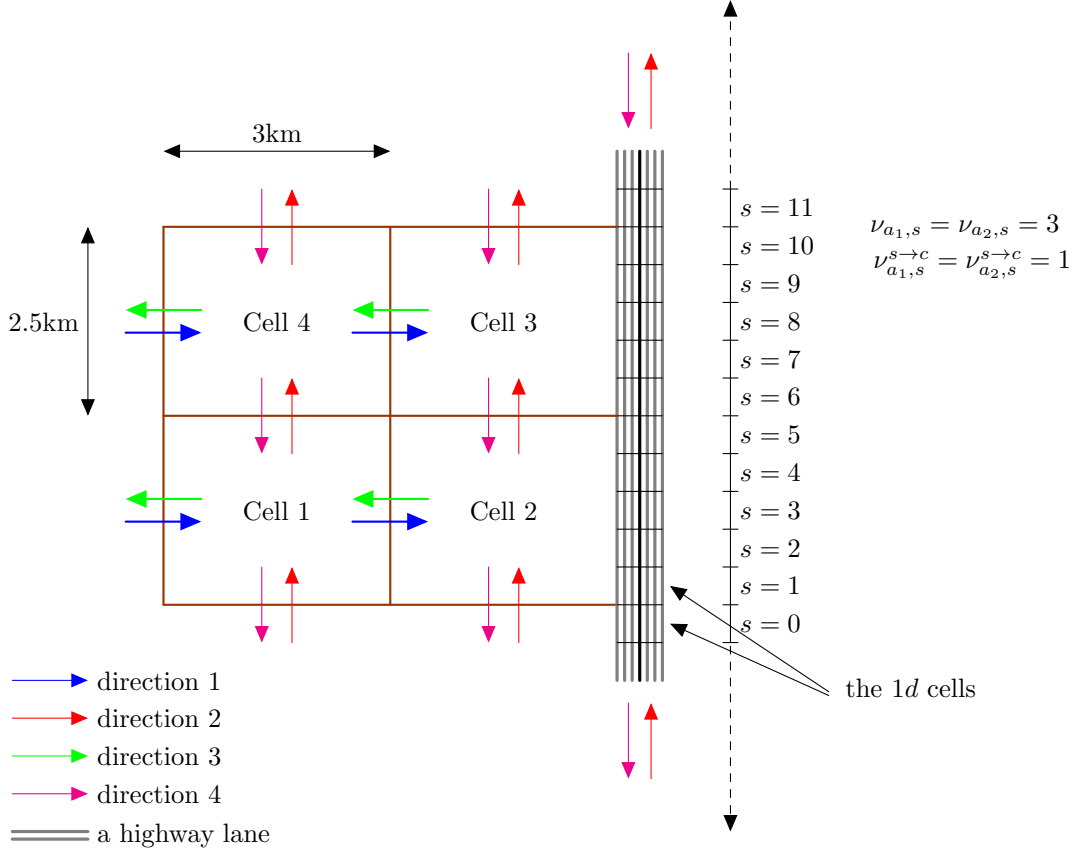
Figure 5.3: Network domain comprising secondary roads and a multi-lane highway.

A surface network represented by such network domain (see above Fig. 5.3) could derived from peri-urban traffic area connected to a metropolitan city.

Common data

We set artificial turning rates for internal movements of the bi-dimensional cells. We attribute the same stochastic matrix Γ_* (respectively Γ^*) to cells 1 and 4 (respectively to cells 2 and 3).

$$
\Gamma_* = \begin{pmatrix} 0.4686 & 0.2236 & 0 & 0.3078 \\ 0.0405 & 0.469 & 0.4905 & 0 \\ 0 & 0.3109 & 0.2904 & 0.3987 \\ 0.3512 & 0 & 0.4097 & 0.2391 \end{pmatrix} \quad \Gamma^* = \begin{pmatrix} 0.4686 & 0.2236 & 0 & 0.3078 \\ 0.0405 & 0.469 & 0.4905 & 0 \\ 0 & 0.3109 & 0.2904 & 0.3987 \\ 0.3512 & 0 & 0.4097 & 0.2391 \end{pmatrix}
$$

The $1d$ cells are numbered from 0 to 11. $s = 0$ and $s = 11$ are $1d$ boundaries cells of the artery $a = (a_1, a_2)$ and have no connection (no commun interface) with the bi-dimensional cells. Only the $1d$ cells $s \in \{1, 2, \cdots 10\}$ share together with the bi-dimensional cells $c = 2$ and $c = 3$. We observe them in the above figure 5.3.

Let us recall that $\gamma_{a,s \to c}$ denotes the turning rates of flow from artery to cell. The matrix of these turning rates are then, with respect to the considered mixed-network of Fig. 5.3:

$$\left(\gamma_{a,s \to c}\right)_{s,c} = \begin{pmatrix} 0 & \gamma_{a_1,s_1 \to c_2} & \gamma_{a_1,s_2 \to c_2} & \gamma_{a_1,s_3 \to c_2} & \gamma_{a_1,s_4 \to c_2} & \gamma_{a_1,s_5 \to c_2} & 0 & 0 & 0 & 0 & 0 & 0 \\ 0 & 0 & 0 & 0 & 0 & 0 & \gamma_{a_2,s_6 \to c_3} & \gamma_{a_2,s_7 \to c_3} & \gamma_{a_2,s_8 \to c_3} & \gamma_{a_2,s_9 \to c_3} & \gamma_{a_2,s_{10} \to c_3} & 0 \end{pmatrix}^T$$

(5.9)

where if A is a matrix, A^T denotes its transpose matrix; and $\gamma_{a_k,s_\ell \to c_m}$ is the turning rates of flow from the lane of a_k of the link $s = \ell$ to the bi-dimensional cell $c = m$.

Testing results

We set the traffic demand constant and equal to 1620 Veh/h/lane at the entry of the artery a_1 and 2520 Veh/h/lane at the entry of the artery a_2. For the residual traffic supply of the $1d$ cells/links, we set the same value equals to 2700 Veh/h/lane. The input data related to the bi-dimensional cells are the same as in the case study 1 of Chap. 3. The matrix of turning rates from artery cells to bi-dimensionals cells is $\left(\gamma_{a,s \to c}\right)_{s,c}$.

On arteries of the highway, we obtain the following numerical results. We show below the evolution of flows accross $1d$ links of arteries a_1 and a_2. Colors 'red' and 'magenta' are specific to directions 2 and 4 respectively. Then, the first color represents physical quantities of artery a_1 and the second color is for artery a_2.
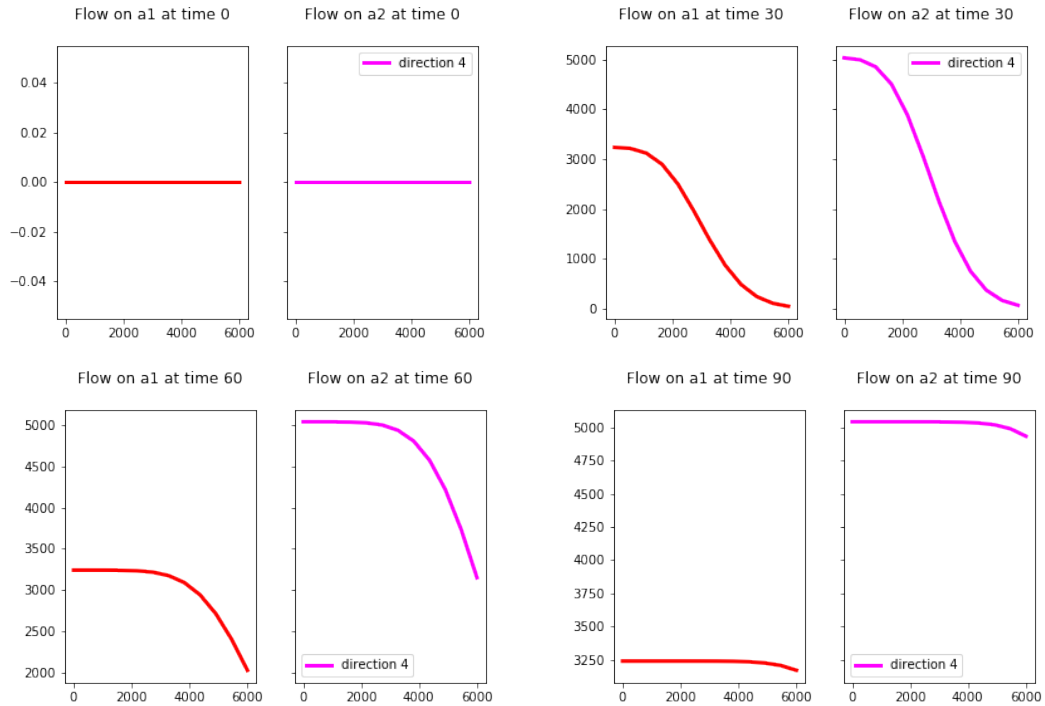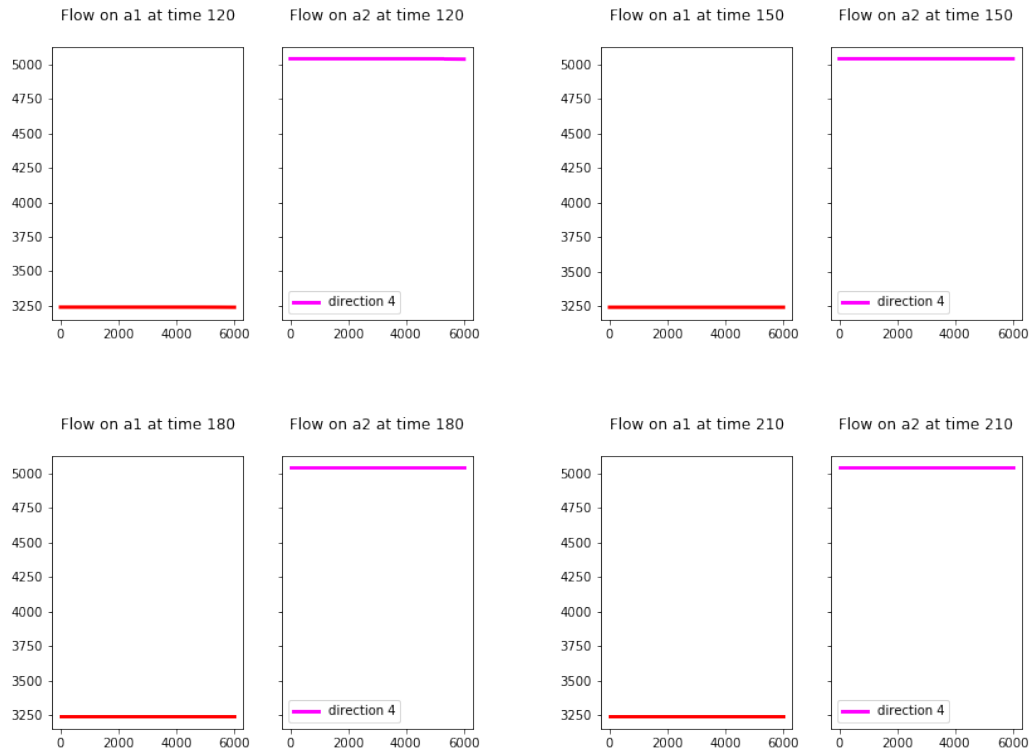
Figure 5.4: Flow on the arteries at certain time steps.
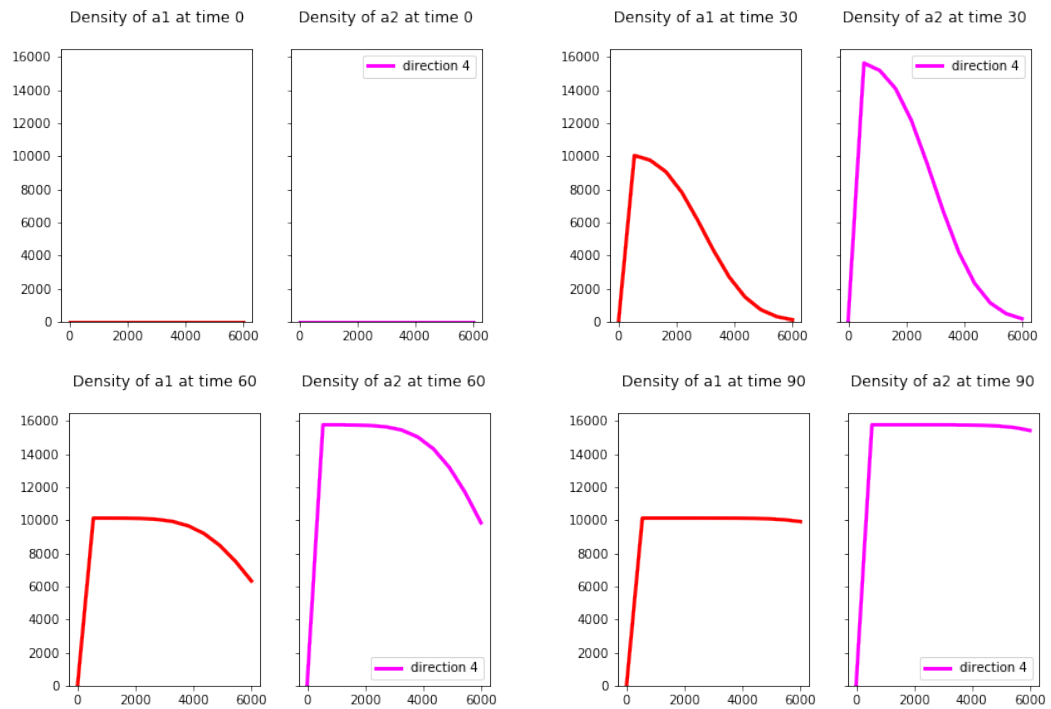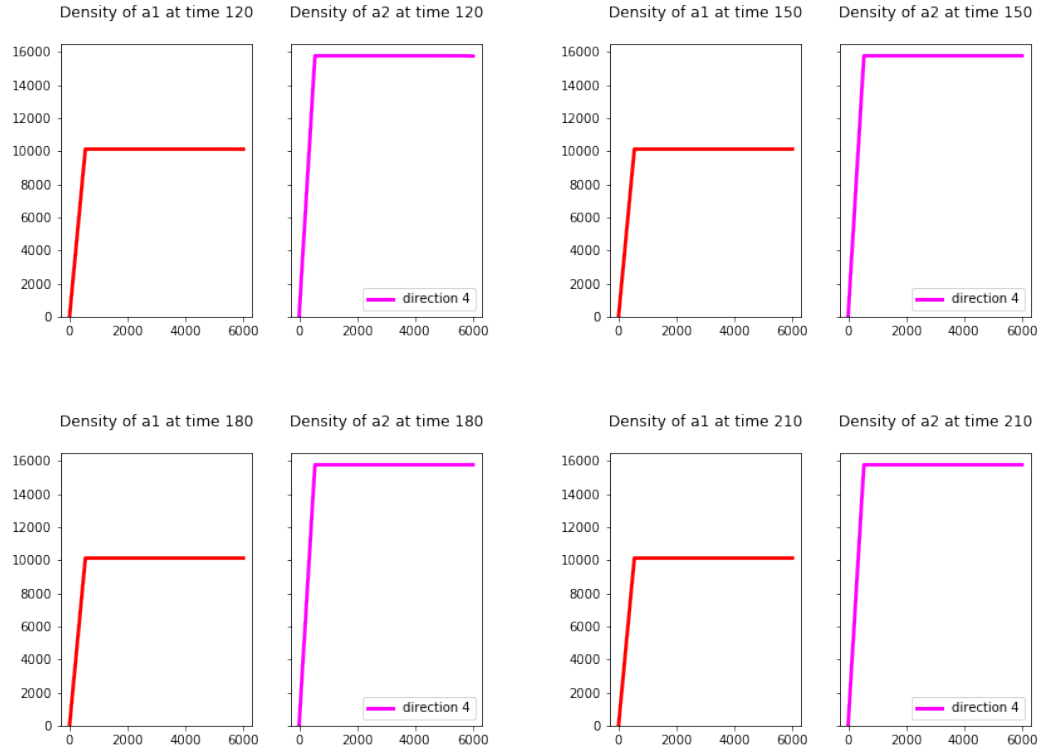
Figure 5.5: Density of arteries at certain time steps.

Let us zoom in on the traffic flows between the considered traffic urban area and the highway. Traffic flows originating from the highway to traffic urban area constitute the travel demand at the border of the bi-dimensional cells 2 and 3, following the dominant direction 3 of propagation. Besides, traffic flows originating from the bi-dimensional cells 2 and 3, precisely outflows of cell 2 and 3, in the direction 1 are travel demand to the $1d$ cells of arteries of the highway.

Figure 5.6: Flows between the bi-dimensional cells and the highway.

On the bi-dimensional cells which represent the urban traffic area, the numerical results are the following.

Figure 5.7: Inflows of the bi-dimensional cells.

Figure 5.8: Outflows from the bi-dimensional cells.

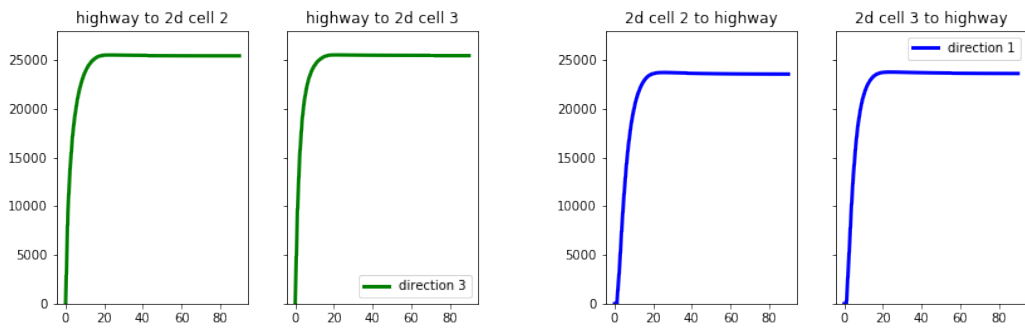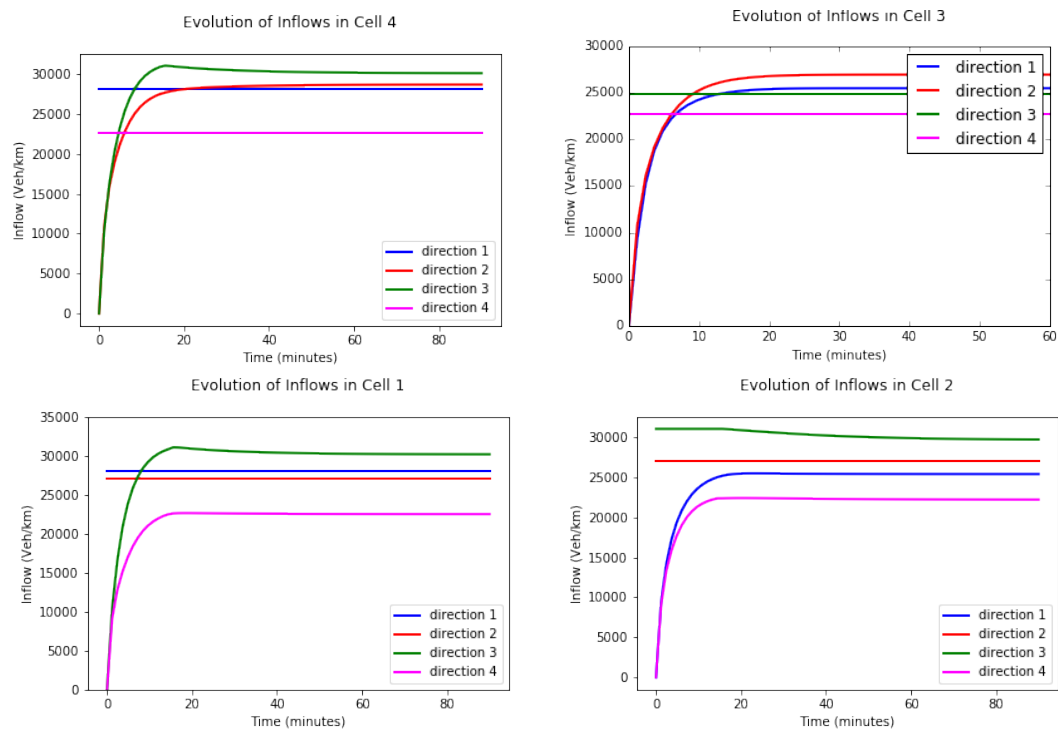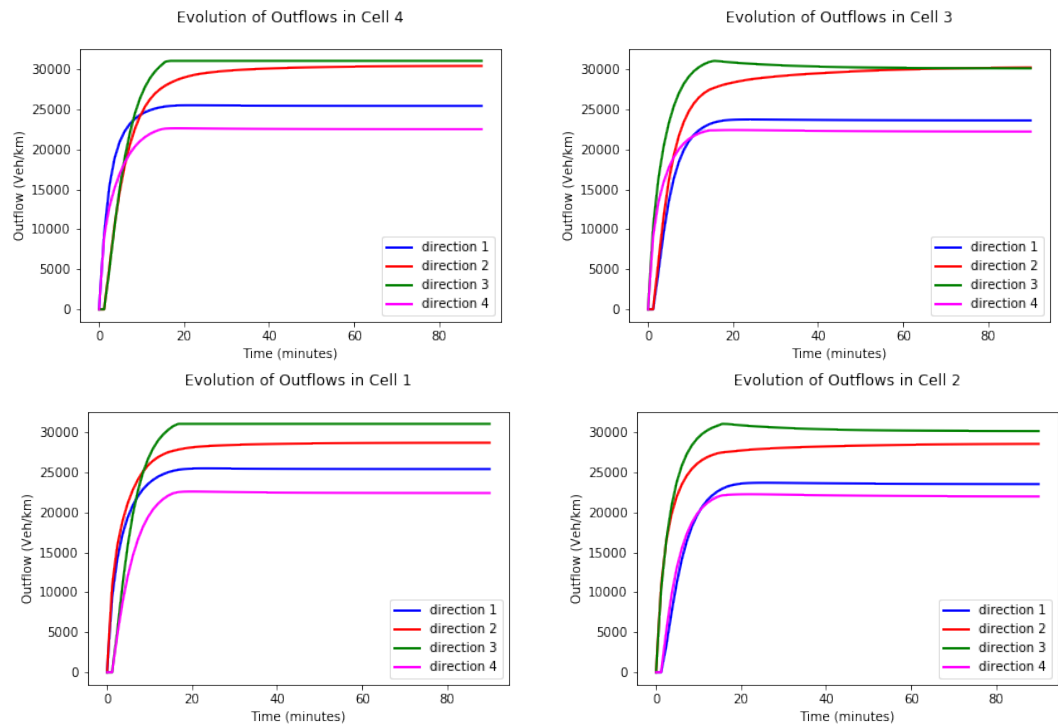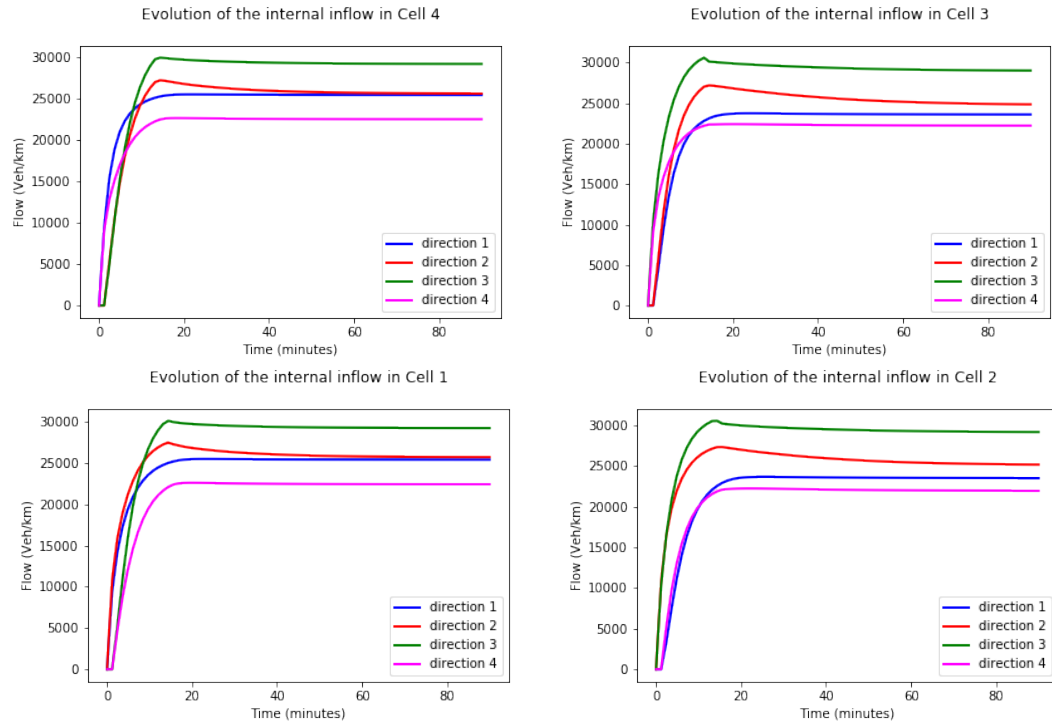Figure 5.9: Internal Inflows in the bi-dimensional cells.
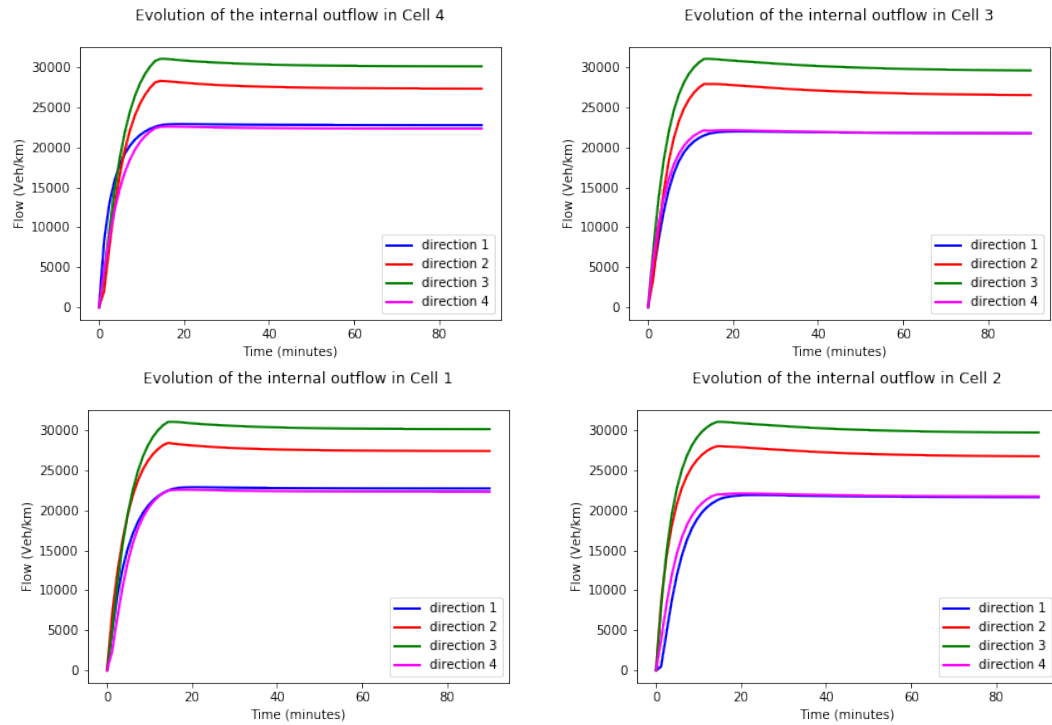
Figure 5.10: Internal Outflows in the bi-dimensional cells.
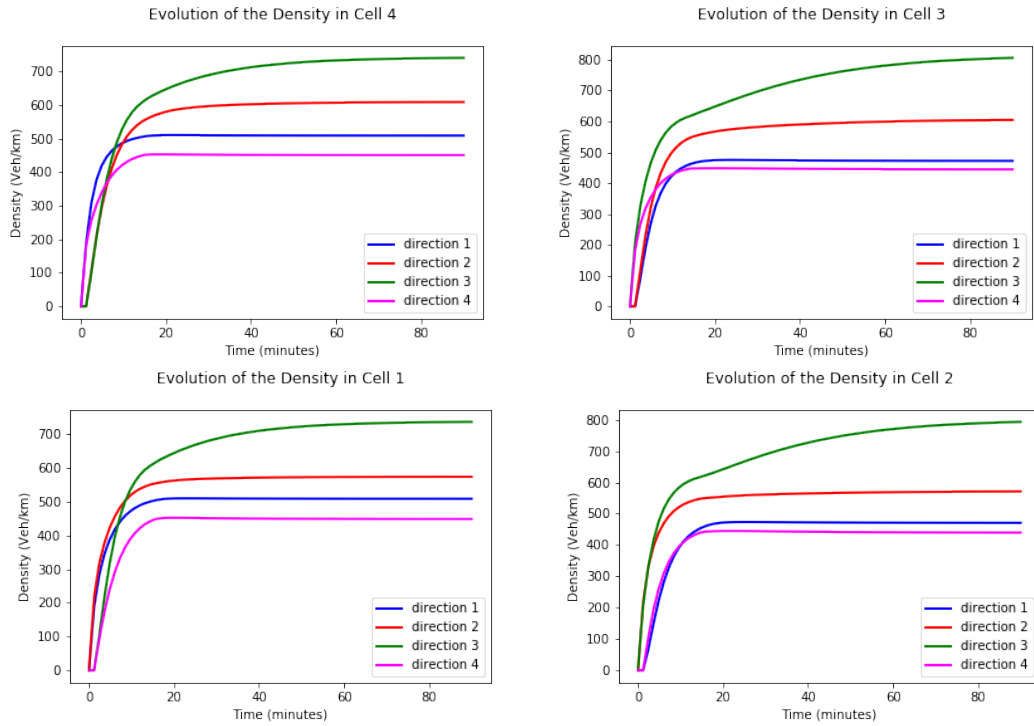
Figure 5.11: Density of the bi-dimensional cells.

We have proved in the previous chapter 3 and this current chapter 5 that one can estimate traffic flows and densities by following at once macroscopic and two-dimensional traffic flow theories. That is the way we argue to reduce intensive calculations in the case of very large surface networks comprising an urban traffic area (secondary roads) and highways. Since the consideration of large and dense surface networks is not the only focus of this Report, we will go through the next section 5.3 to provide how to take into account the vehicular multimodality in the estimation of vehicles flow and density over large networks.

Therefore, in the next section we discuss about considering traffic attributes such like transportation modes to provide estimation of traffic flows and densities estimation per theses attributes. For instance we consider transportation modes such as mass transportation (bus, train, tram, metro), specific modes via demand responsive transport systems, carpooling systems, share and ride travel systems, personal rapid transit systems. The traffic area involved will be large and dense, and comprise ground traffic area and specific air traffic area. The latter traffic area is the one we have discussed in the section 4.2 of the chapter 4.

5.3 Multiscale coupling

This section provides a model which could be applied to traffic area of urban network comprising different transportation modes which share a ground traffic area and a specific air traffic area. It is a question of coupling models of different scales: the microscopic, macroscopic and bi-dimensional scales.

Issues of multiscale modeling

Remarkably, existing models at the same scale typically follow different modeling approaches and, hence, it is difficult to relate these models to each other. In addition, models at different modeling scales are rarely coupled. For example, a macroscopic model typically lacks a microscopic basis and a microscopic model does not have its macroscopic counterpart. Therefore, an ideal multiscale modeling approach should emphasize not only model quality at each individual scale but also the coupling between different scales.

Governing equations

Let U be the traffic area of a multimodal network. We assume that this multimodal network is very large and dense. Since U is large, we could apply the bi-dimensional modeling approach and then mesh or disaggregate the traffic area U in $2d$ elementary cells $c \in \mathfrak{C}$, where $\mathfrak{C}$ is the set of all $2d$ elementary cells of U.

Let (c) be an element of $\mathfrak{C}$ and that it comprises at least a part of roads used by a bus-line and a demand responsive system (DRS).

We already know that global flows of such $2d$ computing cell (c) per its dominant directions could be easily compute. We have fully developed the dynamical bi-dimensional traffic flow model for that in Chap. 3. However, to compute these directional cell flows in the situation where buses-lines and/or DRS-lines cross the area of a $2d$ elementary cell (c), we shall consider the flow originating from buses of commun transportation and the flow originating from the DRS vehicles. In that way, we provide a governing system that describes dynamics of vehicles from different forms of mobility inside any same $2d$ elementary cell. Is to do multi-scale modeling. The main variables and parameters of the multiscale model we introduce are the following.

- The lenght of lanes in the 4 privileged directions of the cell (c) is L_c^{*c} without accounting the lanes of buses and of DRS's vehicles;

- The number of buses in the cell (c) at the time t is $N_c^{*b}(t)$;

- The lenght of buses lines in the cell (c) is L_c^{*b};

- The density $\rho_c^{*b}(t)$ of buses in the cell (c) at the time t is defined as
$\rho_c^{*b}(t) = N_c^{*b}(t)/L_c^{*b}$;

- The inflow of buses in the cell (c) at the time t is $q_c^{*b}(t)$;

- The number of DRS's vehicles in the cell (c) at the time t is $N_c^{*s}(t)$;

- The lenght of DRS's vehicles in the cell (c) is L_c^{*s};

- The density $\rho_c^{*s}(t)$ of DRS's vehicles in the cell (c) at the time t is defined as
$\rho_c^{*s}(t) = N_c^{*s}(t)/L_c^{*s}$;

- The inflow of DRS's vehicles in the cell (c) at the time t is $q_c^{*s}(t)$.

The dynamic of heterogeneous particles such as the buses for commun transportation, and vehicles for demand responsive travel and personal vehicles is difficult to describe. In the following we suggest a physical approach to describe such dynamic.

Let us denote by $K_c(t)$ the density of the cell (c) in its dominant/privileged directions accounting other roads dedicated to commun transportation or responsive travel. We define this variable density as

$$K_c(t) = \chi_c^b \rho_c^{*b}(t) + \chi_c^s \rho_c^{*s}(t) + \chi_c^c \left(\sum_{i=1,2,3,4} \Gamma_{c,ii}^t \rho_{c,i}(t) \right) \tag{5.10}$$

with $\chi_c^c + \chi_c^b + \chi_c^s = 1$. For each cell (c), $\Gamma_{c,ii}^t$ is the rate of vehicles going straight from the same direction i within the cell at time t. We recall that $\left(\Gamma_{c,ij}^t \right)_{i,j=1,2,3,4}$ is the stochastic matrix of assignment of flows within the cell (c) at time t. χ_c^b and χ_c^s are respectively the fraction of flow of (c) located on the bus lines, and the fraction of flow of (c) located on the DRS routes.

Thus, the conservation law results in

$$L_c \frac{d}{dt} K_c(t) = (r_c(t) - q_c(t)) + \sum_{g \in Neighbor(c)} \left(Q_{gc}(t) - R_{cg}(t) \right) \tag{5.11}$$

with $L_c = L_c^{*c} + L_c^{*b} + L_c^{*s}$.

$Q_{gc}(t)$ represents the inflow of (c) taking into account $q_c^{*b}(t)$ and $q_c^{*s}(t)$. Correspondingly, $R_{cg}(t)$ accounts the outflow $r_c^{*b}(t)$ and the outflow $r_c^{*s}(t)$. $r_c(t)$ and $q_c(t)$ are same variables (of Chap. 3) which denote the solution of the linear-quadratic intersection traffic flow model (3.21).

5.4   Perspectives

This chapter presents a perspective on traffic flow modeling at a spectrum of three scales: microscopic, macroscopic and bi-dimensional. In order to ensure modeling consistency, it is critical to address the coupling among models at different scales, i.e. how less detailed models are derived from more detailed models and, conversely, how more detailed models are aggregated to less detailed models. Consequently, traffic flow is modeled as the motion and interaction of all vehicles.

We should implemented these hybrid and multiscale models respectively presented in Sec. 5.2 and Sec. 5.3 in a real case scenario. However we argue that our case study is right since it results from efficient hybridization and multicoupling thechnics.

Chapter 6

RDTA over large transport networks

Contents

The acronym RDTA of this chapter 6 is referred to Reactive Dynamic Traffic Assignment. It is a way for making dynamic traffic assigment by using a reactive scheme relying on the traffic flow prediction and traffic information rather than on an equilibrium dynamic traffic assignment.

6.1   Introduction

Traffic assignment is one of the recurring issues in the preoccupations of networks operators. Particular attention is taken in the case of transport since large urban networks allow people to move every day providing to them means of mobility. The government and territorial

communities are concerned. There are many static equilibrium allocation models dedicated to transport planning with respect to assignment problems in the literature. There are also dynamic allocation models. We are focusing on the second kind of assignment. Most algorithms rely on shortest paths schemes (this is assumed to results from the preferences of drivers). Versatile algorithms such genetic algorithms, greedy algorithms, evolutionary algorithms, have been developed addressing assignment issues in traffic control over networks. Traffic flow models incorporating such algorithms are of good quality depending on the purposes for which they are deployed, and the particular networks concerned. Nevertheless, it is not obvious whether they represent accurately the dynamic aspects of network flows when very large transport networks are involved.

Organization of the chapter

In this chapter we propose a model of dynamic assignment of vehicles flow to predicte and estimate the traffic on wide and dense networks. Using instantaneous travel times of users over networks, the RDTA model developped by Khoshyaran and Lebacque [43] and applied on networks allows to adequately describe movements of users over networks. It allows with specific accomodations that we provide in this Report in Chap. 3, Chap. 5 and Chap. 6, to compute accurately two-dimensional cell flows of large surface networks. The specific accomodations are set out below. (i) We consider that traffic information flows from one bi-dimensional cell to another, along arcs that connect them together. Bi-dimensional cells are modeled as nodes with internal traffic flows along dominant/privileged directions. (ii) Traffic flows are propagated from bi-dimensional cell to another through links/arcs connecting bi-dimensional cells. (iii) Travel costs are estimated based on traffic information in time, traffic densities over the considered network and the variability of paths used.

Our developed RDTA model is a Logit-based model and is fully described in Sec. 6.2. Paths of users are allocated along the directional inflows and directional outflows of bi-dimensional cells. In the previous Chapter 5, we have proposed a versatile hybrid/multiscale traffic simulation for discrete-continuous networks. *Bi-dimensional transport simulator* will denote transport simulator based on (the semi-discretized shape of) the bi-dimensional traffic flow model and the proposed RDTA scheme. The implementation of its simulation model has been provided in [80].

6.2 Reactive dynamic assignment

Let us introduce our RDTA model applied to the Lagrangian two-dimensional traffic flow model developed in the previous chapter 3. Given time-dependent OD matrices, a first allocation of traffic demands is based both on averaged travel times (from cell to cell, pointed by directional outflows) and traffic states in all cells of the whole network domain. Cells refer to $2d$ elementary/bi-dimensional cells which are fully described in Chap. 3.

The traffic assignment model shall identify travel paths of minimum cost, and related directional outflows of cells of these paths. Let us recall that cell flows could be computed with the bi-dimensional traffic flow engine (depicted by Fig. 3.7) which is fully implemented, tested and validated in Chap. 3.

Let us summarize the principle of the approach. The paths are considered from bi-dimensional cell to bi-dimensional cell. Trips inside bi-dimensional cells are approximated by trips from cell center to boundary or from boundary to cell center. The main difficulties reside in modeling trips, and estimating travel costs. Trips are the succession of crossed cells.

Notations are the following.

- $\pi_c^d(t)$: the weight of the path of minimum cost at the time t that reaches the destination cell (d) originating from the cell (c). The destination (d) could be a border of a cell.

- $\pi_c^{d,k}$: the weight of the path of minimum cost at the time t that reaches the cell destination or the cell border (d) from the cell (c), consisting in k-routes. Here we assume that k is equal to 2. This is related to a simplifying assumption on possible directions vehicles or users will use when moving out of a cell towards a destination. We highlight this later in this Sec. 6.2.

- $\Gamma_{c,ij}(t)$: turning rate movements of vehicles within the cell (c), from direction (i) to direction (j), at time t. We recall that $\left(\Gamma_{ij}\right)_{ij}$ is the stochastic traffic assignment matrix depending on the time and cells.

- $\Gamma_{c,ij}^d(t)$: turning rates of incoming flow at the time t in the cell (c) in the direction (i) which going to the direction (j), in order to reach the cell (d) as its destination.

- $\varpi_{cc'}(t)$: the cost of the arc (c,c') at the time t. An arc is the link between two adjacent

cells. So the arc (c, c') is a link that connects the cell c to the cell c', and vice versa. The arc (c, c') is different from the arc (c', c) depending on the direction of travel. We mean that considered bi-dimensional network domains are modeled as direct and weighted graph.

From a simple mesh of a transportation network area (depicted by Figure 6.2) we are able to construct a new network graph at the two-dimensional scale (see figure 6.2).

Travel cost

The cost of travelling from the cell (c) to the cell (g), denoted by ϖ_{cg}^t, can be estimated in the framework of the proposed model by the instantaneous travel time, which itself can be estimated at each time-step t by the following approximation:

$$\varpi_{cg}(t) \approx N_{c,i}(t)/R_{cg}(t) \tag{6.1}$$

if the cell (g) is such that the exit direction (i) of the cell (c) is its entry direction (see the below figure). The above approximation (6.1) of the travel cost $\varpi_{cg}(t)$ is valid only if $N_{c,i}(t)$ and $R_{cg}(t)$ are different of zero, and lower bounded by strictly positive number.
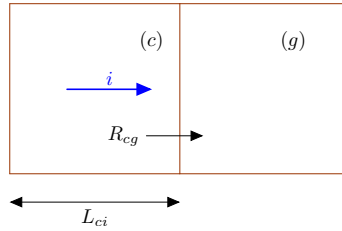
In other way, by default we have the following:

$$\varpi_{cg}(t) = \frac{1}{2} \left(\frac{L_{c,i}}{V_{c,i,max}} + \frac{L_{g,j}}{V_{g,j,max}} \right) \tag{6.2}$$

where $V_{c,i,max}$ is the maximal exit speed of vehicles from the cell (c) follows direction i, and $L_{c,i}$ is the length of lanes in cell (c) in direction i.

The unit of measurement of $N_{c,i}(t)/R_{cg}(t)$ is $\left[\frac{N_{c,i}(t)}{R_{cg}(t)} \right] = \frac{Veh}{Veh/s} = s$. Therefore units of measurement of $\varpi_{cg}(t)$ and $N_{c,i}(t)/R_{cg}(t)$ are the same.

The instantaneous travel time from one origin to a destination via a path is the sum of instantaneous travel time of the cells located on such path.
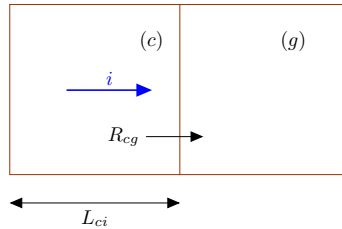
Instantaneous travel time

Let $(c) \in \mathfrak{C}$ be a cell. For (i) a direction, we denote by $V_{c,i}^t$ the cell exit speed of (c) in the direction $(i) = c \rightarrow g$. We are defining instantaneous travel time (ITT) for cell links: that is the links in $2d$-cell that lie in the preferred directions of flow propagation. It is a good approximation since flows will assign through these preferred directions of propagation. This is even the main expected feature in two-dimensional modeling: reduce the great number of links and nodes of dense network in a simplified network while still ensure a way of providing good sufficient information about network traffic states. Let us mention that instantaneous travel time in two-dimension space shall be describe as an integral along the path a user or vehicle will follow with respect to its velocity. A formal definition of ITT is the following (see [49]).

$$ITT(\text{path}; t) = \int_{\text{path}} d\chi / V(\chi, t) \tag{6.3}$$

This formula is valid in non-interrupted traffic flow, particularly when velocity is always bound by a strictly positive lower speed.

The authors of [49] have give clear computational definition of the ITT in interrupted traffic. The cell exit speed defined as $V_{c,i}^t = R_{cg}(t)L_{c,i}/N_{c,i}(t)$ permits emulation of 'First In First Out' (FIFO) behavior within each $2d$-cell [84]. A proper discretization constraint such $R_{cg}(t)\delta t \leq N_{c,i}^t$ is set.

Let us use instantaneous travel time for an arc/link, and adapted it to a bi-dimensional cell with respect to its dominant directions of propagation. Let us denote by $T_{c,i}^t$ the instantaneous travel time from the entire length of the cell (c) in direction (i), estimated at time t.

Hence, introducing the cell travel time $ITT_{c,i}^t = T_{c,i}^t - T_{f,i}^t$, the below (6.4) formulas hold

along the cells of a path:

$$
\left[
\begin{aligned}
ITT_{c,i}^{t+1} - L_{c,i}/V_{c,i}^t &= \left(1 - \frac{\alpha_{c,i}\,\nu_{c,i}^t}{1-\nu_c^t}\right)\left(ITT_{c,i}^t - L_{c,i}/V_{c,i}^t\right) - \left(T_{f,i}^{t+1} - T_{f,i}^t\right), \\[2mm]
&\qquad\qquad\qquad\qquad \text{if } \nu_{c,i}^t \le \tfrac{1}{1+\alpha_{c,i}} \\[4mm]
ITT_{c,i}^{t+1} - L_{c,i}/V_{c,i}^t &= -\frac{1-\alpha_{c,i}}{\alpha_{c,i}^t\,\nu_{c,i}^t}\left(T_{f,i}^{t+1} - T_{f,i}^t\right) \text{ if } \nu_{c,i}^t \ge \tfrac{1}{1+\alpha_{c,i}}
\end{aligned}
\right.
\tag{6.4}
$$

Coefficients $\alpha_{c,i}$ and $\nu_{c,i}^t$ are defined such as:

$$
\alpha_{c,i} \overset{def}{=} V_{c,i,max}\delta t/L_{c,i} \text{ and } \nu_{c,i}^t \overset{def}{=} V_{c,i}^t/V_{c,i,max} = R_{c,g}^t \delta t/\left(\alpha_{c,i} N_{c,i}^t\right).
\tag{6.5}
$$

$V_{c,i,max}$ is the maximal exit speed of vehicles from the cell (c) with respect to the direction i.

Logit formulation

Let us introduce a Logit model for the choice of neighbor cells, and address shortest paths computation. From a cell, vehicles have 4 possible choices for their next motion since there are 4 exit directions. Let d be a destination. d can be a cell or a border of cell. Let (c) is any cell. We assume that (c) is different from d in case where d is a cell.

From cell (c), vehicles/users have generally just 2 possible directions that they may take when they are going out of the cell. This is a simplifying assumption.

Figure 6.2 depicts the 2 possible directions, from a cell (c) to other cell or a border of other cell, named d which could be a destination.
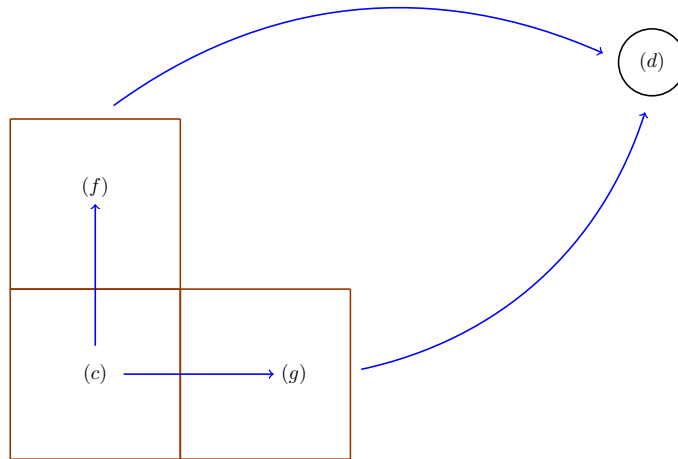

Figure 6.1: Possible paths, with respect to the traffic information and exit speeds in dominant directions of propagation of cells located on the paths, from cell (c) (which could be origin) to other cell or a border of other cell (named d as destination).

Therefore, the weight of the path of minimum cost $\pi_c^d(t)$ at the time t can be decomposed as below:

$$\pi_c^d(t) \quad \rightarrow \quad \begin{cases} \varpi_{cf}^t + \pi_f^d(t + \varpi_{cf}^t) = C_f^d(t) \\ \varpi_{cg}^t + \pi_g^d(t + \varpi_{cg}^t) = C_g^d(t). \end{cases} \tag{6.6}$$

This approximation (6.6) is justified because there are privileged/dominant directions of travel in each cell.
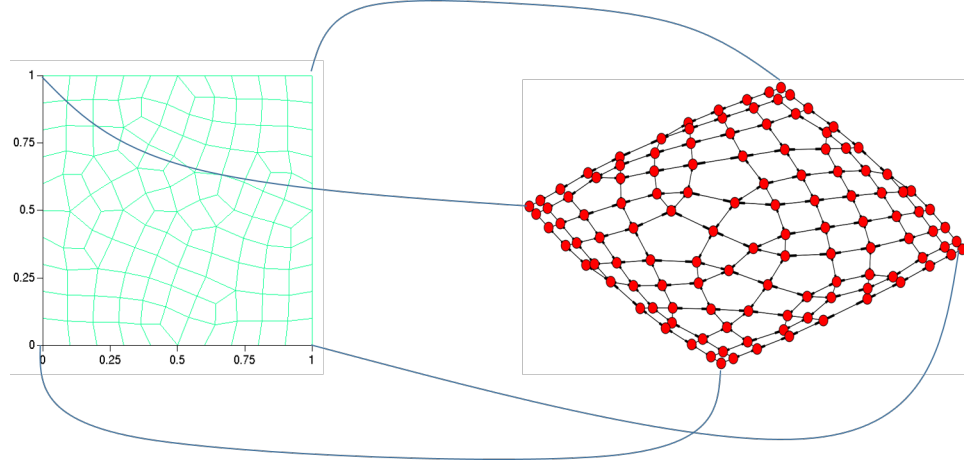

Figure 6.2: Zone-based surface newtork representation

Each node represents a zone. Each arc is a connection between two adjacent zones, from zone center to zone center. Zones are two-dimensional computing cells, with at most 4-directions of propagation of the vehicles flows: (4-inflows and 4-outflows for each cell/node or zone).

We can determine the probability of choice of users for choosing either one cell between neighbor cells from the cell they are located, at time t. The formulation of this probability is given by Eq. (6.7):

$$\left[\begin{array}{l} P\left((\text{choice} = (f)/\text{Dest.} = d)(t)\right) = \dfrac{\exp\left(-\theta C_f^d(t)\right)}{\exp\left(-\theta C_f^d(t)\right) + \exp\left(-\theta C_g^d(t)\right)} = \mathscr{F}_{cf}^d(t) \\[4mm] P\left(\text{choice} = (g)/\text{Dest.} = d\right)(t) = \dfrac{\exp\left(-\theta C_g^d(t)\right)}{\exp\left(-\theta C_f^d(t)\right) + \exp\left(-\theta C_g^d(t)\right)} = \mathscr{F}_{cg}^d(t). \end{array} \right. \tag{6.7}$$

Parameters $\mathscr{F}_{cf}^d(t)$ and $\mathscr{F}_{cg}^d(t)$ allow the calculation of coefficients of turning rates.

Therefore, the time-dependent cost of the path from (c) to d is defined in the following.

$$\forall (c,d) \in \mathfrak{C} \times \mathfrak{C}, \forall t, \quad \begin{aligned} \pi_c^d(t) &= \mathscr{F}_{cf}^d(t) \cdot C_f^d(t) + \mathscr{F}_{cg}^d(t) \cdot C_g^d(t) \\ &= \mathscr{F}_{cf}^d(t) \cdot C_f^d(t) + \left(1 - \mathscr{F}_{cf}^d(t)\right) \cdot C_g^d(t) \end{aligned} \tag{6.8}$$

159

This is a recursive formula on the calculation of the cost of shortest paths with respect to the bi-dimensional traffic flow prediction and traffic information. Nevertheless, we can easily compute $\pi_c^d(t)$ by the below array formula of algebra $(min, +)$ type, which can be improved as a Dijkstra algorithm (see Table 6.1).

Dijkstra based $(min, +)$ algebra for time-dependent shortest paths computation

For each time-step $t > 0$, $\forall (c, d) \in \mathfrak{C} \times \mathfrak{C}$,

- $\pi_c^{d,1}(t) = 0$ (Initialization).
- If $c \neq d$, $\pi_c^{d,1}(t) = \varpi_{cd}(t)$ if exists arc (c, d), or $= \infty$ if not.
- $\pi_c^{d,k+1}(t) = \min \left[\pi_c^{d,k}(t) , \min_{c' \in Succ(c)} \left[\varpi_{cc'}(t) + \pi_{c'}^{d,k}\left(t + \varpi_{cc'}(t)\right) \right] \right]$.

Table 6.1: Time-dependent shortest paths findings.

$Succ(c)$ is the set of successors of the cell (c), since (c) represents a node of the graph corresponding to the network domain.

The RDTA scheme

Let us recall the algorithmic scheme used, from Chap. 3, to compute traffic flow of surface networks. It is a scheme without assignment since we do not calculate the stochastic matrix of assignment $\Gamma_{c,ij}^t$ along the previous simulations. We recall that the assignment matrix we have used has been generated according to the works of Sautmally et al. [78] in case of a static assignment. In the following, let us recall the actual scheme without assignment from Chap. 3. It is the scheme with which we calculated bi-dimensional cell flows in its dominant or preferred or privileged directions.

The scheme from Chap. 3: a scheme with static assignment

Let us assume to be at the time step t of the computation of cell flows in the directions of propagation.

We could assume that we have values of N_{ci}^t and ρ_{ci}^t for all $c \in \mathfrak{C}$ and $i \in \{1, 2, 3, 4\}$ at this time step t. Let us then summarize steps to compute N_{ci}^{t+1} and ρ_{ci}^{t+1} for all $c \in \mathfrak{C}$ and $i \in \{1, 2, 3, 4\}$.

- Internal traffic demand and internal traffic supply are set to be:

$$\delta_{ci}(\rho_{ci}^t) = \lambda_{ci} \nu_{ci} \Delta_{ci}(\rho_{ci}^t) \quad \text{and} \quad \sigma_{ci}(\rho_{ci}^t) = \lambda_{ci} \nu_{ci} \Sigma_{ci}(\rho_{ci}^t)$$

$\Delta_{ci}()$ and $\Sigma_{ci}()$ are lineic traffic demand and lineic traffic supply functions of cell (c) follows direction i. Hence, $\Delta_{ci}(\rho_{ci}^t)$ and $\Sigma_{ci}(\rho_{ci}^t)$ are the internal traffic demand and internal traffic

supply per lane and direction.

- The traffic demand and traffic supply at the border of the network domain are

$\Delta_{cg}^t = v_{cg}\Delta_{ci}(\rho_{ci}^t)$ if the cell (g) is the cell in the direction (i) when being in the cell (c), and

$\Sigma_{hc}^t = v_{hc}\Sigma_{ci}(\rho_{ci}^t)$ if (h) is the cell as shown below.

v_{cg} and v_{hc} are numbers of lanes of cell (c) in directions $j = c \rightarrow g$ and $i = h \rightarrow c$ respectively.

- Calculation of internal flows: q_{ci}^t and r_{ci}^t.

We recall that these variables are solution of the below linear-quadratic optimization problem, which we have solved with the 'CVXOPT' Python based solver.

$$
\max_{(q_c, r_c)} \left(\sum_{i=1}^{4} \Phi_i(q_{ci}) + \sum_{j=1}^{4} \Psi_j(r_{cj}) \right)
$$

$$
\text{s.t.} \quad \left|
\begin{array}{ll}
0 \leq q_{ci} \leq \delta_{ci}^t, & \forall i \in \{1, 2, 3, 4\}, \\
0 \leq r_{cj} \leq \sigma_{cj}^t, & \forall j \in \{1, 2, 3, 4\}, \\
r_{cj} = \sum_{i=1}^{4} q_{ci}\Gamma_{c,ij}^t, & \forall j \in \{1, 2, 3, 4\}.
\end{array}
\right.
\tag{6.9}
$$

with $q_c = (q_{c1} \; q_{c2} \; q_{c3} \; q_{c4})$ the vector inflow of cell (c) and $r_c = (r_{c1} \; r_{c2} \; r_{c3} \; r_{c4})$ its vector outflow.

- Calculation of flows at the border: $q_{cg}^t = \min\left(\Delta_{cg}^t, \Sigma_{cg}^t\right)$.
- Intermediate important variable is $N_{ci}^{t+1/2} = N_{ci}^t + \Delta t \left(r_{ci}^t - q_{ci}^t\right)$ at time step $t + 1/2$.
- In doing so, we can at the end compute $N_{ci}^{t+1} = N_{ci}^{t+1/2} + \Delta t \left(Q_{gc}^t - Q_{ch}^t\right)$ is the number of vehicles in cell (c) at the next time step $t + 1$.
- $\rho_{ci}^{t+1} = N_{ci}^{t+1}/L_{ci}$ is the density of the cell (c) in the direction (i) at the time step $t + 1$, where L_{ci} is the length of lanes of cell (c) in the direction i.

We are going to introduce the destination attribute denoted by d and itineries in the above scheme. With these notions, we deduce a scheme of dynamic assignment. The resulted scheme is commonly known as a kind of reactive DTA. At each time step, values of the stochastic matrix assignment $\left(\Gamma_{c,ij}^t\right)_{i,j=1,2,3,4}$ of each cell (c) may change and then are recalculated.

Scheme of reactive DTA: calculation of the stochastic matrix of assignment

In this section, we provide the analytical expression of the stochastic matrix of assignment $\Gamma_c = \left(\Gamma_{c,ij}^t\right)_{i,j=1,2,3,4}$ for each $c \in \mathfrak{C}$ and its calculation over time during a simulation. For

$c \in \mathfrak{C}$, Γ_c is related to the following coefficients of turning rates $\gamma_{c,j}^{d,t}$ according to the destination attribute d.

Let us pose $\chi_{ci}^{d,t} = N_{ci}^{d,t}/N_{ci}^t$. Then $\chi_{ci}^{d,t} = \rho_{ci}^{d,t}/\rho_{ci}^t$. $\chi_{ci}^{d,t}$ is the fraction of cell (c) concentration', which is moving at the time t towards the destination $d \in \mathfrak{D}$.

$\forall c \in \mathfrak{C}$, $\forall i, j = 1, 2, 3, 4$, we have:

$$\Gamma_{c,ij}^t = \sum_{d \in \mathfrak{D}} \gamma_{c,j}^{d,t} \, \chi_{ci}^{d,t} \tag{6.10}$$

The relevant variable is then the turning rates $\gamma_{c,j}^{d,t}$ related to the destination attribute d. Its formulation is given by (6.13) below.

• **Calculation of $\gamma_{c,j}^{d,t}$, coefficients of turning rates in cell (c) follows direction j towards destination d.** First, we need to know the travel time when traveling from a cell to its neighbor cells. Let us recall its formulation. Given the following figure,
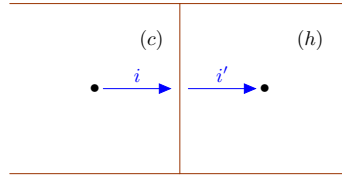
the travel time or travel cost from the cell (c) to the cell (h) is given by:

$$\varpi_{ch}^t \approx \frac{1}{2}\left(\frac{N_{ci}^t}{Q_{ch}^t} + \frac{N_{hi'}^t}{Q_{ch}^t} \right) = \frac{N_{ci}^t + N_{hi'}^t}{2Q_{ch}^t}. \tag{6.11}$$

We initialize the Dijkstra-based algorithm as below:

$$\left| \begin{array}{rcl} \pi_c^{1,t} & = & \dfrac{N_{c1}^t}{R_{c1}^t} \ \text{ if the cell } (c) \text{ is on the border (1)} \\ \pi_c^{1,t} & = & +\infty \end{array} \right.$$

Next we execute the Dijkstra-based algorithm and find k-shortest paths from (c) to d, and then compute the travel cost $\pi_c^{d,t}$. Let us mention that, according to the RDTA routes of probability non nil to be used, $k = 2$.

Given the above precedent figure, we write:

$$C_{ch}^{d,t} = \varpi_{ch}^t + \pi_h^{d,t} \tag{6.12}$$

Let us specify that $C_{ci}^{d,t} \equiv C_{ch}^{d,t}$ if and only if (h) lies in the direction i from (c).

We argue that the turning rates $\gamma_{ci}^{d,t}$ derives from cross-entropy formulation based on the

travel cost $C_{cj}^{d,t}$, where j represents the directions $i-1$ and $i+1$.

$$\gamma_{ci}^{d,t} = \frac{\exp\left(-\theta C_{ci}^{d,t}\right)}{\exp\left(-\theta C_{c,i-1}^{d,t}\right) + \exp\left(-\theta C_{c,i+1}^{d,t}\right)} \tag{6.13}$$

• **Calculation of $\rho_{c,i}^{d,t}$, the density of cell (c) along direction j per destination attribute d.**
Expression (6.10) will be injected in the convex-optimization problem (6.9). A disaggregation by destination $d \in \mathfrak{D}$ is hence appropriate.

In each cell (c), internal flows are then: $q_{c,i}^{d,t} = \chi_{ci}^{d,t} q_{c,i}^{t}$ and $r_{c,j}^{d,t} = \left(\sum_i q_{c,i}^{d,t}\right)\gamma_{cj}^{d,t}$. The cell crossing flows are simply: $Q_{ch}^{d,t} = Q_{ch}^{t}\chi_{ci}^{d,t}$ according to the figure below.
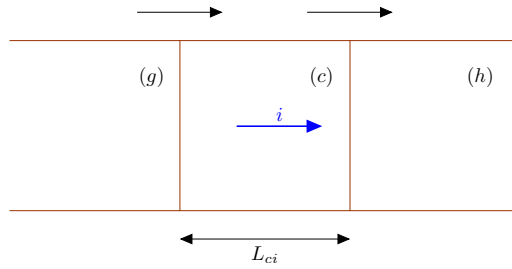
We formulate the number of vehicles in cell (c) per destination d as the following:

$$\left[\begin{array}{rcl} N_{ci}^{d,t+1/2} & = & N_{ci}^{d,t} + \Delta t \left(r_{ci}^{d,t} - q_{ci}^{d,t}\right) \\ N_{ci}^{d,t+1} & = & N_{ci}^{d,t+1/2} + \Delta t \left(Q_{gc}^{d,t} - Q_{ch}^{d,t}\right) \end{array}\right. \quad \forall (c,d) \in \mathfrak{C} \times \mathfrak{D}, \forall t \tag{6.14}$$

according to the same figure (in above). The cell density is easy to compute knowing above variables. We have: $\rho_{ci}^{d,t+1} = N_{ci}^{d,t+1}/L_{ci}$.

Algorithm of RDTA and Bi-dimensional assignment coefficients

> Loop on all bi-dimensional computing cells $c \in \mathfrak{C}$
>
>> loop on neighbor cells f of the cell c
>>
>>> compute ϖ_{cf}^{t} with (6.11)
>
>
> Initialisation of Dijkstra-based algorithm for each destination $d \in \mathfrak{D}$
>
> Execute Dijkstra-based for each destination $d \in \mathfrak{D}$
>
>> compute $\pi_{c}^{d,t}$ from all $c \in \mathfrak{C}$
>
>
> Loop on all bi-dimensional computing cells $c \in \mathfrak{C}$
>
>> loop on dominant neighbor directions i and f of the cell c
>>
>>> compute $C_{cf}^{d,t}$ and $\gamma_{ci}^{d,t}$ with (6.12) and (6.13)
>
> computation of $\Gamma_{c,ij}^{t}$ with the Formula (6.10)
>
>
> computation of flows, densities and number of vehicles, and per destination.

In doing so, the traffic assignment model identifies the minimum cost travel paths, and the directional outflow within cells of each path, which is discussed in this Section 6.2. The general structure of the reactive algorithm is shown in Figure 6.3.
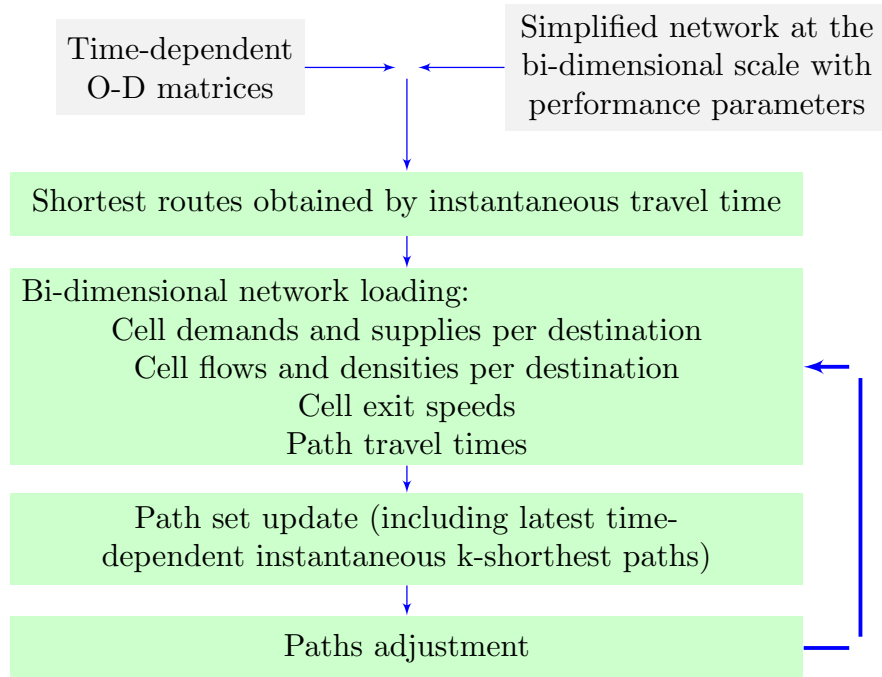
Figure 6.3: Structure of solution algorithm to the RDTA (Reactive Dynamic Traffic Assignment) problem.

The constructed assignment model of Figure 6.3 enables flow assignment of big cities, if their transportation networks areas could be approximated into two-dimensional (orthotropic or anisotropic) media.

6.3   Numerical experiments

We provide in this section the simulation results based on our proposed reactive dynamic traffic assignment scheme. Let us use an hypothetical network domain represented by the network-graph depicted by the Figure 6.4. The network domain has 12 rectangular cells and then 12 bi-dimensional nodes.
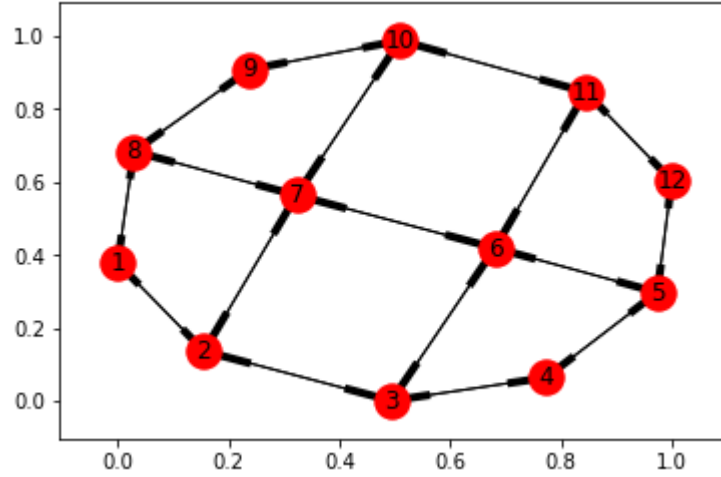

Figure 6.4: Graph of an hypothetical network-domain for the RDTA scheme application.

The resulted traffic simulator associated to the Reactive DTA allow the calculation of time-dependent origin-destination matrices. In fact, we develop a travel demand generator that handled the input travel demand from some cells referred as origins to other cells referred as destinations. More precisely, origins and destinations are located in the set of bound interfaces of the network domain.

A serie of graphics for outflows, inflows and densities of all bi-dimensional cells are shown below.
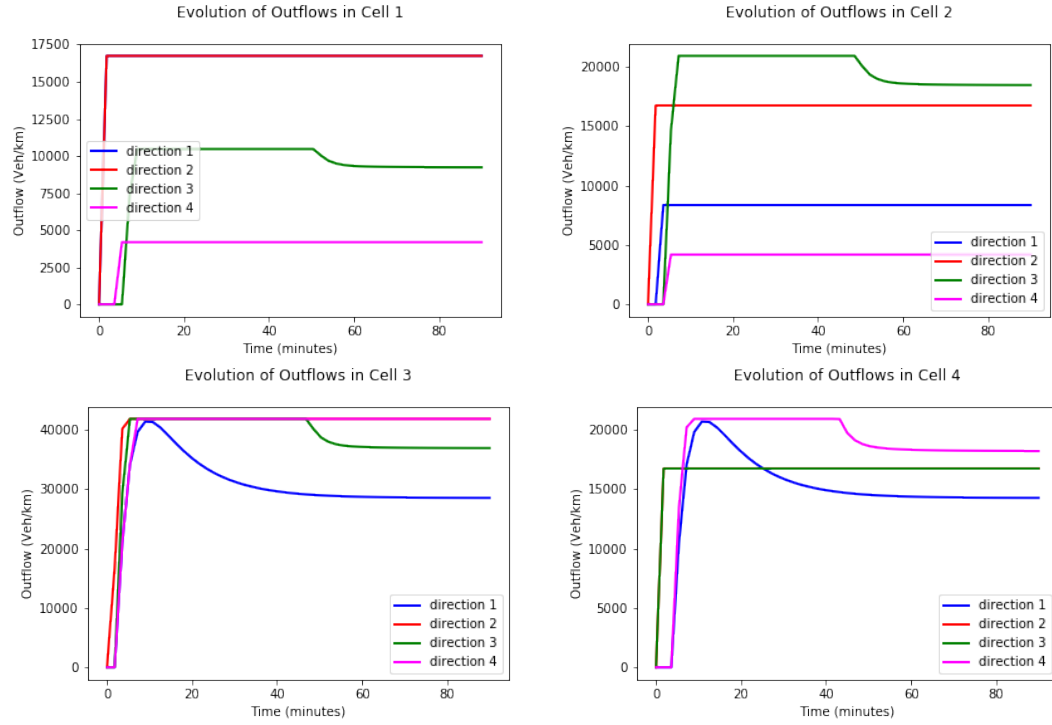
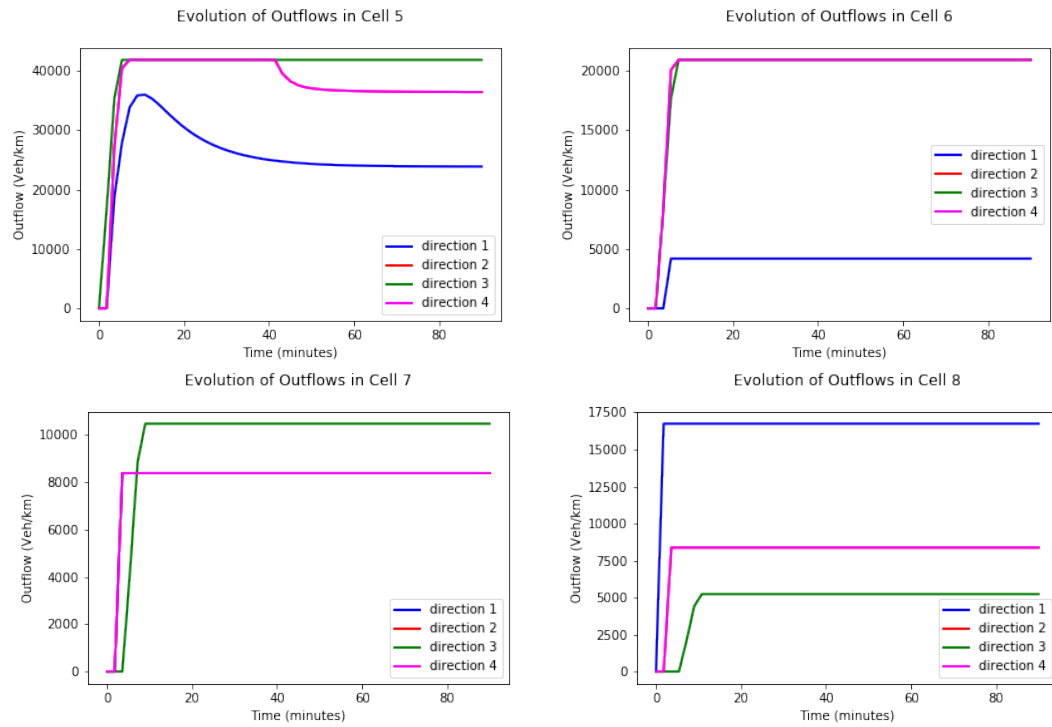Figure 6.5: Outflows of cells 1, 2, 3, and 4.
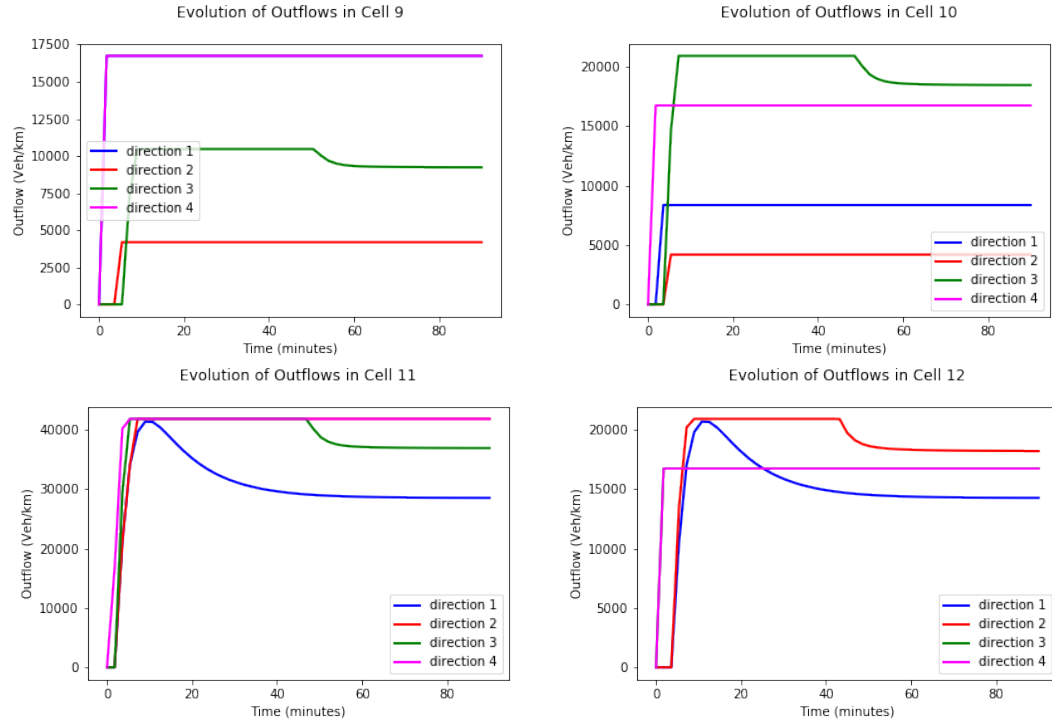

Figure 6.6: Outflows of cells 5, 6, 7 and 8.

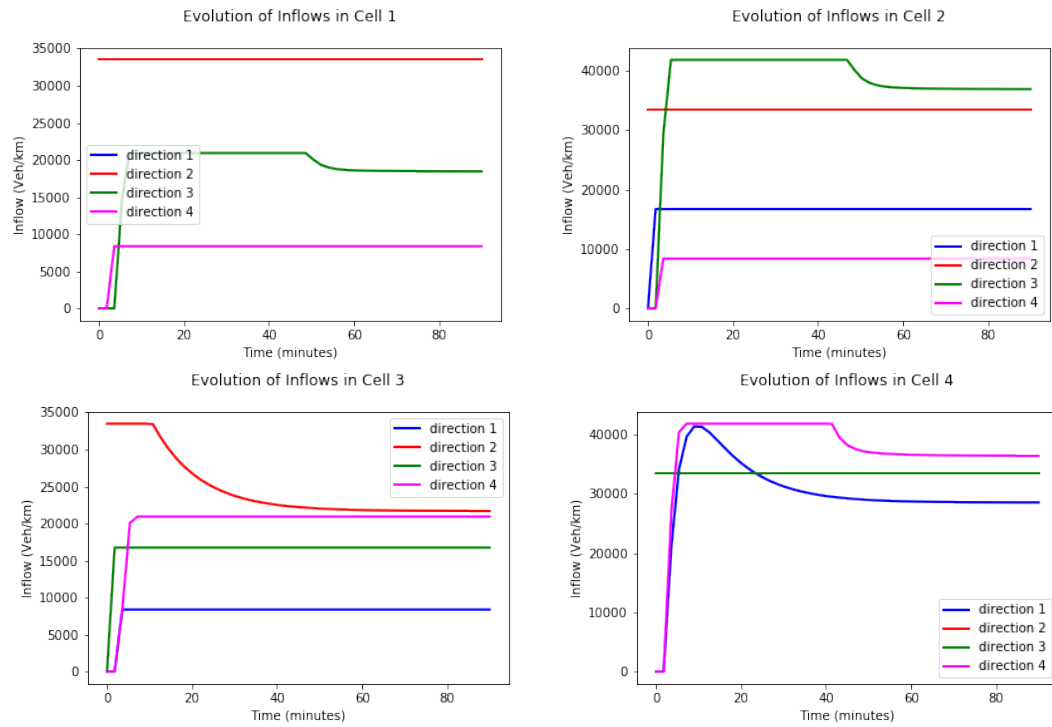Figure 6.7: Outflows of cells 9, 10, 11 and 12.

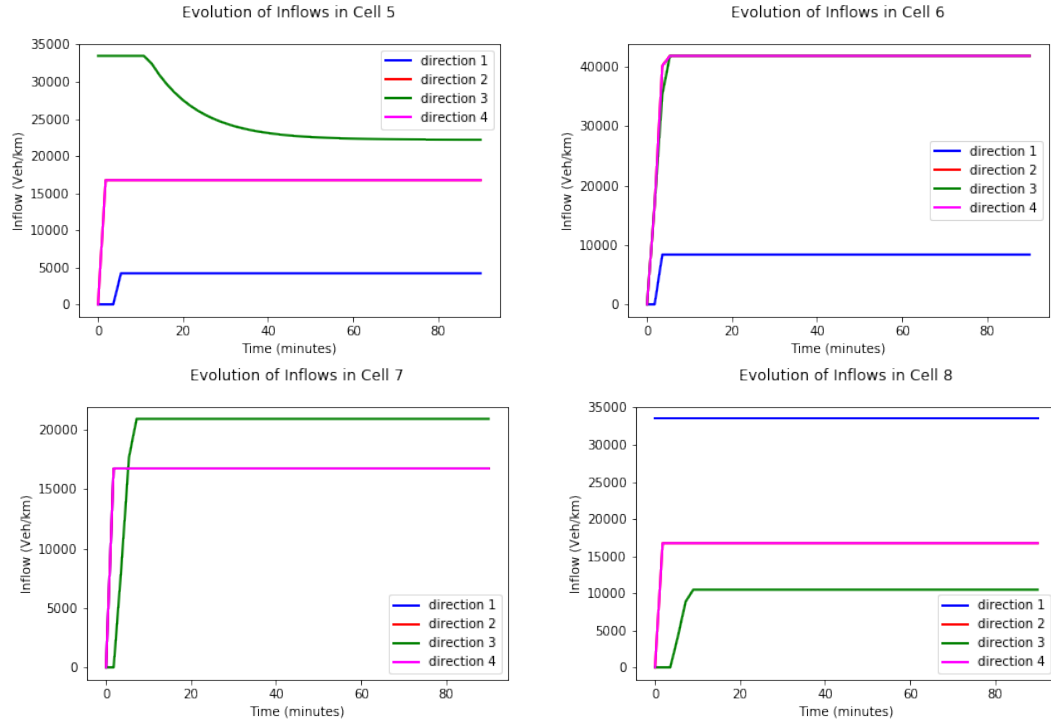Figure 6.8: Inflows of cells 1, 2, 3, and 4.

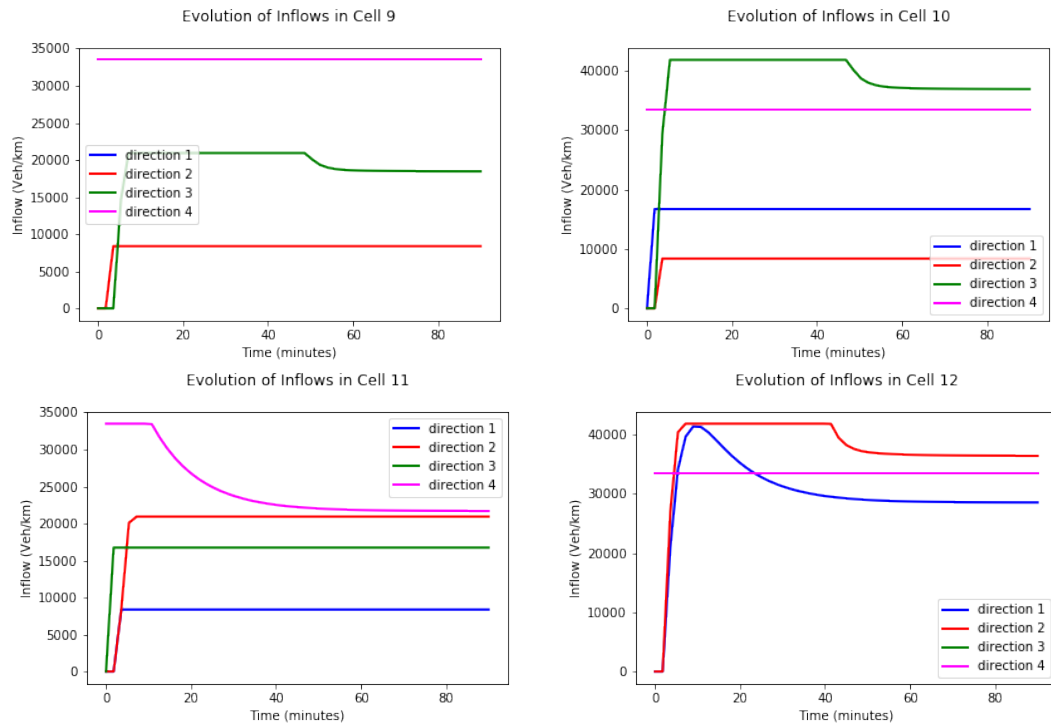Figure 6.9: Inflows of cells 5, 6, 7 and 8.

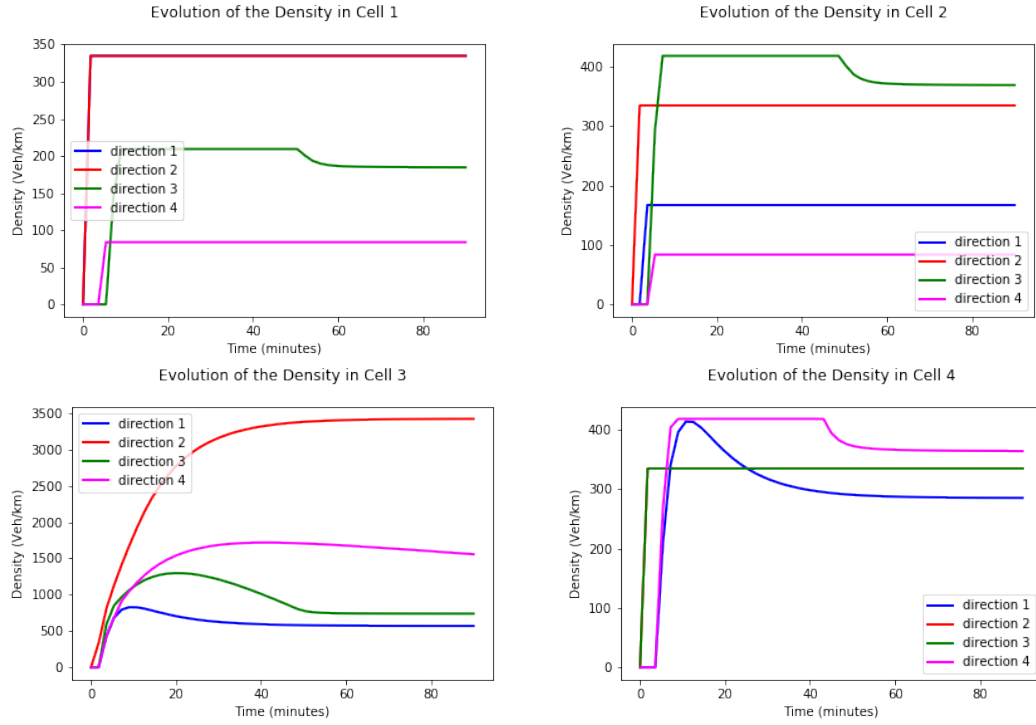Figure 6.10: Inflows of cells 9, 10, 11 and 12.
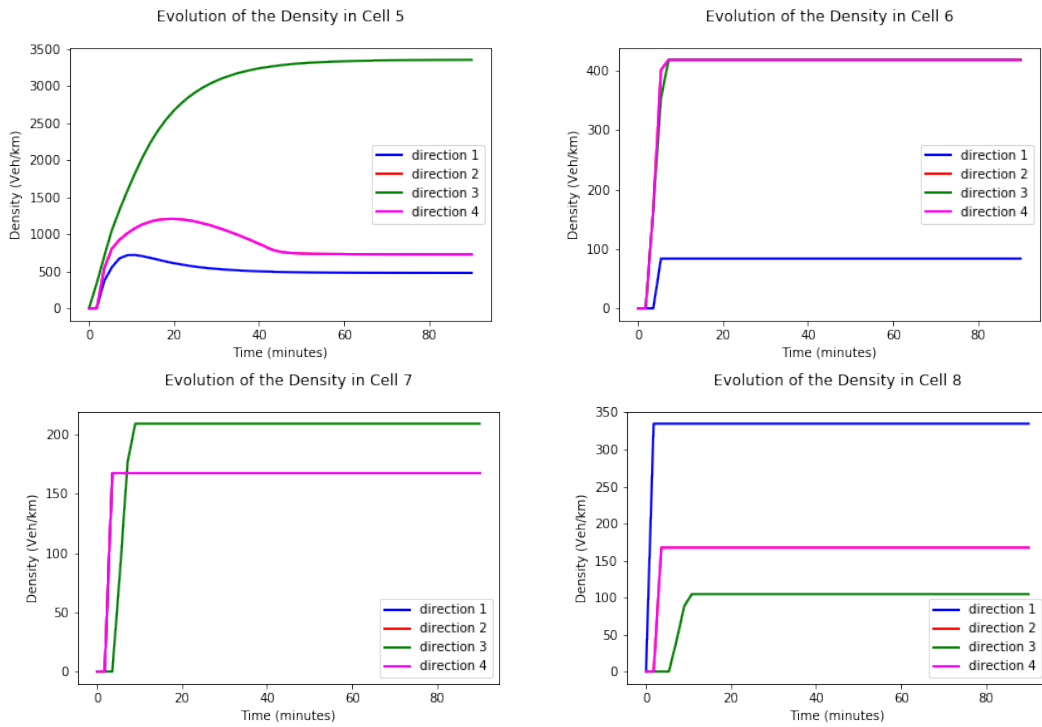
Figure 6.11: Density of cells 1, 2, 3, and 4.

Figure 6.12: Density of cells 5, 6, 7 and 8.
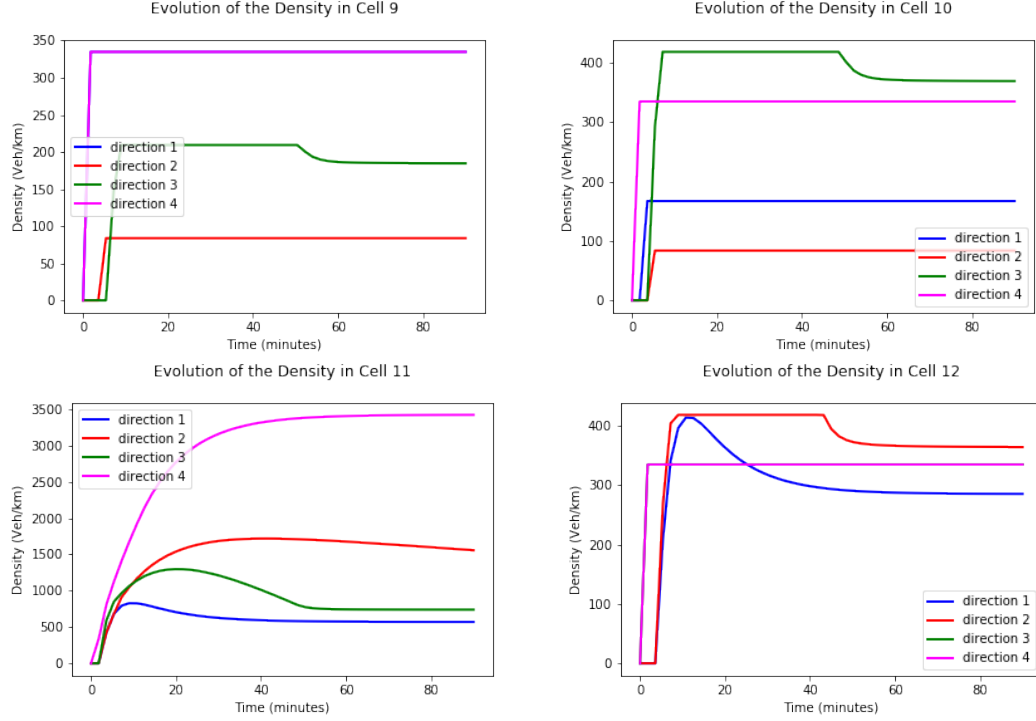
Figure 6.13: Density of cells 9, 10, 11 and 12.

The constructed assignment process and the optimization models allow easy computation of traffic flow at bi-dimensional scale. We show that the application of the two-dimensional traffic flow theory and the reactive dynamic traffic assignment theory allow adequately to simulate very large surface networks. The algorithm based on the principle of reactive dynamic assignment owes its reliability to the fact that it makes possible to obtain the real state of the traffic in comparison with the algorithms related to the user-equilibrium or dynamic user-equilibrium. In addition, our numerical results prove that the algorithm is flexible and fast. Its speed is linked even to the simplicities approaches of two-dimensional traffic theory. They lead to traffic control and supervision of large and dense (orthotropic and anisotropic) surface networks whether the trafic is homogeneous or inhomogeneous.

6.4 Conclusion

Reactive dynamic traffic assignment framework is compatible with vehicular multimodality (distinguishing between private cars, taxis, electric vehicles, demand responsive systems etc). By modifying the estimated travel time, the network is monitored. We refer to works of Atmani [2] and references therein. We could extend the multiscale coupling, presented in

Sec. 5.3, and adapt it to vehicular multimodality of very large transportation systems. We could then apply the reactive dynamic traffic assigment model, the RDTA model, to any large multimodal transportation system. That will highlight traffic interactions between different forms of mobility that are present in the considered multimodal transportation network, even when the traffic domain of the network is meshed in bi-dimensional cells.

This page is intentionally left blank.

Chapter 7

Conclusion et perspectives

Contents

7.1 Summary

We find out that large scale surface networks require specific modeling approaches of the traffic flow theory. We have developed a dynamic bi-dimensional traffic flow (BTF) model which is adequate for traffic flow management from a high level of road networks simplification. The numerical results obtained show that this flow aggregation model predicts, estimates and manages the traffic flow of very large road networks efficiently.

The BTF model is very fast compared to macroscopic traffic flow models. Chapter 3 showed this. However, in the context of vehicular multimodality, it is essential to couple this model with a specific macroscopic model especially the GSOM (Generic Second Order Model) along with microscopic transport models. The coupling of GSOM traffic flow approach with the two-dimensional traffic flow approach is successful. It suits very large and dense road transportation networks. We further respond to the three main objectives which are summed up in

- the reduction of involved cumbersome calculations and prohibitive computational time in case of macroscopic simulators deployment on large and dense surface networks,

- the traffic regulation and control, and

- the estimation of vehicle flows per mode of transportation with respect to its related transportation system.

7.2 Research relevance

The research relevance of this thesis is described in terms of theoretical achievements and practical results.

- **Theoretical relevance**

The developed models provide an extension and refinement of the current multilane traffic flow theory of Farhi *et. al* [18], the dynamical bidimensional model of Saumtally [78], the current dynamic network loading model for large-scale dynamic traffic assignment of Ziliaskopoulos [94]. The final multiscale traffic flow model gives insights into traffic interactions between different road transport modes (or forms of mobility) and the impact of PRT (personal rapid transit) demand responsive system within a multimodal transportation system. Furthermore, the *urban network traffic module* of the multiscale traffic flow simulation model accounts for interactions between traffic streams going through traffic zones. Consequently, dynamics of traffic flow at two-dimensional scale are predicted even from scarce transport data.

- **Practical relevance**

The research results will be applied for traffic flow estimation and traffic control over large and dense networks (comprising a huge number of secondary roads and/ or principal roads (the highways)). The module upon traffic of PRT (personal rapid transit) demand responsive system can be applied as generic model for other kind of this system for control approaches.

7.3 Open Problems & Future Prospects

Since we focus on studies of vehicle flows and networks supply, there are somes traffic issues related to the vehicular multimodality which are not addressed in this Report. Let us mention notably the dynamic of passagers in multimodal transportation.

Besides, we should compare the bi-dimensional traffic flow model with the multi-agent transport simulator called MATSim [36], since this latter is widely used for traffic flow management of any kind of ground transportation system. Some traffic module has been recently developed by the MATSim group to integrate multimodal aspects in the MATSim simula-

tor. However all the transport models implemented in such a simulator are for the most part microscopic, mesoscopic or macroscopic. They estimate the number of vehicles as the number of agents moving in the systems. Moreover, the agent-based approach is literally different from the flux approach. Thus the comparison of these two competitive simulation approaches (the MATSim and the Bi-dimensional transport simulator) is difficult to make and requires specific methodological developments.

This page is intentionally left blank.

Appendix A

CVXOPT convex optimization python package

We present in details the resolution of the intersection model (3.21) resulted from internal traffic within $2d$ elementary cells. Let us recall it below.

In each cell $(c) \in \mathfrak{C}$, it is a question of finding the optimal solution of A.1.

$$
\max_{(q,r)} \left(\sum_{i=1}^{4} \Phi_i(q_i) + \sum_{j=1}^{4} \Psi_j(r_j) \right)
$$

$$
\textbf{s.t.} \left| \begin{array}{ll}
0 \leq q_i \leq \Delta_{ci}^{t+1/2}, & \forall i \in \{1,2,3,4\}, \\[2mm]
0 \leq r_j \leq \Sigma_{cj}^{t+1/2}, & \forall j \in \{1,2,3,4\}, \\[2mm]
-r_j + \sum_{i=1}^{4} q_i \Gamma_{c,ij}^{t} = 0, & \forall j \in \{1,2,3,4\}.
\end{array} \right.
\tag{A.1}
$$

with $q = (q_1 \; q_2 \; q_3 \; q_4)$ and $r = (r_1 \; r_2 \; r_3 \; r_4)$ unknown variables, and Φ_i and Ψ_j being quadratic functions: $\Phi_j(x) = \Psi_j(x) = -\frac{1}{2}x_j^2 + x_j \cdot x_{j,max}$, $\forall j = 1,2,3,4$; $x = (x_1 \; x_2 \; x_3 \; x_4)$ and $x_{max} = (x_{1,max} \; x_{2,max} \; x_{3,max} \; x_{4,max})$ a given vector.

A.1 Resolution of the linear-quadratic optimization problem

Let us rewrite explicitly such a problem (A.1). For the sake of simplicity, we omitt the index of time and indexes of cells.

We obtain the below formulation:

$$\max_{(q,r)} \sum_{\ell=1}^{4} -\tfrac{1}{2}\left(q_\ell^2 + r_\ell^2\right) + \left(q_\ell q_{\ell,max} + r_\ell r_{\ell,max}\right)$$

$$\textbf{s.t.} \quad \left|\begin{array}{ll} -q_i \leqslant 0 & \forall i \in \{1,2,3,4\}, \\ -r_j \leqslant 0 & \forall j \in \{1,2,3,4\}, \\ q_i \leqslant \sigma_i & \forall i \in \{1,2,3,4\}, \\ r_j \leqslant \delta_j & \forall j \in \{1,2,3,4\}, \\ \sum_{i=1}^{4} q_i \Gamma_{ij} - r_j = 0 & \forall j \in \{1,2,3,4\}, \end{array}\right. \tag{A.2}$$

with $q = (q_1 \ q_2 \ q_3 \ q_4)$ and $r = (r_1 \ r_2 \ r_3 \ r_4)$.

In its matrix form, we obtain as follows.

$$\min_{z=(q,r)} \tfrac{1}{2} z^T M z + L z$$

$$\textbf{s.t.} \quad \left|\begin{array}{l} Gz \leqslant h \\ Az = b \end{array}\right. \tag{A.3}$$

with

$z = (q_1 \ q_2 \ q_3 \ q_4 \ r_1 \ r_2 \ r_3 \ r_4)^T$; $M = \mathrm{Id}_{8,8}$; $L = -(q_{1,max} \ q_{2,max} \ q_{3,max} \ q_{4,max} \ r_{1,max} \ r_{2,max} \ r_{3,max} \ r_{4,max})'$;

$h = (0 \ 0 \ 0 \ 0 \ 0 \ 0 \ 0 \ 0 \ \sigma_1 \ \sigma_2 \ \sigma_3 \ \sigma_4 \ \delta_1 \ \delta_2 \ \delta_3 \ \delta_4)^T$;

$G = \begin{pmatrix} -\mathrm{Id}_{8,8} \\ \mathrm{Id}_{8,8} \end{pmatrix}$; $\Gamma = (\Gamma)_{1 \leq i,j \leq 4}$ is the stochastic matrix of assignment coefficients.

Figure A.1 depicts the attribute function Ψ_j with respect to characteristics of lanes in direction (j), $j = 1,2,3,4$.
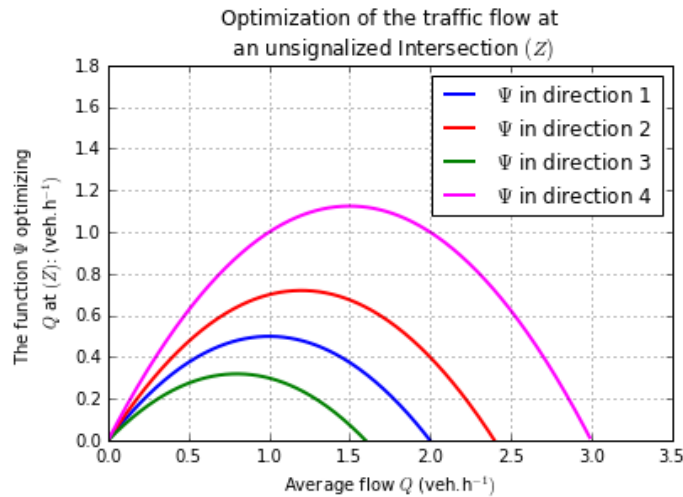

Figure A.1: Optimization profile of car-flows at intersection without signaling

We take for numerical tests values below for the stochastic matrix Γ (from Saumtally [77]).

$$\Gamma = \begin{pmatrix} 0.4686 & 0.2236 & 0 & 0.3078 \\ 0.0405 & 0.469 & 0.4905 & 0 \\ 0 & 0.3109 & 0.2904 & 0.3987 \\ 0.3512 & 0 & 0.4097 & 0.2391 \end{pmatrix}.$$

The equality constraint of (3.7) or (A.2) in a matrix format gives: $Az = b$, with

$$A = \begin{pmatrix} \Gamma_{11} & \Gamma_{21} & 0 & \Gamma_{41} & -1 & 0 & 0 & 0 \\ \Gamma_{12} & \Gamma_{22} & \Gamma_{32} & 0 & 0 & -1 & 0 & 0 \\ 0 & \Gamma_{23} & \Gamma_{33} & \Gamma_{43} & 0 & 0 & -1 & 0 \\ \Gamma_{14} & 0 & \Gamma_{34} & \Gamma_{44} & 0 & 0 & 0 & -1 \end{pmatrix} = \begin{pmatrix} \Gamma^T & | & -\text{Id}_{4,4} \end{pmatrix} \quad \text{and } b = O_{8,1}.$$

We solve the obtained optimization models in Python with the CVXOPT Python package for Convex Optimization [1]. The update of the stochastic matrix Γ is due by routes calculation with the Python Networkx library and the application of the cross-entropy method. Hence, traffic assignment easily identifies minimum cost travel paths, and directional outflows of cells of each path. The constructed assignment process and optimization models applied to very large networks allow easy computation of traffic flow at bi-dimensional scale.

This page is intentionally left blank.

BIBLIOGRAPHY

[1] ANDERSEN, M., DAHL, J., AND VANDENBERGHE, L. CVXOPT Python Software for Convex Optimization, 2004.

[2] ATMANI, D. *Dynamic assignment of users in a multimodal transportation system*. Theses, Université Paris-Est, Dec. 2015.

[3] AW, A., KLAR, A., RASCLE, M., AND MATERNE, T. Derivation of continuum traffic flow models from microscopic follow-the-leader models. *SIAM Journal on Applied Mathematics 63*, 1 (2002), 259–278.

[4] AW, A., AND RASCLE, M. Resurrection of "second order"; models of traffic flow. *SIAM J. Appl. Math. 60*, 3 (Feb. 2000), 916–938.

[5] BAGNERINI, P., AND RASCLE, M. A multi-class homogenized hyperbolic model of traffic flow. *SIAM J. Math. Anal 35* (2003), 2003.

[6] CASSIDY, M. J., JANG, K., AND DAGANZO, C. F. Macroscopic fundamental diagrams for freeway networks: Theory and observation. *Transportation Research Record: Journal of the Transportation Research Board Traffic Flow Theory and Characteristics 2011* (2011), 8–15.

[7] COCLITE, G. M., GARAVELLO, M., AND PICCOLI, B. Traffic flow on a road network. *SIAM Journal on Mathematical Analysis 36*, 6 (2005), 1862–1886.

[8] COSTESEQUE, G., AND LEBACQUE, J. Intersection modeling using a convergent scheme based on hamilton-jacobi equation. *Procedia - Social and Behavioral Sciences 2012* (2012), 343–363.

[9] COSTESEQUE, G., AND LEBACQUE, J. P. Intersection modeling using a convergent scheme based on hamilton-jacobi equation. *Procedia-Social and Behavioral Sciences 54* (2012), 736–748.

[10] COURBON, T., AND LECLERCQ, L. Cross-comparison of Macroscopic Fundamental Diagram Estimation Methods. *Procedia - Social and Behavioral Sciences 20* (2011), 417 – 426.

[11] DAGANZO, C. F. Urban gridlock: Macroscopic modeling and mitigation approaches. *Transportation Research Part B: Methodological 41*, 1 (2007), 49 – 62.

[12] DAGANZO, C. F., AND GEROLIMINIS, N. An analytical approximation for the macroscopic fundamental diagram of urban traffic. *Transportation Research Part B: Methodological 42*, 9 (November 2008), 771–781.

[13] DAGANZO, C. F., AND LAVAL, J. A. Moving bottlenecks: A numerical method that converges in flows. *Transportation Research Part B: Methodological 39*, 9 (Nov. 2005), 855–863.

[14] DAGANZO, C. F., AND LAVAL, J. A. On the numerical treatment of moving bottlenecks. *Transportation Research Part B: Methodological 39*, 1 (Jan. 2005), 31–46.

[15] DUBOC, F., ENAUX, C., JAOUEN, S., JOURDREN, H., AND WOLFF, M. High-order dimensionally split lagrange-remap schemes for compressible hydrodynamics. *Comptes Rendus Mathematique 348*, 1-2 (Jan. 2010), 105–110.

[16] EYMARD, R., GALLOUËT, T., AND HERBIN, R. *Finite Volume Methods*, vol. VII of *Handbook of Numerical Analysis*. North-Holland, Amsterdam, 2000, ch. 5.1, pp. 713–1020.

[17] FAN, S., AND SEIBOLD, B. A comparison of data-fitted first order traffic models and their second order generalizations via trajectory and sensor data.

[18] FARHI, N., HAJ-SALEM, H., KHOSHYARAN, M., LEBACQUE, J.-P., SALVARANI, F., SCHNETZLER, B., AND DE VUYST, F. The logit lane assignment model: First results. *arXiv preprint arXiv:1302.0142* (2013).

[19] FLOTTEROD, G., AND ROHDE, J. Operational macroscopic modeling of complex urban road intersections. *Transportation Research Part B: Methodological 45*, 6 (July 2011), 903–922.

[20] GEUZAINE, C., AND REMACLE, J.-F. Gmsh: A 3-D finite element mesh generator with built-in pre- and post-processing facilities. *International Journal for Numerical Methods in Engineering 79*, 11 (sep 2009), 1309–1331.

[21] GOATIN, P. The aw-rascle vehicular traffic flow model with phase transitions. *Math. Comput. Model. 44*, 3-4 (Aug. 2006), 287–303.

[22] GODVIK, M., AND HANCHE-OLSEN, H. Existence of solutions for the aw-rascle traffic flow model with vacuum. *Journal of Hyperbolic Differential Equations 05*, 01 (2008), 45–63.

[23] GREENBERG, J. M. Extensions and amplifications of a traffic model of aw and rascle. *SIAM Journal on Applied Mathematics 62*, 3 (2002), 729–745.

[24] HAJ-SALEM, H., LEBACQUE, J.-P., AND MAMMAR, S. An intersection model based on the gsom model. *Proceedings of the 17th World Congress The International Federation of Automatic Control 17*, 1 (2008), 7148–7153.

[25] HART, W. E., LAIRD, C., WATSON, J.-P., AND WOODRUFF, D. L. *Pyomo–optimization modeling in python*, vol. 67. Springer Science & Business Media, 2012.

[26] HART, W. E., WATSON, J.-P., AND WOODRUFF, D. L. Pyomo: modeling and solving mathematical programs in python. *Mathematical Programming Computation 3*, 3 (2011), 219–260.

[27] HARTEN, A., LAX, P. D., AND VAN LEER, B. On upstream differencing and godunov-type schemes for hyperbolic conservation laws. *SIAM Review 25*, 1 (1983), 35–61.

[28] HAUT, B., AND BASTIN, G. A second order model of road junctions in fluid models of traffic networks. *Networks and Heterogeneous Media 2*, 2 (2007), 227.

[29] HELBING, D. Gas-kinetic derivation of navier-stokes-like traffic equations. *Phys. Rev. E 53* (Mar 1996), 2366–2381.

[30] HELBING, D. Modeling multi-lane traffic flow with queuing effects. *Physica A: Statistical Mechanics and its Applications 242*, 1 (1997), 175 – 194.

[31] HERTY, M., AND KLAR, A. Modeling, simulation, and optimization of traffic flow networks. *SIAM Journal on Scientific Computing 25*, 3 (2003), 1066–1087.

[32] HOLDEN, H., AND RISEBRO, N. H. *A Mathematical Model of Traffic Flow on a Network of Roads*. Vieweg+Teubner Verlag, Wiesbaden, 1993, pp. 329–335.

[33] HOOGENDOORN, S. *Multiclass continuum modelling of multilane traffic flow*. PhD thesis, Civil Engineering and Geosciences, 1999.

[34] HOOGENDOORN, S., AND BOVY, P. Multiclass macroscopic traffic flow modelling: a multilane generalisation using gas-kinetic theory. In *14th International Symposium on Transportation and Traffic Theory* (1999).

[35] HOOGENDOORN, S. P., AND BOVY, P. H. Continuum modeling of multiclass traffic flow. *Transportation Research Part B: Methodological 34*, 2 (2000), 123 – 146.

[36] HORNI, A., NAGEL, K., AND AXHAUSEN, K. W. *The Multi-Agent Transport Simulation MATSim*. Ubiquity Press, London, Aug. 2016.

[37] HUANG, H.-J., AND LI, Z.-C. A multiclass, multicriteria logit-based traffic equilibrium assignment model under ATIS. *European Journal of Operational Research 176*, 3 (Feb. 2007), 1464–1477.

[38] JIANG, Y., WONG, S., HO, H., ZHANG, P., LIU, R., AND SUMALEE, A. A dynamic traffic assignment model for a continuum transportation system. *Transportation Research Part B 45* (2011), 343–363.

[39] KESSELS, F. L. M. *Multi-class continuum traffic flow models: analysis and simulation methods*. PhD thesis, TRAIL, Delft, 2013.

[40] KEYVAN-EKBATANI, M., KOUVELAS, A., PAPAMICHAIL, I., AND PAPAGEORGIOU, M. Exploiting the fundamental diagram of urban networks for feedback-based gating. *Transportation Research Part B: Methodological 46*, 10 (2012), 1393 – 1403.

[41] KEYVAN-EKBATANI, M., PAPAGEORGIOU, M., AND KNOOP, V. L. Controller design for gating traffic control in presence of time-delay in urban road networks. *Transportation Research Part C: Emerging Technologies 59* (2015), 308 – 322. Special Issue on International Symposium on Transportation and Traffic Theory.

[42] KEYVAN-EKBATANI, M., YILDIRIMOGLU, M., GEROLIMINIS, N., AND PAPAGEORGIOU, M. Multiple concentric gating traffic control in large-scale urban networks. *IEEE Transactions on Intelligent Transportation Systems 16*, 4 (Aug 2015), 2141–2154.

[43] KHOSHYARAN, M., AND LEBACQUE, J. *A Reactive Dynamic Assignment Scheme*. Mathematics in Transport Planning and Control (Default Book Series, Volume), 1998, ch. 13, pp. 131–143.

[44] KHOSHYARAN, M., AND LEBACQUE, J. Numerical solutions to the logit lane assignment model. *Procedia - Social and Behavioral Sciences 54* (2012), 907 – 916.

[45] KLAR, A., GREENBERG, J., AND RASCLE, M. Congestion on multilane highways. *SIAM Journal on Applied Mathematics 63*, 3 (2003), 818–833.

[46] KLAR, A., GREENBERG, J. M., AND RASCLE, M. Congestion on multilane highways. *SIAM Journal on Applied Mathematics 63*, 3 (2003), 818–833.

[47] KLAR, A., AND WEGENER, R. Enskog-like kinetic models for vehicular traffic. 1996.

[48] KNOOP, V. L., VAN LINT, H., AND HOOGENDOORN, S. P. Traffic dynamics: Its impact on the macroscopic fundamental diagram. *Physica A: Statistical Mechanics and its Applications 438*, C (2015), 236–250.

[49] LEBACQUE, J. Instantaneous travel times for macroscopic traffic flow models. Tech. rep., CERMICS, 1996.

[50] LEBACQUE, J., MAMMAR, S., AND HAJ-SALEM, H. Generic second-order traffic flow modeling. In *Proceedings of the 17th International Symposium on Transportation and Traffic Theory* (London, 2007), B. H. E. R.E. Allsop, M.G.H. Bell, Ed., pp. 749–770.

[51] LEBACQUE, J.-P. The godunov scheme and what it means for first order traffic flow models. In *International symposium on transportation and traffic theory* (1996), pp. 647–677.

[52] LEBACQUE, J.-P., AND KHOSHYARAN, M. *First-order macroscopic traffic flow models: Intersection modeling, network modeling*. Elsevier, 2005, ch. 19, pp. 365–386.

[53] LEBACQUE, J.-P., AND KHOSHYARAN, M. A variational formulation for higher order macroscopic traffic flow models of the gsom family. *Procedia-Social and Behavioral Sciences 83* (2013), 370–394.

[54] LECLERCQ, L., CHIABAUT, N., AND TRINQUIER, B. Macroscopic fundamental diagrams: A cross-comparison of estimation methods. *Transportation Research Part B: Methodological 62* (2014), 1 – 12.

[55] LEVEQUE, R. J. Wave propagation algorithms for multidimensional hyperbolic systems. *Journal of Computational Physics 131*, 2 (1997), 327 – 353.

[56] LEVEQUE, R. J., AND SHYUE, K.-M. Two-dimensional front tracking based on high resolution wave propagation methods. *Journal of Computational Physics 123*, 2 (1996), 354 – 368.

[57] LIGHTHILL, M. J., AND WHITHAM, G. B. On Kinematic Waves. {II}. A Theory of Traffic Flow on Long Crowded Roads. *Proc. Royal Soc.* (1955), 317–345.

[58] LOUAIL, T., LENORMAND, M., PICORNELL, M., CANTÚ, O. G., HERRANZ, R., FRIAS-MARTINEZ, E., RAMASCO, J. J., AND BARTHELEMY, M. Uncovering the spatial structure of mobility networks. *Nature Communications 6, 6007* (2015).

[59] MA, T. A hybrid cross entropy algorithm for solving dynamic transit network design problem. *CoRR abs/1211.5371* (2012).

[60] MA, T., AND LEBACQUE, J. A dynamic packet-based multi-agent approach for large scale multimodal network simulation. In *10th International Conference on Application of Advanced Technologies in Transportation* (2008).

[61] MA, T.-Y. *Modèle dynamique de transport basé sur les activités*. PhD thesis, Ecole des Ponts ParisTech, 2007.

[62] MAHMASSANI, H. S. Dynamic network traffic assignment and simulation methodology for advanced system management applications. *Networks and Spatial Economics 1*, 3-4 (2001), 267–292.

[63] MAHMASSANI, H. S., AND PEETA, S. Network performance under system optimal and user equilibrium dynamic assignments: implications for advanced traveler information systems. *Transportation Research Record* (1993).

[64] MAHROUS, R. F. A. *Multimodal Transportation Systems : Modelling Challenges*. PhD thesis, Enschede, 2012.

[65] MERCHANT, D. K., AND NEMHAUSER, G. L. A model and an algorithm for the dynamic traffic assignment problems. *Transportation Science 12*, 3 (1978), 183–199.

[66] MERCHANT, D. K., AND NEMHAUSER, G. L. Optimality conditions for a dynamic traffic assignment model. *Transportation Science 12*, 3 (aug 1978), 200 – 207.

[67] MOUTARI, S., AND RASCLE, M. A hybrid lagrangian model based on the aw-rascle traffic flow model. *SIAM Journal on Applied Mathematics 68*, 2 (2007), 413–436.

[68] NELSON, P. A kinetic model of vehicular traffic and its associated bimodal equilibrium solutions. *Transport Theory and Statistical Physics 24*, 1-3 (1995), 383–409.

[69] NGODUY, D. *Macroscopic discontinuity modeling for multiclass multilane traffic flow operations*. PhD thesis, Netherlands TRAIL Research School, 2006.

[70] NICHOLSON, B., SIIROLA, J. D., WATSON, J.-P, ZAVALA, V. M., AND BIEGLER, L. T. pyomo.dae: A modeling and automatic discretization framework for optimization with differential and algebraic equations. *http://www.optimization-online.org* (May 2016), 28.

[71] NIE, Y. M. A cell-based merchant-nemhauser model for the system optimum dynamic traffic assignment problem. *Transportation Research Part B: Methodological 45*, 2 (2011), 329 – 342.

[72] PAVERI-FONTANA, AND S.L. On boltzmann-like treatments for traffic flow: A critical review of the basic model and an alternative proposal for dilute traffic analysis. *Transportation Research* (1975), 225–235.

[73] PHILLIPS, W. F. A kinetic model for traffic flow with continuum implications. *Transportation Planning and Technology 5*, 3 (1979), 131–138.

[74] PREZ, L. M. R., AND BENITEZ, F. G. Traffic flow continuum modeling by hypersingular boundary integral equations. *International journal for numerical methods in engineering 82*, 3 (2010), 47–63.

[75] PRIGOGINE, I., AND HERMAN, R. Kinetic theory of vehicular traffic. *Transportation Research Board. 500 Fifth St. NW, Washington, D.C. 20001* (1971).

[76] RICHARDS, P. I. Shock-waves on the highway. *Operations Research 4*, 1 (1956), 42–51.

[77] SAUMTALLY, T. *Modèles bidimensionnels de trafic*. PhD thesis, Université Paris-Est, 2012. Thèse de doctorat dirigé par Haj-Salem H., Transport Paris Est 2012.

[78] SAUMTALLY, T., LEBACQUE, J.-P., AND HAJ-SALEM, H. A dynamical two-dimensional traffic model in an anisotropic network. *Networks and Heterogeneous Media* (September 2013), 663–684.

[79] SIEBEL, F., AND MAUSER, W. On the fundamental diagram of traffic flow. *SIAM Journal on Applied Mathematics 66*, 4 (2006), 1150–1162.

[80] SOSSOE, K. Biditsim: Dynamic bi-dimensional traffic flow simulator. Tech. rep., msoi Mobilité Intelligente, 2017.

[81] SOSSOE, K., LEBACQUE, J., MOKRANI, A., AND HAJ-SALEM, H. Traffic flow within a two-dimensional continuum anisotropic network. *Transportation Research Procedia 10* (2015), 217–225.

[82] SOSSOE, K., AND LEBACQUE, J.-P. A multiclass vehicular dynamic traffic flow model for main roads and dedicated lanes/roads of multimodal transport network. In *Proceedings of the International Conference on Numerical Analysis and Applied Mathematics 2014 (ICNAAM-2014)* (2015), vol. 1648, AIP Publishing, pp. 1–4.

[83] SOSSOE, K., AND LEBACQUE, J.-P. *Dynamic Model for Assignment in a 'Sky-Car' Transit System: Spatial Interactions with Other Common Transport Modes*. Springer International Publishing, Cham, 2016, pp. 499–506.

[84] SOSSOE, K., AND LEBACQUE, J.-P. *Reactive Dynamic Assignment for a Bi-dimensional Traffic Flow Model*. AISC 539, ICSS 2016, 2017, ch. 17.

[85] TAMPERE, C., ET AL. *Human-kinetic multiclass traffic flow theory and modelling with application to advanced driver assistance systems in congestion*. TU Delft, Delft University of Technology, 2004.

[86] TAMPÈRE, C. M., CORTHOUT, R., CATTRYSSE, D., AND IMMERS, L. H. A generic class of first order node models for dynamic macroscopic simulation of traffic flows. *Transportation Research Part B: Methodological 45*, 1 (2011), 289–309.

[87] TRANGENSTEIN, J. A. J. A. *Numerical solution of hyperbolic partial differential equations*. Cambridge, UK ; New York : Cambridge University Press, 2009. Formerly CIP.

[88] VAN DEN BERG, M., HEGYI, A., SCHUTTER, B. D., AND HELLENDOORN, J. A macroscopic traffic flow model for integrated control of freeway and urban traffic networks. In *Decision and Control, 2003. Proceedings. 42nd IEEE Conference on* (Dec 2003), vol. 3, pp. 2774–2779 Vol.3.

[89] VAN NES, R. *Design of multimodal transport networks; A hierarchical approach*. PhD thesis, The Netherlands TRAIL Research School, 2002.

[90] VIDES, J., NKONGA, B., AND AUDIT, E. A Simple Two-Dimensional Extension of the HLL Riemann Solver for Gas Dynamics. [research report] rr-8540, hal-00998235v2, Project-Team Castor, 2014.

[91] WARDROP, J. G., AND WHITEHEAD, J. I. Correspondence. some theoretical aspects of road traffic research. *Proceedings of the Institution of Civil Engineers 1*, 5 (1952), 767–768.

[92] WEGENER, R., AND KLAR, A. A kinetic model for vehicular traffic derived from a stochastic microscopic model. *Transport Theory and Statistical Physics 25*, 7 (1996), 785–798.

[93] WONG, S. Multi-commodity traffic assignment by continuum approximation of network flow with variable demand. *Transportation Research Part B: Methodological 32*, 8 (1998), 567 – 581.

[94] ZILIASKOPOULOS, A. K., WALLER, S. T., LI, Y., AND BYRAM, M. Large-scale dynamic traffic assignment: Implementation issues and computational analysis. *Journal of Transportation Engineering 130*, 5 (2004), 585–593.